Geologic Description, Sampling, and Petroleum Source Rock Potential of the Awatubi and Walcott Members, Kwagunt Formation, Chuar Group of the Sixtymile Canyon Section, Grand Canyon, Arizona

Bruce H. Wiley[1], Carol M. Dehler[2], Samir A. Ghazi[3], Lung-Chuan Kuo[3],
and Steven L. Rauzi[4]

January 2002
(Revised February 2002)

ARIZONA GEOLOGICAL SURVEY
OPEN-FILE REPORT 02-01

Cooperatively prepared by the Arizona Geological Survey and Conoco

Includes 1 plate and 84 pages of text (including title page)

[1]Current address: Burlington Resources, Inc., P.O. Box 51810, Midland, TX 79710
[2]Utah State University, Department of Geology, 4505 Old Main Hill, Logan, UT 84322
[3]Conoco Inc, Conoco Center, P.O. Box 2197, Houston, TX 77252
[4]Arizona Geological Survey, 416 W. Congress #100, Tucson, AZ 85701

Acknowledgements

Contents

Contents (continued)

Tables

Figures and Plate

Abstract

In November 1997, a stratigraphic section of the Awatubi and Walcott Members of the Late Proterozoic Kwagunt Formation, Chuar Group, located in the Sixtymile Canyon area, of the eastern Grand Canyon National Park, Arizona, was measured, described and sampled. The goals of the study were: 1) to further characterize the petroleum source rock potential of the Awatubi and Walcott Members, previously concluded to constitute the significant source rock potential of the Chuar Group (Wiley, et al., 1998); 2) to add to the Chuar Group reference sample collection at the Arizona Geological Survey which is available for future study; 3) to integrate and synthesize Chuar Group source rock data from the Sixtymile Canyon section with that from the Nankoweap Canyon and Carbon Canyon sections (Wiley, et al., 1998); and 4) to review the range of possible organic-rich depositional environments and their characteristics to identify the most likely depositional environments for the Chuar Group.

A total of 1480 ft (452 m) of section [653 ft (199 m) = Awatubi; 827 ft (252 m) = Walcott] was measured and 30 samples were collected (9 samples from the Awatubi Member, and 21 samples from the Walcott Member). All 30 samples were analyzed for total organic carbon (TOC) as a measure of organic richness and by Rock-Eval pyrolysis, which included Tmax as a measure of thermal maturity.

A wide variance was obtained in estimates of organic richness from the various indices of richness. For the Awatubi Member, a minimum of 10 ft (2% of the 456 ft of sampled Awatubi) based on genetic potential, and a maximum of 355 ft (78%) based on total organic carbon (TOC) is potential source rock. For the Walcott Member, a minimum of 489 ft (60% of the 814 ft of sampled Walcott) based on genetic potential, and a maximum of 814 ft (100%) based on total organic carbon (TOC) is potential source rock.

A wide variance is also seen in estimates of organic maturity obtained from the various indices of maturity. The maturity of the Awatubi Member based on Tmax has an average value in the immature window, and the Tmax gradient was entirely within the early oil window. Based on productivity index, 434 ft (95%) of the 456 ft of sampled Awatubi section is early oil or higher maturity and 182 ft (40%) ranges up to late oil and postmature (gas windows). For the Awatubi Member, all of the Tmax values are unreliable, and productivity index values also have relatively large errors but may be a more reliable indicator of thermal maturity. Based on the maturity deduced for the Walcott Member, the Awatubi Member is likely to be in the peak to late oil generation window.

Both Tmax and productivity index rate much of the upper part of the Walcott Member as immature, but for the lower part of the Walcott Member, maturity indicated by productivity index is generally higher than that indicated by Tmax. The Tmax gradient of the upper 420 ft (51%) of the 827 ft of total Walcott section is immature, and the lower 407 ft (49%) is in the early oil window. Productivity index ranks 358 ft (44%) of the 814 ft of sampled Walcott Member as immature, 456 ft (56%) as early oil or higher, 317 ft (39%) as early oil-peak oil gap or higher, 112 ft (14%) as peak oil or higher, and 20 ft (2%) as late oil and postmature (gas windows). The Tmax values for the Walcott Member are reliable, but due to their high-TOC content exhibit a delayed release of their S2 material resulting in exaggerated Tmax values. We conclude that the Walcott Member samples range from immature to early mature to the onset of peak oil generation. This is consistent with the productivity index values in the Walcott Member samples for which Tmax is reliable, which vary from 0.05 to 0.15. The unusually high productivity index of sample S10-60-25 may be due to contamination. Samples in the lower part of the Walcott Member (S10-60-18 to S10-60-10) have higher productivity index values due to the very small S1 and S2 values and therefore larger analytical error. The average Tmax maturity of the Walcott Member anomalously exceeds that of the underlying Awatubi Member, which is probably due to unreliable Tmax values for the Awatubi due to low kerogen S2 values.

The potential source rocks of the Awatubi Member are gas prone. The Walcott Member is definitely a potential gas source, with some of the indicators suggesting oil potential as well.

For the Awatubi Member, hydrocarbons in 40% of the section indicate a migrated origin, in 5% indicate a mixed origin, and in 55% indicate an indigenous origin. For the Walcott Member hydrocarbons in 95% of the section have an indigenous origin, and only in 2% indicate a migrated origin, and in 3% indicate a mixed origin.

The Sixtymile Canyon section has thicker organically rich facies in both the Awatubi and Walcott

Members than in the neighboring Carbon Canyon (Walcott Member thin and not sampled) and Nankoweap Canyon areas, suggesting that it was deposited in a deeper, possibly more basinal portion of the Chuar Basin, with more of its deposition below the anaerobic water column.

Tmax maturities in the Sixtymile Canyon section are consistent with the previously reported pattern from the Carbon Canyon and Nankoweap Canyon sections, whereby Tmax maturity windows have an apparent dip to the southeast. This suggests longer or deeper burial to the northwest or higher heat flow to the northwest.

The range of possible depositional environments of the Chuar Group is interpreted utilizing the euxinic basin biofacies and lithofacies model of Byers (1977), seven possible euxinic and five possible oxic organic-rich basin models, and data on the present-day photic zone, lithofacies of the shore zone and inner and outer shelf, ocean water temperature variations and mixing, shallowing upward carbonate sequences, and stromatolites. The range of possible basin models proposed for the Chuar Group include three euxinic models (1, 3, or 4) and two oxic models (10 or 12), all of which are to some degree restricted. The euxinic models include the restricted hypersaline (>37 per mille) euxinic marine basin models with two-way (model 3) or one-way (model 4) flow through the portal, or the isolated tropical humid climate euxinic lake model (model 1). Stable carbon isotope ratios (del C13 Aromatic vs. del C13 Saturate) indicate the lacustrine model is less likely, at least for the Tanner, Carbon Canyon, Awatubi, and Walcott Members (Wiley, et al., 1998). Two oxic, restricted marine models, the shallow saline/hypersaline lagoon (model 10), or an epeiric sea model (model 12) are also possibilities. Some cyclical alternation of these five models is also possible. The lack of bedded gypsum or higher grade evaporites in the Chuar Group implies that for any of the restricted basin depositional models under consideration, the degree of restriction was less than that necessary to concentrate seawater to a salinity of 124‰ at which gypsum precipitation begins. Lucia (1972) has shown that gypsum is not deposited when the ratio (Ao/At) of the surface area of the restricted basin (Ao) to the cross-sectional area of the inlet (At) is less than 10^6. Highly organic, sulphur-bearing, black shales, found primarily in thin beds of the Tanner and Carbon Canyon Members, in the upper portion of the Awatubi Member, and in most of the Walcott Member, indicate deposition in the dysaerobic (50-150 m) to anaerobic (>150 m) zones, or alternatively the deeper parts of a shallow saline/hypersaline oxic lagoon or epeiric sea with anoxic bottom sediments. Stromatolitic and algal-bearing beds indicate deposition under oxygenated conditions in the photic zone (80-200 m maximum, 50 m if nearshore), but more probably at intertidal or shallow subtidal marine depths. A maximum depositional depth of 150 ft (46 m) has been suggested for deepwater stromatolites in the Devonian of Western Australia (Playford and Cockbain, 1969). These beds record shallowing to within the aerobic zone. Alternatively, they may have been deposited in the shallow margins of a shallow saline or hypersaline oxic lagoon or oxic epeiric sea. The Flaky Dolomite Bed at the base of the Walcott Member has characteristics of flocculose cyanobacterial mat deposition. Bouyancy produced by entrapped mat photosynthetic oxygen may explain the contorted bedding restricted to this horizon. Other possible explanations for the contorted bedding of the Flaky Dolomite Bed include slumping, storm generated traction currents (rip-up), or deposition in desiccation-flooding-dessication cycles. Alternatives similar to the stromatolitic and algal beds are possible for the red, gray, and green, low organic shales of the Jupiter, Carbon Canyon, and Duppa Members which also indicate deposition under oxygenated conditions. The Carbon Butte sandstones were deposited under shallow marine tidal influences (Wiley, et al., 1998; Dehler, 1998; Dehler and Elrick, 1998; Dehler, et al., 2001). The lower Chuar Group was deposited under generally shallow aerobic depths (<50 m) and the organic-rich upper Awatubi and Walcott Members record a deepening episode to dysaerobic or anaerobic depths (>50 m) and the initiation of prolonged euxinic basin conditions, perhaps associated with Butte Fault movement if the contorted bedding and carbonate clasts in the basal Walcott Member Flaky Dolomite Bed are interpreted as slumping. Euxinic conditions were interrupted by up to eight periods of carbonate deposition.

If the Chuar Group was deposited in a shallow saline or hypersaline oxic lagoon or epeiric sea, carbonate deposition may represent periods of decreased water depth and/or sediment input. Low- and high-organic shale deposition may represent periods of increased water depth and/or sediment input. The black organic-rich shales could indicate deposition as soft fluid (soupy or watery) clay, lacking in mechanical strength, and having anoxic bottom sediments near the water-sediment interface.

Introduction

In November 1997, a stratigraphic section of the Awatubi and Walcott Members of the Kwagunt Formation, Chuar Group, located in the Sixtymile Canyon area of the eastern Grand Canyon, Arizona (Figures 1-3), was measured (Dehler, PhD, in prep.), described and sampled. The Chuar Group is Late Proterozoic in age. An ash at the top of the Walcott Member yields an U-Pb age of 742 Ma (Dehler, et al., 1999). Elston (1989, p. 97, 104) estimated an age of 850 million years for the base of the Kwagunt Formation and reported a Rb-Sr isotope date of 1,070 Ma ± 70 Ma for flows of the Cardenas Basalt. This study supplements that of Wiley et al. (1998) which sampled the entire Chuar Group in the Nankoweap Canyon and Carbon Canyon areas of the eastern Grand Canyon. The first goal of this study was to further characterize the petroleum source rock potential of the Awatubi and Walcott Members of the Kwagunt Formation, previously concluded to constitute the significant source rock potential of the Chuar Group (Wiley, et al., 1998). A total of 1480 ft (451 m) of section [653 ft (199 m) = Awatubi; 827 ft (252 m) = Walcott] was measured (Dehler, PhD, in prep.) and 30 samples were collected (21 samples from the Walcott Member, and 9 samples from the Awatubi Member).

About one half of each of the 30 samples were analyzed geochemically for source rock potential by Humble Geochemical Services Division of Humble, Texas as a subcontractor to Baseline Resolution, Inc. of Plano, Texas. These were all analyzed for total organic carbon (TOC) as a measure of organic richness and by Rock-Eval pyrolysis which included Tmax as a measure of thermal maturity. Tables 2 to 3 summarize the analytical results for the two members. The details of these analytical results are plotted stratigraphically on Plate 1 beside the measured section, and are included in Appendix 1 in tabular form. Field notes of the study are recorded in Appendix 2.

As with the previous study, the half portion of each of the samples not used for analysis have been deposited with the Arizona Geological Survey to provide a stratigraphically allocated reference collection for future study. Supplementing the Arizona Geological Survey's Chuar reference collection was a second goal of this study. A third goal was to integrate and synthesize Chuar Group source rock data from the Sixtymile Canyon section with that of the Nankoweap Canyon and Carbon Canyon sections (Wiley, et al., 1998). A fourth goal was to review the range of possible organic-rich depositional environments and their characteristics to identify the most likely depositional environments for the Chuar Group.

Previous and Ongoing Work

The reader is referred to Wiley et al. (1998) for: 1) a review of previous work, 2) a discussion of the evolution of a petroleum play concept, 3) reservoir and source rock evaluation guidelines, and 4) a review of the previous status of Grand Canyon Chuar Group source rock potential. Also see Plate 1 of this report for references to evaluation guidelines. The Sixtymile Canyon area has been studied previously by Ford and Breed (1973) in their measured section "H", the type section for the Sixtymile Formation.

Rauzi (1990) mapped the possible distribution of the Chuar Group in northern Arizona and southern Utah. Cook (1991) measured and described the Walcott Member in the Sixtymile Canyon area and provided detailed analysis of its source rock potential. Summaries of his measured thicknesses and his source rock TOC and Tmax data as compared to the present study are shown in Tables 1 and 2.

Dehler, et al., (1999), Karlstrom, et al. (2000), Dehler, et al., (2001), and Dehler (PhD, in prep.) measured and sampled the Chuar Group towards understanding the basin evolution and C-isotope stratigraphy.

Methods

Field

The mapping used in this report was again essentially that of Ford and Breed (1973), slightly modified by Ford (1990) and Huntoon et al. (1996). Due to the remoteness of the Sixtymile Canyon area,

the area was reached by helicopter transport. The section was measured and sampled by a three-person field party comprised of authors Ghazi and Dehler, and Andrew H. Knoll of Harvard University, Cambridge, Massachusetts. Localities were plotted on the U.S. Geological Survey Cape Solitude 7.5' Topographic Quadrangle, Coconino County, Arizona (Figure 3). Outcroping strata were sampled approximately every 1.5 to 3 m (4.5 to 9 ft).

Analysis

The stratigraphic column in Plate 1 was modified by Wiley from more detailed measured sections by Dehler (PhD, in prep.) in order to conform with the format and scale of the previous companion study of Wiley et al. (1998). Plate 1, however, shows several additional columns as compared to Plates 1 and 2 of Wiley et al. (1998). In this closer look at the Awatubi and Walcott Members: 1) plots of hydrogen index (H.I.) and S2/S3 are included as hydrocarbon type indicators, 2) a plot of genetic potential (S1 + S2) is added as an additional source richness rating, and 3) productivity index or transformation ratio [S1/(S1 +S2)] is included as an indication of maturity, product, and migration.

Stratigraphy

Table 1 compares the measured thicknesses of the Awatubi and Walcott Members in the Sixtymile Canyon section, as measured in the present study, with those of previous workers in the Sixtymile Canyon area, and also with the Nankoweap Canyon, and Carbon Canyon areas of Wiley, et al. (1998). In the Sixtymile Canyon section, the Walcott Member measured 827 ft thick and the Awatubi Member measured 653 ft thick. In the Nankoweap Butte section, Ford and Breed (1973) measured the Walcott Member at 838 ft thick and the Awatubi Member at 1128 ft thick. Cook (1991) measured the Walcott Member at 763 ft thick in the Sixtymile Canyon section. Ford and Breed (1973) designated their section "H" from the Sixtymile Canyon area as the type section for the Sixty Mile Formation. Plate 1 shows the Sixtymile Canyon columnar section lithology and sampling localities for the Walcott and Awatubi Members. Further lithologic description is given in the field notes of Appendix 2. The location of the measured section and sample localities are shown on Figure 2, a geologic map after Ford and Breed (1973), and Figure 3, the Cape Solitude 7.5' Topographic Quadrangle Map.

Source Rock Potential by Stratigraphic Unit

Appendix 1, Analytical Data, provides the source rock analysis for each of the nine Awatubi Member samples and the twenty-one Walcott Member samples. Table 2 summarizes the range and average of the organic richness (TOC) and organic maturity (Tmax) for each member and compares these averages to those of Cook (1991) for the Walcott Member. Table 3 summarizes the source rock potential of each member on the basis of hydrocarbon type (hydrogen index and S2/S3), source richness (TOC and genetic potential), source maturity (Tmax and productivity index or transformation ratio), and whether it is indigenous, mixed, or migrated (productivity index or transformation ratio). These categories are also plotted stratigraphically on Plate 1. Interpretations are based on point-to-point curve graphing for all categories except Tmax, which is based on an eyeball best-fit straight line through the points. The x axis, or abcissa, of each source rock category is subdivided by vertically defined cutoffs or interpretive guidelines. See Plate 1 for references to the vertical guidelines or "cutoffs" for each category. All interpretations are accurate only within the approximately 3 meters stratigraphic sampling increment.

Awatubi Member of Kwagunt Formation

The Awatubi Member is 653 ft thick in the Sixtymile Canyon section. Nine samples were collected. The lowest was from 197 ft above the base and the highest was from 110 ft below the top, so for

purposes of point-to-point graphing, the the upper 456 ft of section was sampled (because the first point was 197 ft above the base). Organic richness as measured by total organic carbon in percent (% TOC) ranged from 0.39% (poor) to 1.87% (good) and averaged 1.11% (good). Organic richness as measured by genetic potential, by comparison, is not as high. Genetic potential ranged from 0.04 (non-oil source, some gas potential) to 0.42 (moderate source rock), and averaged 0.14 (non-oil source, some gas potential).

Stratigraphically, in terms of total organic carbon content the 456 ft of sampled Awatubi section contained 101 ft of section rated as poor, 355 ft rated as fair or better (17 ft in fair category *stricto senso* (*s.s.*)), 338 ft rated as good or better (238 ft in good category *s.s.*), and 100 ft rated as very good. In the Sixtymile Canyon section, the upper 345 ft of the Awatubi Member was fair or better based on TOC. By comparison, in the Nankoweap Canyon section the upper 195 ft mostly rated as fair or better. In the Carbon Canyon section, the upper 390 ft of the Awatubi Member mostly had TOC ratings of fair or better. As was previously concluded by Wiley, et al. (1998), it is this upper part of the Awatubi Member plus the Walcott Member which constitutes the significant Chuar Group source rock.

In terms of genetic potential, the 456 ft of sampled Awatubi section contained 446 ft of section rated as non-oil source, some gas potential, and 10 ft of moderate source rock potential.

Source maturity of the nine samples as measured by Tmax ranged from 301°C (immature) to 436°C (early oil), and averaged 389°C (immature). Three samples had Tmax values below 380°C and if these are excluded, the remaining six samples ranged from 416°C (immature) to 436°C (early oil), and averaged 428°C (immature). The eyeball best fit straight line through all thirty Tmax data points of the Sixtymile Canyon section, is entirely within the early oil window for the entire 653 ft of the Awatubi Member section. The top of the Awatubi is projected at 437°C (early oil window) and the base of the Awatubi is projected at 440°C (early oil window). It should be noted that for all nine Awatubi samples Tmax data was not reliable due to low kerogen S2 values. For the upper 345 ft of organically rich Awatubi (TOC = fair or better), the average Tmax of all 7 samples from this interval is 379°C. (immature). For the same 345 ft of section, the average Tmax of the four samples with a Tmax of greater than 380°C is 429°C.(immature).

Productivity index or transformation ratio [S1/(S1 + S2)] values ranged from 0.11 (early oil window) to 0.60 [late oil and postmature (gas windows)], and averaged 0.37 (peak oil window). For this measure of maturity, the 456 ft of sampled Awatubi section contained 22 ft rated as immature; 434 ft rated as early oil or higher maturity (97 ft rated as early oil *s.s.*); 337 ft rated in the early oil-peak oil gap or higher (119 ft in the early oil-peak oil gap *s.s*); 218 ft rated as peak oil or higher (36 ft rated peak oil *s.s.*); and 182 ft rated late oil and postmature (gas windows).

Using productivity index (transformation ratio) as a measure of indigenous, mixed or migrated origin, the 456 ft of sampled Awatubi section included 182 ft ranked as migrated; 22 ft ranked as mixed (204 ft mixed or migrated) and 252 ft ranked as indigenous.

Using the hydrogen index as an indication of hydrocarbon type the 456 ft of sampled Awatubi section included 419 ft of basal section with no hydrocarbon potential and the upper 37 ft of section which ranked as gas prone.

Similarly, the S2/S3 ratio, as a hydrocarbon or kerogen type indicator, ranks 356 ft of the 456 ft sampled as having no hydrocarbon potential and 100 ft as gas prone.

All nine Awatubi samples plot in the gas prone portion of the crossplot of reactive carbon index [RCI = 10(S1 + S2)/TOC] vs. productivity index (Figure 4).

On the modified van Krevelen diagram (Figure 5) the Awatubi samples cluster in the lower left corner of the diagram. This plot is not definitive as to kerogen type, apparently due to a fairly high maturity, [probably at least greater than 0.5% Ro by comparison to Figures 5.1A and 5.2 of Peters and Cassa (1994, p. 96 and 97)].

Walcott Member of the Kwagunt Formation

The Walcott Member is 827 ft thick in Sixtymile Canyon. Twenty-one samples were collected.

Since the highest sample was taken 21 ft below the top of the member, for purposes of point-to-point graphing 814 ft of section were sampled. Organic richness as measured by total organic carbon in percent (% TOC) ranged from 0.96% (fair) to 9.39% (excellent), and averaged 2.83% (very good). Again, as for the Awatubi Member, organic richness as measured by genetic potential is lower. Genetic potential (S1 + S2) ranged from 0.17 (non-oil source, some gas potential) to 27.01 (excellent source rock), and averaged 3.75 (moderate source rock).

In terms of total organic carbon content, the 814 ft of sampled Walcott section contained 814 ft (i.e. the entire Walcott section) rated as fair or higher (6 ft in fair category s.s.); 808 ft rated as good or higher (388 ft in good category s.s.); 420 ft rated very good or higher (303 ft rated very good s.s.), and 117 ft of section in the excellent category.

In terms of genetic potential, the 814 ft of sampled Walcott section contained 325 ft rated as non-oil source, some gas potential; 489 ft rated as moderate or higher (397 ft rated in the moderate category s.s.); 92 ft rated as good or higher (40 ft rated in the good category s.s.); and 52 ft rated as excellent.

Source maturity of the 21 Walcott samples as measured by Tmax ranged from 427°C. (immature) to 447°C. (peak oil), and averaged 435°C. (immature/early oil boundary). This is somewhat lower than the range [436°C. (early oil) to 451°C. (late oil)] and average [443°C. (early oil)] reported for the Sixtymile Canyon Walcott section by Cook (1991). Six of the 21 Walcott samples had Tmax data considered unreliable due to low kerogen S2 values (see Appendix 1). The eyeball best fit straight line through all 30 Tmax data points of the Sixtymile section (the Tmax gradient), places the upper 420 ft of the Walcott Member in the immature window, and the basal 407 ft of the Walcott Member in the early oil window. This Tmax gradient ranges from 432°C. (immature) at the top of the Walcott Member to 437°C. (early oil) at the base of the Walcott Member.

Productivity index or transformation ratio [S1/(S1 + S2)] values ranged from 0.05 (immature) to 0.53 [late oil and postmature (gas windows)]; and averaged 0.16 (early oil/peak oil gap). For this measure of maturity, the 814 ft of sampled Walcott section contained 358 ft rated as immature, 456 ft rated as early oil or higher maturity (139 ft rated early oil s.s.); 317 ft early oil-peak oil gap or higher maturity (205 ft rated early oil-peak oil gap s.s.); 112 ft rated peak oil or higher maturity (92 ft rated peak oil s.s.); and 20 ft rated late oil and postmature, i.e. gas windows.

Using productivity index (transformation ratio) as a measure of indigenous, mixed, or migrated origin, the 814 ft of sampled Walcott section included 20 ft ranked as migrated, 22 ft ranked as mixed (42 ft mixed or migrated), and 772 ft ranked as indigenous.

Using hydrogen index as indicative of hydrocarbon type, the 814 ft of sampled Walcott section included 224 ft with no hydrocarbon potential (occurring primarily in the basal 300 ft of the Walcott), 555 ft ranked as gas prone, and 35 ft ranked as mixed oil and gas prone.

Similarly the S2/S3 ratio, as a hydrocarbon or kerogen type indicator, ranks 119 ft of the 814 ft of Walcott sampled as having no hydrocarbon potential (again occurring primarily in the basal 300 ft of the Walcott); 321 ft as gas prone; 282 ft as mixed oil and gas prone, and 92 ft as oil prone.

On the crossplot of reactive carbon index [RCI = 10 (S1 + S2)/TOC] vs. productivity index (Figure 4), all but 3 of the 21 Walcott samples plot in the gas prone area. Two Walcott samples plot in the uncertain area, and 1 sample plotted in the oil prone area.

On the modified van Krevelen diagram (Figure 5) approximately 12 (57%) of the 21 Walcott samples plot in the Type I (alginite) and II (exinite) kerogen region (terminology of Nuccio and Fouch, 1992, p.71). Peters and Cassa (1994, p. 97) combine kerogen Types I and II in the liptinite or exinite maceral group. As was the case for the Awatubi Member, clustering of the Walcott Member data points toward the lower left corner of the modified van Krevelen diagram suggests a fairly high maturity, probably at least greater than 0.5% Ro. Similar conclusions were reached for the Walcott Member by Summons et al. (1988) who determined kerogen from a bituminous and argillaceous dolomite sample of the Walcott Member was a Type I-II kerogen of the mature region of the van Krevelen diagram. Cook (1991) determined Walcott kerogen was Type II. Kerogen Types I and II are generally oil prone (Nuccio and Fouch, 1992, p. 71; Peters and Cassa, 1994, p. 96).

Discussion: Unusual Aspects of the Sixtymile Canyon Geochemical Data

Areal Thickness Variations of Organically Rich Awatubi Member

One of the four puzzling results reported by Wiley, et al. (1998) for the the Chuar Group of Carbon Canyon and Nankoweap Canyon is the lateral variation in the thickness of the organically rich source rock (fair or better) of the Awatubi Member in the two sections (Figure 6). In both sections a distinct increase in organic richness occurs in the uppermost part of the Awatubi Member, but in the Nankoweap Canyon section this occurred in the upper 195 ft of the Awatubi Member and in the Carbon Canyon section it occurred in the upper 390 ft of the Awatubi Member. In the Sixtymile Canyon section, this increase in the organic richness (TOC = fair or higher) of the Awatubi section occurs in the upper 345 ft of the member, a thickness which is intermediate between the other two sections.

Vertical Maturity Anomaly: Average Maturity of the Walcott Member Exceeding that of the Underlying Awatubi Member

A second puzzling result reported by Wiley, et al. (1998) for the Chuar Group of Nankoweap Canyon is that the the average Tmax maturity for the the Walcott Member (433°C.) was higher than that of the underlying Awatubi Member [428°C. for samples above a Tmax of 390°C. in the upper 195 ft (rich Awatubi); 410°C. for all Tmax samples in the upper 195 ft (rich Awatubi)]. In the Carbon Canyon section, the Walcott Member was estimated at only 50 ft thick and was not sampled. In the Carbon Canyon section, the upper 390 ft of the organically rich Awatubi Member had an average Tmax of 427°C. for samples above a Tmax 390°C. and 412°C. for all samples. Maturity is a function of time and temperature (Hood, et al., 1975; Waples, 1980; Dow and O'Connor, 1982, p. 140-141; van Gijzel, 1982, p. 161-163). Temperature increases with depth (Schlumberger, 1979, p. 2) and deeper strata are older and buried longer than shallower strata by the law of superposition (Steno, 1669), unless structurally deformed (overthrusted). The result of these factors is that maturity normally increases with depth.

Like the Nankoweap Canyon section, the average Tmax maturity of the Sixtymile Canyon section Walcott Member (435°C. = immature/early oil boundary) is greater than the average Tmax maturity of the underlying organically rich upper 345 ft of the Awatubi Member (429°C. = immature for the four Awatubi samples with Tmax greater than 380°C., or 379°C. = immature for all 7 organically rich Awatubi samples). This higher Awatubi average Tmax maturity than the Walcott average maturity is probably a data artifact owing to Awatubi Tmax values being unreliable due to low kerogen S2 values. See the discussion under "Discrepancies between Organic Maturity Indicators, Awatubi Member and Walcott Member" concerning the reliability of the Tmax values for each member.

Tmax Maturity Windows Dipping to the Southeast

A third puzzling result reported by Wiley, et al. (1998) for the Chuar Group of Carbon and Nankoweap Canyons is that stratal units of the Nankoweap Canyon section were more mature than equivalent units of the Carbon Canyon section, on the basis of Tmax as a measure of organic maturity (Figure 7). Tmax maturity windows, therefore, appeared to be dipping to the southeast.

Figure 7 is a southeast-northwest stratigraphic cross section through the Carbon Canyon, the Sixtymile Canyon, and the Nankoweap Canyon sections with the Tmax maturity windows superimposed. This shows that the Tmax maturity of the upper half of the Walcott Member is immature and the lower half is in the early oil window, which is similar to the Nankoweap Canyon Walcott Member. The Sixymile Canyon Awatubi Member, however, is entirely in the early oil window. By comparison, the Nankoweap Canyon section Awatubi Member is in the peak oil and late oil windows, i.e. a higher maturity than the Sixtymile Canyon Awatubi Member. The Carbon Canyon section Awatubi Member Tmax maturity is in

the immature and early oil windows, i.e. a lower maturity than the Sixtymile Canyon section Awatubi Member. These findings are consistent with the previously reported pattern of lower maturities to the southeast (Carbon Canyon area) and higher maturities to the northwest (Nankoweap Canyon area) in equivalent strata. That the Sixtymile Canyon section is consistent with the previously reported pattern of maturity windows dipping to the southeast, suggests that the pattern is real and not a data artifact. Two possible explanations were offered by Wiley, et al. (1998, p. 53-54). The first possibility is that the area to the northwest experienced longer and/or deeper burial during any of three major periods of tectonism: 1) the Late Precambrian Grand Canyon disturbance, or 2) the late Mesozoic to early Tertiary Laramide orogeny, or 3) Miocene to Pliocene Basin and Range extension (Elston and McKee, 1982; Elston, 1989, p.96-98; Huntoon, 1989; Ford, 1990, p.63; Middleton and Elliot, 1990, p. 86; Sears, 1990, p. 78-82) The two major periods of movement on the Butte Fault occurred during Grand Canyon disturbance extension which created half grabens, and during Laramide-age compression which created the East Kaibab Monocline (Sears, 1990, p. 81-82; Billingsley and Elston, 1989, p. 15-16, fig. 1.17). Timmons, et al. (2001) document movement within the Butte fault system throughout Chuar Group deposition. A second possible explanation is that the area to the northwest experienced higher heat flow during any of the 3 periods of volcanism or plutonism which occurred during the Cretaceous-Paleocene, Miocene, and Pliocene-Quaternary (Huntoon, 1989; Huntoon, 1990).

Discrepancies Between Organic Maturity Indicators

A fourth puzzling result reported by Wiley, et al. (1998) for the Chuar Group of Carbon and Nankoweap Canyons is that for 71% of the samples, maturity as determined from organic petrologic indicators was higher than maturity as determined from Tmax. Organic petrologic indicators included the following six measures: 1) vitrinite reflectance equivalent (VRE) from bitumen Ro, 2) measured mean bitumen reflectance, 3), measured mean vitrinite-like reflectance, 4) thermal alteration index (TAI) using maturity zones of DGSI, 5) TAI using maturity zones of Peters and Cassa (1994) and Waples (1980), and 6) extinction of sporinite and alginite fluorescence indicating an Ro of 1.20 or greater. In the Nankoweap Canyon section Tmax maturity of the Walcott Member is immature and early oil window, and the Tmax maturity of the organically rich, upper 195 ft of the Awatubi Member is peak oil window. In the Carbon Canyon section the Walcott Member and upper 390 ft of organically rich (fair or higher) Awatubi Member are both immature based on Tmax. Organic petrologic based maturity estimates for the Nankoweap Canyon section Walcott and organically rich Awatubi Members are both peak oil to condensate/wet gas windows. Organic petrologic based maturity estimates for the Carbon Canyon section organically rich Awatubi Member are immature to condensate/wet gas windows.

While the present study of the Sixtymile Canyon section has not included organic petrology, the same sort of discrepancy between various maturity indicators has been observed, as discussed below.

Awatubi Member

In the Sixtymile Canyon section, maturity of the Awatubi Member, based on Tmax is lower than that based on productivity index (transformation ratio). Based on productivity index 434 ft (95%) of the 456 ft of the sampled Awatubi section is early oil or higher maturity and 182 ft (40%) of the 456 ft of the sampled Awatubi section ranges up to late oil and postmature (gas windows). The average productivity index for the Awatubi samples was in the peak oil window.

The Awatubi Member maturity based on Tmax, however, was much lower, with an average value in the immature window. The Awatubi Member Tmax gradient was entirely within the early oil window.

The Tmax values for all the Awatubi Member samples are really unreliable, so they should not be considered for assessing the thermal maturity of these samples. The productivity index values also have relatively large errors due to the small S1 and S2 values, but they may be a more reliable indicator of the thermal maturity of these samples. Based on the following discussion of the maturity of the Walcott

Member, the Awatubi Member is likely to be in the peak to late oil generation window.

<u>Walcott Member</u>

In the Sixtymile Canyon section, the two measures of maturity, Tmax and productivity index, are somewhat more consistent for the Walcott Member. Based on Tmax, the average value of the Walcott Member samples is at the immature/early oil boundary. The Tmax gradient of the upper 420 ft (51%) of the 827 ft total Walcott section is in the immature window, and the Tmax gradient of the lower 407 ft (49%) of the 827 ft total Walcott section is in the early oil window.

Based on productivity index, the average value of the Walcott Member samples is in the early oil-peak oil gap. Based on productivity index, 358 ft (44%) of the 814 ft of the sampled Walcott section is immature and 456 ft (56%) of the 814 ft of sampled Walcott section is early oil or higher. Three hundred seventeen feet (39%) of the sampled Walcott section rated early oil-peak oil gap or higher; 112 ft (14%) rated peak oil or higher, and 20 ft (2%) rated late oil and postmature (gas) windows.

For the Walcott Member the two measures rate much of the upper part of the member as immature. For Tmax however, a maximum maturity of peak oil is seen in 1 sample and the basal section Tmax maturity gradient only reaches early oil. By contrast, on the basis of productivity index, 14% of the section is peak oil or higher.

Most of the Tmax data for the Walcott Member samples are reliable, but do not correlate well with their stratigraphic positions. In fact, these Tmax values correlate strongly with the TOC content of the samples, with higher TOC samples having higher Tmax values. This is also the case in the Walcott Member samples from the Nankoweap Canyon area. This phenomenon is occasionally observed on high-TOC samples. Because the S2 peak is very large, and temperature continually rises during the release of S2 material, the instrument will register a higher Tmax because it takes a little longer to reach the apex of the S2 peak. But this "delay" effect seems to be enhanced in this suite of samples. Perhaps S2 material is a little more difficult to release in these very old rocks.

In general we conclude that the Walcott Member samples range from immature (Tmax lower than 435 degrees C.) to early mature (Tmax between 435 and 445 degrees C.) to the onset of peak oil generation (Tmax higher than 445 degrees C.) This is also consistent, in general, with the productivity index values which vary in the group for which Tmax is reliable (see Tmax values in Appendix 1 which are not asterisked) from 0.5 to 0.15. One sample with an unusually high productivity index value (S10-60-25) may be due to contamination. Samples in the lower part of the Walcott Member (S10-60-18 to S10-60-10) have higher productivity index values due to the very small S1 and S2 values and therefore larger analytical error.

Discrepancies Between Organic Richness Indicators

<u>Awatubi Member</u>

Using genetic potential to rate source richness only the uppermost 10 ft (2%) of the 456 ft sampled had moderate (oil) source rock potential, with the remaining 98% of the sampled Awatubi section rated as non-oil source/some gas potential. Hydrogen index indicated that only the upper 37 ft (8%) was gas prone with the remaining basal section section having no hydrocarbon generation potential. The S2/S3 ratio indicated only 100 ft (22%) was gas prone, with the remaining section having no hydrocarbon potential.

This contrasts with organic richness rated by total organic carbon, whereby 355 ft (78%) of the 456 ft of sampled Awatubi section rated as fair or better in richness, i.e. potential source rock. Three hundred thirty eight feet (74%) rated good or better, and 100 ft (22%) rated very good.

For the Awatubi Member there is an extreme in the various estimates of organic richness from only 2% of the section having moderate oil potential to 78% of the section with fair or better richness, i.e. potential source rock. Even if the discrepancy is in part based on the fact that the Awatubi Member appears

to be gas prone (RCI vs. PI plot, fig. 5), the hydrogen index predicts only 8% of the section has gas potential and the S2/S3 ratio predicts only 22% of the section has gas potential with both indices indicating no hydrocarbon potential for the rest of the Awatubi section.

Walcott Member

Again for the Walcott Member a contrast is seen in the amount of section rated as potential source rock by different indices. On the basis of total organic carbon (TOC) the entire 814 ft (100%) of the sampled Walcott Member was fair or higher, ie. potential source rock; however on the basis of genetic potential only 60% (489 ft of the 814 ft sampled) of the Walcott section rated as moderate or higher (oil) potential. The Walcott Member, too, appears to be gas prone based on the RCI vs. PI plot (fig. 5). Based on hydrogen index 28% (224 ft of 814 ft sampled) of the Walcott Member sampled has no hydrocarbon potential and based on S2/S3 ratio 15% (119 ft of 814 ft sampled) of the Walcott sampled has no hydrocarbon potential.

Discrepancies In Hydrocarbon/Kerogen Type

The various geochemical indices also show discrepancies in the predicted hydrocarbon/kerogen type. Most samples of the Awatubi and Walcott Members plot in the gas prone region of the crossplot of reactive carbon index (RCI) vs. productivity index (PI) (Figure 4). On the other hand, 57% (12/21 samples) of the Walcott Member samples plot in the Type I and II region of the Modified van Krevelen diagram (Figure 5). Type I and II kerogen are oil prone.

For the Awatubi Member, hydrogen index rates the upper 37 ft (8%) as gas prone and the remaining section as having no hydrocarbon potential. The S2/S3 ratio rates 100 ft (22%) as gas prone, with the remaining section as having no hydrocarbon potential.

For the Walcott Member, hydrogen index rates 28% (224/814 ft) of the sampled section as having no hydrocarbon potential, 68% (555/814 ft) as being gas prone, and 4% (35/814 ft) as being mixed oil and gas prone. The S2/S3 ratio rates 15% (119/814 ft) of the sampled Walcott Member as having no hydrocarbon potential, 39% (321/814 ft) as being gas prone, 35% (282/814 ft) as being mixed gas and oil prone, and 11% (92/814 ft) as being oil prone.

Synthesis and Integration with Nankoweap Canyon and Carbon Canyon Source Rock Data

Organic Richness

Figure 6 is a southeast-northwest stratigraphic cross section of the Awatubi and Walcott Members through the Carbon Canyon, Sixtymile Canyon, and Nankoweap Canyon sections with total organic carbon (TOC) source richness superimposed. The top of the Carbon Butte Member is used as a (flattened) datum and one possible correlation of organic facies is shown. The Awatubi Member shows a thickening of the good and very good facies in the Sixtymile Canyon section relative to the other two sections. The Walcott Member was thin (estimated at 50 ft thick) in the Carbon Canyon section due to erosional truncation by the Great Unconformity and was not sampled. The Walcott Member in the Sixtymile Canyon section has a thicker very good facies in the middle of the section and a thick good facies in the basal section. It also has three excellent facies as compared to two in the Nankoweap Canyon section. The middle of the Walcott Member of the Nankoweap Canyon section has a poor facies which was not seen in the Sixtymile Canyon section. Figure 6 thus illustrates that of the three sections, the thickest organically-rich facies in the Awatubi Member is in the Sixtymile Canyon section and that a thicker organically-rich facies in the Walcott Member occurs in the Sixtymile Canyon section than in the Nankoweap Canyon section (with the Carbon Canyon section being thin and not sampled).

16

Organic Maturity

Figure 7 is a southeast-northwest stratigraphic cross section of the entire Chuar Group through the Carbon Canyon, Sixtymile Canyon, and Nankoweap Canyon sections with Tmax source maturity windows superimposed. This figure illustrates the apparent dip of the Tmax maturity windows to the southeast, suggesting 1) longer and/or deeper burial to the northwest, or 2) higher heat flow to the northwest due to volcanism and/or plutonism. Tmax variation in the southwest-northeast direction, allowing determination of true dip of Tmax maturity windows remains to be established.

Kerogen/Hydrocarbon Type

The Awatubi Member is most likely a gas prone source based on the crossplot of reactive carbon index vs. productivity index (Figure 4), hydrogen index, and S2/S3 ratio; however between 22% (based on TOC) and 98% (based on generative potential) of the section has poor source rock potential.

The Walcott Member contains Type I and II kerogen based on the Modified van Krevelen diagram (Figure 5) which are oil prone, however the plot of reactive carbon index vs. productivity index (Figure 4) indicates that all but three samples plot in the gas prone region. Hydrogen index indicates that 68% of the section is gas prone and that 4% is mixed oil and gas prone (the balance having no hydrocarbon potential). The S2/S3 ratio indicates a greater mix of both oil and gas potential, i.e. 39% gas prone, 35% mixed oil and gas prone, and 11% oil prone (the balance having no hydrocarbon potential).

Migration

For the Awatubi Member, hydrocarbons in 40% of the section had a migrated origin, hydrocarbons in 5% of the section had a mixed origin, and hydrocarbons in 55% of the section had an indigenous origin, based on productivity index.

For the Walcott Member, hydrocarbons in the bulk of the section (95%) had an indigenous origin, with hydrocarbons in only 2% of the section indicating a migrated origin, and hydrocarbons in in only 3% of the section indicating a mixed origin, based on productivity index.

Depositional Environment

Key Evidence

Wiley, et al. (1998, p. 45, 49) presented evidence from stable carbon isotope ratios, using a plot of del C13 Aromatic vs. del C13 Saturate as developed by Sofer (1984), that supported a marine origin for shales of the Tanner, Carbon Canyon, Awatubi, and Walcott Members. Sedimentological evidence was also presented for a tidal, and therefore shallow marine, origin for the Carbon Butte Member (Wiley, et al., 1998, p. 44, 55). Both the upper Chuar Group (Cook, 1991) and the entire Chuar Group (Dehler, et al., 2001) have been interpreted as marine deposits. Cook (1991) based his interpretation on organic geochemistry and sedimentology. Dehler, et al. (2001) based their interpretations on sedimentology, physical stratigraphy, and carbon isotope stratigraphy.

A marine origin for these members is also supported by their microfossils as reported by Bloeser, et al. (1977), Vidal and Knoll (1983), Vidal and Ford (1985), and Vidal (1986), and Porter and Knoll (2000). These authors reported two biofacies. The first was a benthonic facies consisting of algal filaments and small unicells found primarily in the cherty carbonate lithofacies, i.e. the stromatolitic cyanobacterial mats. This facies was interpreted to represent a nearshore, shallow water depositional environment. The second biofacies was an open water, cosmopolitan eukaryotic planktonic biofacies including chitinozoans [which have been reinterpreted as testate amoebae (Porter and Knoll, 2000)], Chuaria, and other acritarchs occuring primarily in the clastic or shale lithofacies, especially the Walcott Member. Similar planktonic

assemblages occur in the Late Proterozoic (Late "Riphean" and Vendian, ca. 800-700 Ma) sequences in the southern Urals of the former U.S.S.R., the East European Platform, Scandinavia, Svalbard, and Greenland (Vidal and Knoll, 1983, p. 270; Vidal and Ford, 1985, p. 349; Vidal, 1986, p. 420). This cosmopolitan distribution implies a planktonic marine origin. The very high organic productivity during deposition of the Kwagunt shales is demonstrated by Bloeser, et al.'s (1977, p. 677) estimate of 10,000 vase-shaped microfossils (chitinozoans) per cubic centimeter of rock.

Two authors have cited evidence of hypersaline conditions during deposition of the Chuar Group. Summons et al. (1988, p. 2626, 2630, and 2633-2635) reported evidence for deposition in a hypersaline environment for samples from 5 to 6 m above the base of the Walcott Member. This included traces of gypsum, quartz and calcite pseudomorphs after gypsum or anhydrite, and solution collapse structures together with dolomite. Their biomarker distributions and heavy carbon isotope signatures also support, in part, the evidence for deposition under hypersaline conditions. The heavy carbon isotope signatures (high $^{13}C/^{12}C$ ratio), however, can also be due to high productivity or high burial rates. Because the dolomites are altered, the heavy carbon isotope signatures may not be primary values. Ford and Breed (1973) cited evidence of hypersaline conditions during deposition of parts of the Jupiter, Carbon Canyon, and Awatubi Members. One bed of the basal stromatolitic limestone of the Jupiter Member contains carbonate casts of gypsum crystals, and the upper Jupiter Member shales contain occassional [rare (Dehler, PhD, in prep.)] salt pseudomorphs (Ford and Breed, 1973, p. 1247, 1248). Salt pseudomorphs are not uncommon [are present (Dehler, Ph.D., in prep.)] in the limestone beds of the Carbon Canyon Member, and some siltstone beds of the Awatubi Member carry salt pseudomorphs (Ford and Breed, 1973, p. 1249, 1251).

Ford and Breed (1973) also found evidence of emergence and desiccation in parts of the Tanner, Jupiter, Carbon Canyon, Carbon Butte, and Awatubi Members. The upper Tanner Member shales bear ripple marks and occassional mud cracks (p. 1247). The upper Jupiter Member shales contain mud cracks on top of almost every surface and rain prints (p. 1248). Dehler's ongoing work indicates the upper Jupiter Member "rain prints" are actually intraclast impressions. The sandstone and limestone cyclical beds of the Carbon Canyon Member are usually mud cracked and ripple marked on bedding plane exposures (p. 1249). In the Carbon Butte Member mud cracks and ripple marks are frequent and both features are usually present in the Awatubi Member siltstone beds (p. 1250, 1251).

Ford and Breed (1973) reported stromatolites at the base of the Jupiter Member and near the top of the Carbon Canyon Member of the Galeros Formation, and reported biohermal stromatolites at the base of the Awatubi Member of the Kwagunt Formation. Ford and Breed assigned these members to an upper Riphean age.

Ford and Breed (1973, p. 1252 and fig. 1) found algae in various portions of the Walcott Member, including their basal "Flaky Dolomite", their pisolitic chert bed, and the lower bed of their double "Top Dolomite" ("dolomite couplet" of Cook, 1991). Wiley, et al. (1998) reported algal beds in the Tanner Member (p. 75, 82), Jupiter Member (p. 73), Carbon Canyon Member (p. 72, 81, 82), Duppa Member (p. 80), Carbon Butte Member (p. 71), Awatubi Member (p. 80), and the Walcott Member (p. 78).

Common dolomite in carbonate beds suggests restricted evaporitic conditions or supratidal sabkha conditions creating dolomitizing magnesium enriched brines, although other mechanisms of dolomitization, for example deep burial dolomitization, are possible. Dehler's ongoing work indicates that although the timing of dolomitization of Chuar carbonates is as yet uncertain, all Chuar carbonates are recrystallized. Ford and Breed (1973) reported massive coarsely crystalline dolomite in the basal Tanner Member (fig. 1), dolomitic limestone in the basal stromatolitic limestone of the Jupiter Member (p. 1247), dolomitized stromatolite columns in the 2 foot stromatolitic limestone of the Carbon Canyon Member (p. 1250), dolomitized limestone stromatolitic columns with a coarsely crystalline dolomite matrix in the basal Awatubi Member (p. 1251), and two dolomitic units in the Walcott Member (p. 1252, and fig. 1), i.e., a basal "Flaky Dolomite" and the double "Top Dolomite" ["dolomite couplet" of Cook (1991)]. The dolomite lithology is supported by grain densities reported for reservoir rocks by Wiley, et al. (1998). Schlumberger (1972, p. 46) cited average matrix densities (zero porosity rocks) of 2.65 gm/cc for quartz (sandstone), 2.71 gm/cc for calcium carbonate (limestone), 2.87 gm/cc for dolomite (dolostone), 2.96 gm/cc for

anhydrite, and 2.32 gm/cc for gypsum. Wiley, et al. (1998) reported grain densities for Chuar carbonate units as follows: Walcott = 2.85-2.87 gm/cc (dolomite); Awatubi = 2.84 gm/cc (dolomitic limestone); Carbon Butte = 2.74 gm/cc (dolomitic limestone); Carbon Canyon = 2.87 gm/cc (dolomite); Jupiter = 2.83-2.86 gm/cc (dolomite or dolomitic limestone); Tanner = 2.86-3.66 gm/cc (dolomite). Dehler (Ph.D., in prep.) reports all Chuar Group carbonates are dominantly dolomitic.

Wiley, et al. (1998, p. 69, 76, 78, 79) reported yellow (sulfur ?), elemental sulfur, sulfide, or sufurous matter or weathering, and yellow sulfur odor and stain, on bedding planes of the Tanner, Awatubi, and Walcott Members. The field notes of the present report document sulfur odor and possible sulfur powder on cleavage planes of the Walcott Member.

Modern Stromatolites

Stromatolites are finely laminated beds, mounds or columns composed of limestone and silica which are formed as successive generations of algal mats trap and bind successive layers of sediment grains and/or mineral precipitates on their gelatinous surface (McAlester, 1968, p. 13; Laporte, 1968, p. 20; Golubic, 1976a, p. 113). Structurally, algal mats form a cohesive fabric of intertwined filaments and/or gelatinous matter produced by both filamentous and coccoid microorganisms (Golubic, 1976a, p. 113). "Algal mats and Recent stromatolites are products of microbial communites composed of cyanophytes, eucaryotic algae, photosynthetic bacteria (thio-, rhodo-, athiorhodo-, and chlorobacteria), and various heterotrophic bacteria. Cyanophytes or blue-green algae are the most significant single group engaged in the formation of stromatolites" (Golubic, 1976b, p. 127).

Cyanophytes are a largely asexually reproducing group of procaryotes (lacking a nucleus) (Golubic, 1976b, p. 129; Fortey, 1998, p. 51, 60). The phylum Cyanophyta is divided into two classes: 1) Coccogonea, or coccoid, unicellular cyanophytes, and 2) Hormogoneae, or filamentous multicellular cyanophytes characterized by chains of cells called trichomes. Both classes produce extracellular gelatinous matter ("mucillage" when soft and amorphous, or "gel" when firm and cohesive) which may provide a cohesive matrix for colony formation (Golubic, 1976b, p. 129).

Golubic (1976a, p. 113-122) has described the taxonomic composition of stromatolite-building algal mats, their communal ecology, and their bathymetric and geographic distribution which is briefly summarized as follows. Within an algal mat, vertically stratified physical and chemical microgradients result in a biological stratification of the mat. Light penetrates the upper few millimeters of the mat establishing a euphotic zone, where organic matter is produced photosynthetically. Rates of photsynthesis vs. respiration produce a vertical gradient of CO_2, O_2, pH, Eh, and ionic composition of interstitial water along the light attenuation gradient. The upper aerobic photosynthetic layers are dominated by cyanophytes and subordinate eucaryotic algae and photosynthetic bacteria. The deeper layers contain progressively less, and finally no oxygen. Organic matter produced by the upper layers is decomposed in the deeper layers into inorganic compounds, both aerobically and anaerobically, by a diverse flora of bacterial and subordinate fungal decomposers. In order to avoid becoming buried and encrusted as the mat traps and binds sediments and precipitated minerals, the entire live algal mat community either grows or moves constantly upward (Golubic, 1976a, p. 116).

An example of a well differentiated stratified algal mat is that of the intertidal zone of the Persian Gulf, which consists of five layers, each about 1 mm thick (Golubic, 1976a, p. 114). The upper two layers, in the aerobic portion of the mat include a brown surface cyanophyte layer which shields the entire mat community from solar radiation with its brown extracellular sheath pigment scytonemine, and the second underlying blue-green cyanophyte layer which produces the mats maximal biomass. The third layer is transitional between the aerobic and anaerobic portion of the mat and consists of salmon-pink filamentous bacteria. The two basal layers occur in the anaerobic portion of the mat and include a purple-pink layer of purple sulphur bacteria, and the deepest black, iron sulphide-stained layer containing mainly non-photosynthetic anaerobic bacteria. Some cyanobacterial mats, such as pustular and domal mats, are not stratified and a single species completely dominates the microflora of the structure (Bauld, 1981b, p. 307,

310).

Geographically, the zonal sequence or distribution of algal mat types in the marine peritidal environments of the Persian Gulf and Shark Bay, Australia are arranged in zones roughly parallel to the coastline, with the zonal variation in predominant genera reflecting increased exposure to air and decreasing water depth (Golubic, 1976a, p. 124-126).

Living cyanobacteria (cyanophytes, or blue-green algae) are found wherever there is constant moisture (Attenborough, 1979, p. 22). Most modern cyanobacteria live in fresh water, but marine and terrestrial kinds occur (Mintz, 1972, p. 142). Several of the sheet-like benthonic colonial forms bind layers of calcium carbonate to form these layered mounds called stromatolites.

Extensive cyanobacterial mats (stromatolites), today, can only flourish where high salinity or excessive heat excludes herbivores and sediment feeders, such as cerithid gastropods or other mollusks, which feed upon them and keep them in check (Friedman and Sanders, 1978, p. 337, 340; Attenborough, 1979, p. 22; Fortey, 1998, p. 57). Cyanobacterial mats are common in marginal marine environments of tropical, semi-arid, and arid climates. They are cosmopolitan in geothermal springs, and are widespread in permanent and ephemeral saline lakes (Bauld, 1981a; 1981b). Warren (1986, p. 447) noted that cyanobacteria and algae thrive in salinities of 40 to 250‰, although some stromatolite-forming genera live in freshwater, such as those of Green Lake, New York (Eggleston and Dean, 1976, p. 479, 481). Mat-forming cyanobacteria in alkaline hot springs have an upper temperature limit of approximately 73 to 74°C (Bauld, 1981b, p. 310). In hypersaline environments, cyanobacteria and algae flourish when hypersaline, nutrient-rich waters are periodically freshened (Warren, 1986, p. 446). Today extensive cyanobacterial mats are found in intertidal environments of arid climatic areas like the Arabian (Persian) Gulf and Shark Bay, Australia, and in supratidal to shallow subtidal environments of humid climatic areas like the Bahamas (Gebelein, 1976, p. 381; Friedman and Sanders, 1978, p. 331, 337). In the Bahamas, algal mats have been observed to depths of 50 m, but grow most rapidly in depths of less than 10 m (Gebelein, 1976, p. 381).

Modern domal and columnar stromatolites are best known from the hypersaline (60,000 to 65,000 parts per million salinity) intertidal (0.3 to 0.5 m above and below mean sea level) and shallow subtidal zone (to at least 3.5 m below mean sea level) of Hamelin Pool (barred) Basin of Shark Bay, Western Australia (Playford and Cockbain, 1976, p. 389, 393; Friedman and Sanders, 1978, p. 330, 331, 340, 380, 525-526). Fortey (1998, p. 58) reported living stromatolites in the hot, inland Gulf of Baja California, Mexico, and at greater depths in the seas around the Bahamas. Dill, et al. (1986) reported giant (>2 m high) columnar stromatolites growing at shallow subtidal depths in 7-8 m of clear normal oceanic salinity (37-40‰) waters, located in current-swept channels between the Exuma Islands on the eastern Bahama Bank. There they grow by trapping ooid and pelletal carbonate sand and synsedimentary precipitation of carbonate cement within a field of migrating 1- to 2.5 m-high, rippled, ooid sand dunes (megaripples). Stromatolites of the Precambrian are believed to have occupied more widespread environments because grazing herbivores and sediment feeders had not yet evolved (Friedman and Sanders, 1978, p. 340; Fortey, 1998, p. 57). For example, Playford and Cockbain (1969) suggested that deepwater marine stromatolites of the Devonian of Western Australia lived at water depths of up to 150 ft (46 m).

In the hypersaline Great Salt Lake of Utah, with a salinity of 200 to 290‰ in this century and a percentage dissolved solids similar to seawater and hypersaline seawater, algal stromatolites are locally abundant (Halley, 1976, p. 435, 437; Friedman and Sanders, 1978, p. 247; Kirkland and Evans, 1981, p. 182). Calcareous bioherms, constructed by several species of blue-green algae, occur in shallow water (shoreline to 4 m) and have an aggregate extent of 260 sq. km (Halley, 1976, p. 435, 437; Kirkland and Evans, 1981, p. 182). Warren and Kendall (1985, p. 1016, 1017, fig. 4) reported both flat algal mats and domal stromatolites from salinas (hypersaline lakes) of South Australia. The flat, laminated algal mats fringe the salina shore. Basinward, domal, laminated stromatolites occur in waters from 0.6 to 1 m deep, with larger laterally linked forms more common in deeper waters. Eggleston and Dean (1976, p. 479, 481) reported extensive freshwater stromatolitic bioherms in Green Lake, New York from lake-surface level to a depth of 10 m. Bauld (1981a) surveyed the worldwide distribution of benthic cyanobacterial mats occurring

in saline lakes and coastal lagoons.

All cyanobacteria are photosynthetic, utilizing CO_2 and H_2O plus light energy to produce organic carbon, O_2 and H_2O. Some cyanobacteria also carry out facultative anoxygenic photosynthesis in which CO_2 and H_2S plus light energy produce organic carbon and S^o (sulfur) (Bauld, 1981b, p. 307). Cyanobacterial mat-produced organic carbon is a carbon and energy source for the production of H_2S by sulfate-reducing bacteria, and subsequent metal sulfide deposition including stratiform sulfide mineral deposits (Bauld, 1981b, p. 307, 308, 314). Such organic matter is also a possible reductant for abiological sulfate reduction to sulfides and is a possible source material for kerogen and subsequent hydrocarbon formation (Bauld, 1981b, p. 307, 308, 314).

Since stromatolites are photosynthetic (Attenborough, 1979, p. 22; Fortey, 1998, p. 52), the maximum penetration of light into the ocean provides a maximum water depth for the specific beds in which they occur. Deposition within the photic zone would also apply to the various algal beds reported by Ford and Breed (1973) and Wiley, et al. (1998) as given in the previous section, unless the algae were planktonic forms which settled into an aphotic zone depositional environment at death.

The Photic Zone

Authors differ on the depth of light penetration in the ocean. Hedgpeth (1957, p. 18-23, figs. 1 and 3) defined the boundary between the lighted photic zone and the lightless aphotic zone as ranging from 46 m in neritic areas to between 65 m and 140 m in oceanic areas (p. 18, fig. 1) or to 100 fathoms (p. 22, fig. 3). He also noted that the term disphotic zone could be used to denote a zone of the sea with intermediate illumination.

Friedman and Sanders (1978, p. 347-348) modified Hedgpeth's zones to include a photic zone from 0 to 80 m with sufficient light for plant growth, a disphotic zone from 80 to 600 m with transitional light levels, and an aphotic zone below 600 m which is lightless and in which plants cannot grow. Laporte (1968, p. 40) and Mintz (1972, p. 54, 57) define only a lighted zone (photic zone) from 0 to 200 m and a dark zone (aphotic zone) below 200 m. Ingle (1980, p. 167 and 177) put the base of the photic zone at approximately 150 m off present-day southern California. Pedersen and Calvert (1990, p. 455) state that photosynthesis is restricted the a relatively thin surface (euphotic) zone, which ranges from about 100-120 m in clear, open ocean waters to a few meters in turbid, nearshore regions. Huc (1980, p. 448-449) states that the euphotic zone ranges from 0 to 200 m in open oceans, to 50 m in coastal waters, and to only a few meters in lagoons. Phleger (1960, p. 9) states that most photosynthesis in the ocean occurs at water depths of less than approximately 50 m, although in tropical offshore areas it may occur as deep as a few hundred meters.

In summary, the maximum base of the photic zone and active photosynthesis is between 80 m (240 ft) and 200 m (600 ft).

Nearshore and Shelf Sands and Wave Base

In open marine clastic shelf systems, sand deposition characterizes the beach and nearshore, or shore zone, at depths of 0 to 20 m (0-66 ft), and can also be significant in inner shelf areas at depths of approximately 20 to 50 m (66-164 ft). Mud and turbidity current deposits characterize outer shelves (50-150 m; 164- 492 ft) with an adequate sediment supply. Reworked relict Pleistocene sediments characterize outer shelves lacking an adequate modern sediment supply. Brenner (1980) applied these same open marine, continental shelf depositional zones to the North American Cretaceous epicontinental seaway. Other authors (Hayes, 1967, p. 120; Heckel, 1972, p. 268; Freidman and Sanders, 1978, p. 361, 373-374) have suggested that because of their shallow depths, ancient epeiric seas lacked periodic lunar tides and were subject to sea waves, but not long-period swells (see Model 12).

Beach and Nearshore (Shore Zone) Sands (0-20 m; 0-66 ft) and Fairweather Wave Base

The beach and nearshore zone, or nearshore turbulent zone (Phleger, 1960, p. 15-17, 258-259; Ingle, 1980, p. 177, fig. 7), or shore zone (Galloway and Hobday, 1983, p. 115-124) has been divided into a supratidal backshore zone, an intertidal foreshore zone, and a subtidal shoreface zone by Harms, et al. (1975, p. 82, fig. 5-1) and Walker (1984, p. 148, fig. 9). The shoreface extends from mean low tide level to fairweather wave base (Galloway and Hobday, 1983, p. 115; Walker, 1984, p. 148, fig. 9). The breaker, surf, and swash zones shift from the upper shoreface during low tide to the foreshore zone during high tide (Harms, et al., 1975, p. 82). Wave action builds a series of bars, of which the outermost is called the longshore bar, that at the high swash line is called the beach bar, and those between are called ridges and runnels (Harms, et al., 1975, p. 82). Shore-zone sands are characteristically, but not invariably, well sorted, quartzose sand (Phleger, 1960, p. 15-16; Galloway and Hobday, 1983, p. 115).

Fairweather wave base defines the the base of the shore zone, with sand deposition in the high energy, wave-induced, continually turbulent water above this depth, and mud deposition in the low energy, quiet waters below this depth during fairweather conditions (Busch, 1974, p. 29-30; Galloway and Hobday, 1983, p. 115-124; Walker, 1984, p. 148). The land-ward asymmetry of fairweather wave-driven currents results in a net shoreward sediment transport and the deposition of sand in the shore zone (Brenner, 1980, p. 1225; Galloway and Hobday, 1996, p. 164). This net shoreward transport of sand in the shore zone has been called the littoral energy fence (Brenner, 1980, p. 1225; Galloway and Hobday, 1996, p. 161, 163, fig. 7.4, 164).

The depth of fairweather wave base varies, but normally lies in the 5 to 15 m range (Walker, 1984, p. 148). Ingle (1980, p. 167, fig. 3, p. 177, fig. 7) estimated effective fairweather wave base at approximately 10 to 15 m. Friedman and Sanders (1978, p. 484) stated that along most coasts, fairweather, everyday wave base is 10 m or less. Galloway and Hobday (1983, p. 1150) cited an average wave base depth of 35 ft (10 m). Lankford (1967, p. RL-5) stated that the beach to 50 ft (15.2 m) is continually turbulent, being within wave base on the West Coast of the U.S. Phleger (1960, p. 15, 258-259) gave a depth of 0-20 m for the nearshore turbulent zone and Brenner (1980, p. 1224-1225) defined a nearshore regime from 0 to approximately 20 m. Phleger (1960) and Brenner (1980) are followed here for depth ranges.

Wave effectiveness is inversely related to tidal range, with microtidal environments (0-2 m; 0-7 ft) being wave dominated, while macrotidal environments (4-6 m; 13-20 ft) are tide dominated. Increasing tidal range causes wave energy to be dissipated over a greater width of shore zone (Galloway and Hobday, 1983, p. 115).

Inner Shelf Sands (20-50 m; 66-164 ft) and Outer Shelf Muds (50-150 m; 164-492 ft)

Efforts to interpret present-day shelf sedimentation are complicated by a vast blanket of relict Pleistocene sand, which has covered much of the world's shelves and which was deposited during periods of lowered or transgressing sea level (Hayes, 1967, p. 111, 126-130). On modern coasts lacking an adequate sediment supply these relict sediments are exposed and possibly are being reworked (Harms, et al., 1975, p. 82; Walker, 1984, p. 141).

The inner shelf (toe of shoreface at about 20 m to 50 m; 66 to 164 ft) is dominated by tidal, wind-driven, storm-wave, and storm-current processes, while the outer shelf (50-150 m; 164-492 ft) is dominated by density stratification, nepheloid (bottom turbid layer) flow, geostrophic flow, and oceanic currents (Brenner, 1980, p. 1224-1225; Galloway and Hobday, 1983, p. 144, fig. 7-1; Galloway and Hobday, 1996, p. 162, fig. 7.1A,B). The depth ranges for the inner and outer shelves followed here are those suggested by Ingle (1980, p. 167, fig. 3, p. 177, fig. 7). Whereas sand is supplied and commonly moved across the entire shoreface zone by fairweather waves, sand is supplied to the offshore shelf by infrequent storm events which erode beaches and move sediment seaward to the shoreface and shelf (Harms, 1975, p. 82; Galloway and Hobday, 1983, p. 145; Galloway and Hobday, 1996, p. 164). The inner shelf is a zone

of seaward gravity-driven, advective storm transport. Of the various storm processes, probably the most effective mechanism for transporting sand from the shore zone, across the littoral energy fence, and onto the shelf, is bottom-return storm flow. This offshore-directed, bottom-return storm flow results from the return of water stacked against the shoreface by longshore storm winds called coastal setup (Galloway and Hobday, 1996, p. 162-164).

On the inner shelf, storm transport produces an inner shelf sand prism consisting of an inner hummocky cross-stratified sand facies and an outer storm-graded sand bed facies (Galloway and Hobday, 1996, p. 163, fig. 7.4, p.164). The zone of hummocky cross-stratification extends between storm-wave base, located on the inner shelf, and fairweather wave base at the toe of the shoreface (Galloway and Hobday, 1996, p. 162). The hummocky cross-stratified sandstones are commonly interbedded with bioturbated mudstones (Walker, 1984, p. 148-149). The width of the inner shelf sand prism depends on shelf energy, gradient, and sediment supply (Galloway and Hobday, 1983, p. 144). Its distal equivalent is an outer shelf mud blanket (Shepard, 1969, p. 218-219; Galloway and Hobday, 1983, p. 144). The outer edge of the inner shelf sand prism, if present, or shore zone sand prism, if the inner shelf sand prism is absent, defines the sand-mud line of Busch (1974, p. 8-9, 24). Busch (1974, p. 8-24) discusses the various stratigraphic sequences resulting from variations in mud, sand, and carbonate supply and subsidence vs. uplift rates. In the mid to outer shelf, long-period swells place bottom sediment, primarily muds, in suspension, allowing diffusive transport by currents or a gravity-driven nepheloid layer (Galloway and Hobday, 1996, p. 161, 163, fig. 7-4, 163). Some outer shelves, such as the northeastern Pacific shelf, have an extensive outer shelf mud belt, localized by low velocity, intruding ocean currents (Galloway and Hobday, 1996, p. 164). On the mid and outer shelf, below storm wave base, turbidite deposits can be preserved. Turbidites may be generated by sediment liquification caused by storm-driven coastal setup (Walker, 1984, p. 154, fig. 21). Outer shelf muds lack stratification due to bioturbation, and inner shelf muds are interlayered with thin discontinuous laminae of sand (Shepard, 1969, p. 218-219). Lagoonal muds also lack stratification due to bioturbation, excepting near deltas, and in arid regions with very high salinities and stagnant conditions which limit benthos and its resultant bioturbation (Shepard, 1969, p. 219).

Active inner shelf sandwaves are found in tide dominated, storm dominated and intruding ocean current dominated shelves. On Georges Bank, a tide dominated shelf, sand ridges and sand waves occur at depths of less than 60 m (Walker, 1984, p. 156). On the Middle Atlantic Bight, a storm dominated shelf, sandwave fields are restricted to the inner shelf at depths of less than 30 m (Walker, 1984, p. 147). On the southeastern shelf of South Africa, a shelf dominated by the intruding Agulhas Current of the Indian Ocean, sandwaves occur in 40-60 m of water (Walker, 1984, p. 165). In the first and last examples, relict sediments are probably being reworked (Walker, 1984, p. 147, 163, 165).

Inner shelf sediments (water depth < 200 ft or 61 m) are strongly influenced by climate. Inner shelf sediments off glaciated landmasses are gravel and silty, chloritic muds. Temperate and arid landmasses have sandy inner shelves. Hot (tropical), humid coasts have muddy inner shelves. Shallow subtropical shelves with low sediment influx are commonly carbonate dominated (Hayes, 1967; Galloway and Hobday, 1996, p.159-160).

Storm Wave Base

Wave base is defined as a water depth of one-half the wavelength. "Just as there are a spectrum of wavelengths and wave periods on the waters surface, so there is a spectrum of wave bases" (Friedman and Sanders, 1978, p. 469). For example, off Whalehead Cove, Oregon, waves with periods of from 8 to 12 seconds, have wave bases of from 50 to 110 m, respectively. Off Fire Island, Long Island, New York, waves with periods of from 3 to 5 seconds have wave bases of from 7 to 20 m, respectively (Friedman and Sanders, 1978, p. 474, fig. A-15).

Sea waves are steep waves, actively being blown by the wind, while low swells originally were

generated as sea waves in a storm center, but have propagated beyond the storm and have become more regular than sea waves (Friedman and Sanders, 1978, p. 364-365). In southern California, the predominant waves in summer months are long, low swells, generated by winter storms in the Antarctic Ocean, with periods of 10 to 12 seconds (Friedman and Sanders, 1978, p. 492). During the winter months the dominant waves are storm waves generated by local storms with periods of 5 to 7 seconds (Friedman and Sanders, 1978, p. 491-492). On the Pacific Coast of North America, typical swells have a period of 10 seconds, a wavelength of 150 m, and a wave base of 75 m. On the Atlantic Coast of the U.S. typical swells have a period of 6 seconds, a wavelength of 57 m, and a wave base of 28.5 m (Friedman and Sanders, 1978, p. 472-473). Ordinary swells have periods of 6 to 14 seconds, and wave bases of about 28 to 175 m (Friedman and Sanders, 1978, p. 465, 469, fig. A-10, 480). Storm waves have periods of 3 to 7 seconds, wavelengths of 15 to 75 m, and wave bases of 7.5 to 37.5 m. Long-period swells, which preceed storm waves, have periods of 14-22 seconds, wavelengths of 300 to 900 m, and wave bases of 150 to 450 m (Friedman and Sanders, 1978, p. 480). The depth of the shelf break, or seaward edge of the continental shelf, ranges from 18 m (59 ft) to 915 m (3002 ft), with an average depth of 124 m (407 ft) (Bouma, et al., 1982, p. 281). At the mean depth of the shelf break, in many parts of the world, swells having periods of greater than about 8 seconds begin to interact with the bottom, as the bottom is within long-period swell wave base (Friedman and Sanders, 1978, p. 469, fig. A-10).

Storm-associated waves are occasionally capable of disturbing the outer shelf to depths of 650 ft (200 m). Threshold velocities for sediment movement on the Washington shelf were exceeded during five days of the year at the 550 ft (167 m) shelf break, and 53 days of the year at the 250 ft (75 m) mid-shelf (Galloway and Hobday, 1983, p. 145). Dunbar and Rodgers (1957, p. 130) noted that the depth of wave action may rise to 300 ft (91 m) or more during heavy storms. On the Pacific Coast of the U.S., depths of 100 ft (30 m) (or deeper off Oregon and Washington) are occasionally (Lankford, 1967, p. RL-5) or frequently (Phleger, 1960, p. 15-16) stirred by turbulence when long-period waves arrive. Shepard (1969, p. 13) cited examples of unusual storms moving rocks and coarse sand off the English and Irish coasts at depths of 100 ft (30 m) to 180 ft (55 m). In the California continental borderland, Ingle (1980, p. 177, fig. 7) used a depth of 50 m (164 ft), the depth of average wave touchdown, to divide the sandy inner shelf from the sand/mud lithology of the outer shelf. Ingle suggested a depth of 150 m (492 ft), the base of the photic zone to approximate the seaward edge of the outer shelf (shelf break). Brenner (1980, p. 1224, 1225, fig. 1) suggested a depth range of approximately 20 m (66 ft), i.e. the toe of the shoreface, to between 50 m (164 ft) and 200 m (656 ft) for the storm influenced inner shelf regime and between 50 m (164 ft) and 200 m (656 ft) to 500 m (1640 ft) for the outer shelf regime. Ingle (1980) is followed here for depth ranges.

Implications for the Chuar Group Shales

Chuar Group shales, largely lacking sands and storm rip-ups (with the notable exception of the contorted, basal Walcott Member Flaky Dolomite bed, by this interpretation), suggest deposition at least below fairweather wave base (5-20 m; 16-66 ft), and possibly at mid to outer shelf depths [approximately 50 to 150 m (164 to 492 ft) following Ingle (1980, p. 167, 177)] below the inner shelf depths dominated by storm wave processes. Several alternatives, however, are possible. One is that the climate of Chuar deposition was hot and humid with a muddy shelf, or subtropical with low sediment influx and with shale and carbonate dominated deposition. A second possibility is that Chuar deposition occurred in a restricted lagoonal or estuarine environment which served as a sediment trap, allowing mud deposition to begin at sealevel. A third possibility is that Chuar shale deposition occurred under limited (Carbon Butte Member) and depleted (Chuar Group shales) sand supply, abundant mud supply, and limited carbonate supply as described by Busch (1974, p. 8-24).

Dehler, et al. (2001) pointed out that no one climate regime existed throughout Chuar Group deposition. They suggested Chuar Group shales and sandstones were deposited during periods of humid climate, whereas dolomites were deposited during periods of arid climate, which alternated in humid/arid climatic cycles. Dehler, et al. (1998) interpreted the paleoenvironments of Chuar Group mudrocks to

include intertidal, shallow subtidal, and possibly deeper subtidal depths, the latter two near or below fairweather wave base.

Seasonal, Latitudinal, and Vertical Ocean Temperatures and Mixing

The shelf break, or seaward edge of the continental shelf, may be as shallow as 18 m or as deep as 915 m, with an average depth of 124 m. The width of the shelf ranges from a few kilometers to more than 1,000 km, with an average width of 75 km (Bouma, et al., 1982, p. 281). Phleger (1960, p. 17) cited 100 to 125 m as the average water depth of the shelf break.

The temperature of sea water varies with latitude, season, and depth. The following review of these variations is from Phleger (1960, p. 5-9, 17-18), Turekian (1968, p. 76), and Ingle (1980, p. 167, fig. 3; 177, fig. 7). There are three distinct bathymetric water layers: the seasonal or surface layer, the permanent thermocline of intermediate depth, and the deep (and bottom) waters.

In the mid-latitudes, winter water is relatively cold, turbulent, and well mixed to 100 m or more, and may cover the entire continental shelf. In the summer, surface water warms and a seasonal thermocline develops in the upper few hundred feet. This upper layer showing seasonal temperature variations (in mid-latitudes) is termed the seasonal layer. For the mid-latitudes, Ingle (1980, p. 167, fig. 3; 177, fig. 7) shows 100 m as the base of the surface or mixed layer.

In the tropics the upper layer is always warm, well mixed, and isothermal to as deep as 150 m in the Trade Winds belt. In these areas, seasonal temperature variations in the upper seasonal layer may be insignificant.

At all but the high latitudes, below the seasonal layer is the permanent thermocline, from about 100 m to between 1000 and 1500 m. This layer exhibits a decrease in temperature with increasing depth, except in high latitudes where the temperature is uniformly cold at all depths. The deep and bottom waters, below 1000 to 1500 m, all have their origin in the high latitudes and are uniformly cold. In the deep (and bottom) waters, temperatures are generally 5°C or less.

"One of the principal characteristics of the (continental) shelf water is that it is mostly or entirely within the seasonal layer, and the seasonal effect extends to the bottom" (Phleger, 1960, p. 17). In the tropics, with little or no seasonal variation, the zone of mixed isothermal water extends to the shelf break or deeper. Along coasts with moderate to high runoff, a seaward thinning surface wedge of nearshore low salinity water may extend to the edge of the shelf and be as deep as 180 ft (55 m) at the shelf break. The seasonal layer reflects the temperature of the ambient average temperature of that latitude (Turekian, 1968, p. 76).

Implications for the Chuar Group

Of the twelve organic-rich shale environments considered as candidates for Chuar Group deposition, seven require total or semi-isolation (restriction) from the sea and five, namely models 5, 6, 7, 9, and 11, are open marine. The above information suggests that **open-marine** waters shallower than a few hundred feet (60-90 m ?) should be well mixed and vertically isothermal at all seasons and at all latitudes. In the surface or seasonal layer anoxia should not be produced by density contrasts resulting from a vertical temperature gradient. In the euxinic basin model 5, closed anoxic depressions in the oxic open ocean, anoxic depressions are generated below the seasonal layer, within the permanent thermocline, when the depression is filled by isothermal water at the temperature of the highest closing contour. Water higher in the thermocline is warmer and less dense. Sill depths for modern examples range from 200 m in the Santa Barbara Basin of the California Continental Borderland to 2200 m for the Orca Basin. In euxinic basin model 7, oxygen minimum zones also occur within the permanent thermocline from 100 to 1500 m (Table 4 of this report; Ingle, 1980, p. 167, fig. 3; 177, fig. 7).

Typical Shallowing Upward Carbonate Sequences

James (1984, p. 216-219) described typical shallowing upward carbonate sequences. The subtidal unit commonly contains stromatolites in deposits older than middle Paleozoic. Intertidal zone limestones or dolomites are characterized by three distinctive features: 1) algal mats (stromatolites), 2) cryptalgal laminates with fenestral porosity, and 3) **desiccation features (polygons, mud cracks)**. In Precambrian and lower Paleozoic deposits these features will be preserved throughout the unit due to lack of prolific browsing or burrowing fauna. The supratidal zone is characterized by lithified storm deposited sediments which are fractured into **desiccation polygons**, and may form flat pebble breccias cemented by cryptocrystalline aragonite or calcite and characteristically containing 25 to 50% fine crystalline dolomite. Supratidal low beach ridges in the Bahamas may consist of up to 80% dolomite (Friedman and Sanders, 1978, p. 334). Supratidal sediments may also consist of well laminated dolomite or limestone with fenestral porosity.

Variations from this general sequence arise from differences in depositional energy and climate. The intertidal unit may be represented by low energy muddy sequences of a tidal flat environment or high energy grainy sequences of a beach environment (James, 1984, p. 214, 218). In humid or semiarid climatic zones, as typified by the Bahamas, non-carbonate evaporites are not precipitated (Friedman and Sanders, 1978, p. 335). In arid climates, as typified by the Persian Gulf, non-carbonate evaporites are precipitated interstitially in the supratidal salt flat or sabkha environment. The supratidal environment of arid climates exhibit three notable differences from those of humid climates: 1) greater abundance of dolomite, 2) presence of gypsum, anhydrite, halite, and possibly other evaporites, and 3) stromatolites may display a greater variety of shapes, e.g. domal or columnal (Friedman and Sanders, 1978, p. 343). Evaporation at the sabkha surface causes interstitial fluids to reach salinities up to ten times that of normal seawater, causing the interstitial precipitation of aragonite, gypsum, and anhydrite. Precipitation of these calcium compounds increases the ratio of magnesium to calcium, causing dolomitization of the lime mud underlying the sabkha (Friedman and Sanders, 1978, p. 337, 339). Nodular anhydrite and dolomite are the signature of a sea-marginal sabkha in an arid climate belt (Friedman and Sanders, 1978, p. 338). Supratidal halite crusts and interstitial precipitation of $CaCO_3$ and $CaSO_4$ are found in both subtropical arid climates such as the Persian Gulf and subtropical subhumid climates such as Broad Sound, Queensland, Australia (Friedman and Sanders, 1978, p. 331-332, 335, 338).

Implications for the Chuar Group

The implications of these carbonate models for the Chuar Group carbonates are fourfold. First, desiccation features such as polygons and mudcracks are characteristic features of carbonate intertidal and supratidal deposits and do not require basin isolation from the sea. Second, since the Chuar Group lacks nodular gypsum or anhydrite which are signature deposits of an arid climate sea marginal sabkha, but does have minor evidence of hypersalinity (see Key Evidence), the Chuar Group carbonates were either deposited in a humid tropical environment or north of 40 degrees from the equator where evaporation rates are less than precipitation rates (Friedman and Sanders, 1978, p. 374). Paleomagnetic evidence suggests that the Chuar Group deposition occurred between 10 and 20 degrees of the equator (Weil, et al., 1999; Karlstrom, et al., 2000), that is, within the tropics. Third, the gypsum and halite pseudomorphs noted by Summons, et al. (1988) and Ford and Breed (1973) may have formed in a subhumid climate such as Broad Sound, Australia. Dehler, et al. (2001) proposed that Chuar Group carbonates indicate more arid climates as opposed to more humid climates indicated by siliciclastics. Lack of nodular gypsum or anhydrite in the Chuar Group may be due to deposition in a subtropical, subhumid setting as in the Broad Sound, Australian modern analogue. Fourth, lack of common grainy sequences (excepting the pisolitic zones of Ford and Breed (1973) in the Chuar Group carbonates suggests deposition in a low energy intertidal tidal flat environment rather than a beach environment.

Euxinic Basin Biofacies and Lithofacies (Byers, 1977)

Euxinic environments are defined as environments which contain H_2S in the bottom water, and no oxygen (Friedman and Sanders, 1978, p. 524; Pedersen and Calvert, 1990, p. 458). Oxygen is removed by oxidation of first-cycle organic matter. Byers (1977) presented a general model of biofacies patterns in euxinic basins which can be utilized to interpret the Chuar Group source rocks. Byers (1977) cited the Baltic Sea, with poorly oxygenated bottom waters, and the Black Sea, with bottom waters entirely lacking in oxygen, as modern examples of euxinic basins. In all cases the mechanism creating euxinic basins is water density stratification produced by a salinity and temperature gradient in combination with a portal silled at depth (Byers, 1977, p. 6). Such basins exhibit a tripartite layering of their water columns based on oxygen concentration. Each water layer results in a distinctive biofacies and lithofacies where that layer intersects the basin's bottom profile (bathymetry/paleobathymetry). Byers (1977, p. 7, fig. 1) based the depth ranges for the three zones of the water column on the Black Sea, the largest modern anoxic sea.

The aerobic zone from approximately 0-50 m is well oxygenated with normal aerobic ranges of 2.0 to 7.0 ml/l dissolved oxygen (Byers, 1977, p. 8), although the minimum oxygen concentration for this facies is 1.0 ml/l (Byers, 1977, p. 8, 16). Water throughout the aerobic layer is of nearly equal salinity and density, and atmospheric oxygen is continually mixed in at the surface due to vertical mixing by waves and thermal overturn. The aerobic biofacies is characterized by a diverse calcareous epifauna, a shelly infauna, and strongly bioturbated lithofacies.

Surface water in temperate climates normally contains 7 ml/l dissolved oxygen (Byers, 1977, p. 7). Maximum oxygen saturation in sea water is about 6 to 8.5 ml/l, depending on water temperature and salinity (Demaison and Moore, 1980, p. 1186 and 1205). The major change in faunal composition, a diversity decrease, occurs below 2.0 ml/l dissolved oxygen in the Gulf of California (Parker, 1964; Byers, 1977, p. 8). In the Black Sea, mollusks and echinoderms are restricted to the upper water column with oxygen values greater than 1.0 ml/l (Bacescu, 1963; Rhodes and Morse, 1971; Byers, 1977, p. 8).

The dysaerobic zone, from approximately 50 to 150 m, is a strongly stratified layer (pycnocline) in which oxygen decreases rapidly with depth from 1.0 ml/l to 0.01 ml/l (Byers, 1977, p. 7 and 8). This is a zone of rapid change in salinity and density, and with little vertical mixing. The dysaerobic biofacies is dominated by soft-bodied infaunal polychaetes and nematodes and poorly calcified crustaceans creating bioturbate lithofacies, lacking the calcareous epifauna and shelly infauna of the aerobic zone.

The anaerobic zone below approximately 150 m, is a layer of deep-basin water of nearly uniform salinity and density with an oxygen content at or near zero (below 0.01 ml/l, Byers, 1977, p. 7, 8). The layer is not mixed vertically and the basin sill prohibits the lateral exchange of oxygenated waters with the open ocean. The anaerobic biofacies lacks all benthos. Shells are absent and the sediment is undisturbed due to lack of infauna, resulting in laminated, organic-rich shaly lithofacies which may contain interbedded turbidites. The characteristic deposit of a euxinic basin having stagnant bottom water is gray to black silt, clay, or marl (Strom, 1939; Trask, 1939, p. 448-450; Shepard, 1969, p. 222; Friedman and Sanders, 1978, p. 529). Modern-day Black Sea sediments contain from 1 or 2% to between 4.54 and 6% weight organic carbon (Caspers, 1957, p. 823; Demaison and Moore, 1980, p. 1190-1191, fig. 8; Pedersen and Calvert, 1990, p. 459) or from 3% to 10% organic matter (Trask, 1939, p. 449). Trask (1939, p. 430) reported that carbon constitutes 50 to 60% of organic matter and suggested that carbon content estimates of 53 to 56% of organic matter are the right order of magnitude. More recently, Aller and Yingst (1980) reported that approximately 40% of organic matter is organic carbon. Euxinic Norwegian fjords commonly have organic carbon contents in excess of 12 per cent, and range up to 16.75 per cent (excluding 23.4% from Fjellangervag, Norway containing wood fiber from a saw mill on the shore) (Strom, 1936, p. 61-66; Strom, 1937; Strom, 1939, p. 361; Trask, 1939, p. 447-448; Friedman and Sanders, 1978, p. 529). In contrast, sediments deposited under oxidizing bottom waters are characteristically gray or green muds and range between 1 and about 2.5 per cent in organic matter (Friedman and Sanders, 1978, p. 529, 531, fig. D-11).

Byers (1977, p. 16) noted that in euxinic evaporite basins the tripartite water zonation might be

achieved at much shallower depths than the 50 m and 150 m boundaries estimated above. In evaporite settings, brine formation greatly increases the density of bottom waters, which results in a rapid density increase with depth, and a thin pycnocline (dysaerobic zone). The solubilty of oxygen decreases with increased salinity. A 200,000 ppm NaCl solution can contain less than 2 ml/l dissolved oxygen (Hite, 1972, p. 332, fig. 2) and waters having salinities exceeding 300,000 ppm can sometimes contain zero dissolved oxygen (Friedman and Sanders, 1978, p. 523, fig. D-3; Warren, 1986, p. 447, fig. 4). Much smaller salinity increases than these can exclude invertebrates long before oxygen becomes limiting. In evaporite basins azoic conditions, due either to high salinity or low oxygen may have been achieved at depths much shallower than 150 m (Byers, 1977, p. 16).

Stoakes and Creaney (1985) used the Byers model to explain the deposition of the Upper Devonian Duvernay Formation of Alberta, Canada, a carbonate source rock.

Modern Euxinic and Organic-rich Basin Models

Tables 4 and 5 are a compilation and classification of modern euxinic basins and organic-rich environments which attempt to include the possible models for deposition of the Chuar Group. Tables 4 and 5 recognize seven major categories of organic-rich, euxinic basins plus five organic-rich, non-euxinic, oxic environments which are briefly defined below and considered as potential models for Chuar deposition. Table 4 compares the percentage organic carbon, depths, and sediments of the anoxic vs. oxic facies of each category. Table 5 summarizes the range of percent organic carbon found in the 12 environments considered in Table 4. Readers are referred to the sources (Strom, 1936, 1937, 1939; Gripenberg, 1939; Trask, 1939; Rickard, 1956; Toombs, 1956; Caspers, 1957; Rusnak, 1960; Neev and Emery, 1967; Watson and Waterbury, 1969; Shaw, 1977; Friedman and Sanders, 1978; Demaison and Moore, 1980; Huc, 1980; Ingle, 1980; Bauld, 1981a; Bauld, 1981b; Kirkland and Evans, 1981; Warren, 1986; and Pedersen and Calvert, 1990), particularly Trask, 1939; Friedman and Sanders (1978), Huc, 1980; Demaison and Moore (1980), Bauld, 1981b; and Warren (1986) for details. Significant differences exist between the euxinic/organic-rich basin classifications of these various source authors, as well as between those of the sources and Tables 4 and 5.

Trask (1932; 1939) was one of the earliest workers to attempt to synthesize the present global distribution of organic matter as depositional models for petroleum source rocks. From an analysis of several thousand samples of aquatic sediments, he determined that nearshore sediments average 2.5% organic matter while open ocean sediments average less than 1% organic matter (Trask, 1932; 1939, p. 428). Categories of organic-rich, near-shore environments recognized were: 1) the continental platform, 2) areas of upwelling, 3) inland seas, 4) fiords, 5) Black Sea, 6) deltas, 7) lagoons, and 8) areas of limestone deposition (Trask, 1939, p. 446).

Friedman and Sanders (1978, p. 528-536) discussed general models of circulation and stagnation of basin waters. Categories recognized included: 1) basins having ventilated waters; 2) basins having euxinic conditions; 3) basins whose waters are ventilated occasionally; 4) closed basins on the sea floor; 4) basins losing large amounts of water by evaporation; 4a) portals with two-way flow; most saline evaporites at margins of basin; 4b) portals with one-way flow; most-saline evaporites at center of basin.

Demaison and Moore (1980) also examined the present distribution of organic matter to construct a general model for the distribution of petroleum source rocks. Their general model stressed preservation of organic matter in anoxic environments produced by global climatic-oceanographic/lacustrine systems. They identified four main anoxic settings having petroleum source rock potential: 1) large anoxic lakes, 2) anoxic silled basins, 3) anoxic layers caused by upwelling, and 4) open-ocean anoxic layers.

Demaison and Moore (1980, p. 1184, 1186, 1205) defined as "anoxic" any water containing less than 0.5 ml/l dissolved oxygen, which is the threshold below which metazoan biomass and bioturbation by deposit feeders become significantly depressed. They proposed this limit of 0.5 ml/l (the threshold of arrested bioturbation), not the total absence of oxygen in the water, as the effective "biochemical fence" between potentially poor or good qualitative and quantitative preservation of organic matter in sediments.

Table 4 utilizes their data and definition of anoxic. For this study, therefore, we modify the oxygen limits defining Byers's (1977) tripartite division of the water column as follows: aerobic zone = 8.5 to 1.0 ml/l (unchanged), dysaerobic zone = 1.0 to 0.5 ml/l, anoxic zone (instead of anaerobic) = <0.5 ml/l. This change retains the lithofacies associated with each zone since the anoxic facies will still lack bioturbation by deposit feeders (burrowers) and thus be laminated. The "oxic" facies of Table 4 and of Demaison and Moore (1980), however, includes waters with oxygen levels equaling those of Byers's (1977) aerobic and dysaerobic zones.

In general Demaison and Moore (1980, p. 1184-1186, and 1204-1205) concluded that the overall range of organic carbon content in sediments deposited under anoxic water is significantly wider and higher, about 1% to over 20% organic carbon, than in sediments deposited under oxygenated water, which typically range between 0.2% to 4% regardless of surface productivities. Data in Tables 4 and 5 indicate that the organic carbon content of the various anoxic facies ranges from 0.22 to 26 or 30%. The organic carbon content of the oxic facies in Tables 4 and 5 ranges from 0.1 to 32%. While the upper range of organic carbon content for oxic facies in Tables 4 and 5 is higher than that given by Demaison and Moore (1980), it is only in three oxic environments that organic carbon values exceed 6%. These three environments are saline lakes, lagoons, and areas of limestone deposition. By comparison four anoxic environments (Models 1, 2, 5, 6, and 7) have an upper range of organic carbon content exceeding 6%. Tables 4 and 5 do not include data from the controversial Holocene (7,000-3000 yrs BP) sapropel [variously called "the old Black Sea" or "unit 2" (Degens and Ross, 1974; Pelet and Debyser, 1977; Demaison and Moore, 1980, p. 1190) or "Unit C" (Calvert, 1990; Pedersen and Calvert, 1990)] which underlies the Black Sea and which contains up to 20 wt. % organic carbon (Caspers, 1957, p. 823; Demaison and Moore, 1980, p. 1190-1192; Pedersen and Calvert, 1990, p. 459-460 and 463) or even 20 to 35% organic matter (Trask, 1939, p. 449). One group of authors (Degens and Ross, 1974; Pelet and Debyser, 1977; Demaison and Moore, 1980, p. 1190) interpreted the unit to be of anoxic origin, while a second group (Calvert, 1990; Pedersen and Calvert, 1990) interpreted the unit to be of oxic origin. The Black Sea data in Table 4 only relate to its modern sediments. The maximum total organic carbon content for the Walcott Member of 9.39% in the Sixtymile Canyon section (this report) and 8.29% in the Nankoweap Canyon section (Wiley, et al., 1998) are within possible ranges for either anoxic or oxic deposition.

Demaison and Moore (1980, p. 1204-1205) further characterized the organic matter in anoxic facies as being more reduced (hydrogen-rich), and more lipid-rich than that in oxic facies. The hydrogen-rich anoxic facies are therefore oil-prone, while the hydrogen-depleted oxic facies are gas-prone. Anoxic sediments also contain abnormally high concentrations of U, Cu, Mo, Ni, P, and S which tend to correlate positively with organic carbon concentrations. The evidence of sulfur in the Tanner, Awatubi, and Walcott Members reported here and by Wiley, et al. (1998) suggests either deposition under an anoxic water column or in anoxic sediments under either an anoxic or an oxic water column for at least parts of these units.

Organic matter oxidation (decomposition) proceeds through a progression of reactions as different electron acceptors are sequentially exhausted (Kinsman, et al., 1973, p. 325; Demaison and Moore, 1980, p. 1183; Pedersen and Calvert, 1990, p. 457-458). The first step utilizes oxygen in aerobic **oxidative** metabolism until dissolved oxygen levels are reduced to between 1 and 2 ppm. The terminal product of aerobic microbial respiration is CO_2 and H_2O (Demaison and Moore, 1980, p. 1183; Bauld, 1981b, p. 311, 313). Steps two through four are types of anaerobic oxidation. The terminal products of anaerobic microbial respiration are CO_2 and CH_4 (Bauld, 1981b, p. 311, 313). The second step occurs as dissolved oxygen levels are reduced to 0.5 to 1.0 ppm and **denitrofying** anaerobic bacteria utilize dissolved molecular oxygen, nitrate, and nitrite ions as nitrogen sources for protein synthesis and generate CO_2, H_2O, and N_2 (Demaison and Moore, 1980, p. 1183). The third step commences when dissolved oxygen levels reach about 0.1 ppm and **sulfate-reducing** anaerobic bacteria utilize sulfates as the oxidant and generate CO_2, H_2O, and H_2S (Demaison and Moore, 1980, p. 1183). The fourth and final step is **fermentation**

29

which utilizes carboxyl (CO_2) groups and organic acids as the electron acceptor. A special type of anaerobic fermentation is bacterial methanogenesis which produces methane, and branched and aromatic hydrocarbons up to butane (Demaison and Moore, 1980, p. 1183; Pedersen and Calvert, 1990, p. 458).

Sulfate-reducing bacteria are involved in the formation of H_2S, calcium carbonate, native sulfur, phosphate, and pyrite (iron sulfide or FeS_2) through the reduction of sulfate ions in formation pore waters (Friedman and Sanders, 1978, p. 130, 131, 217, 245, 536; Kendall, 1984, p. 267). The reaction producing calcium carbonate and hydrogen sulfide proceeds as follows:

$$CaSO_4 = Ca^{2+} + SO_4^{2-}$$
$$\text{then, } SO_4^{2-} + 2CH_2O(\text{organic matter}) = H_2S + 2HCO_3^-$$
$$\text{then, } Ca^{2+} + 2HCO_3^- = CaCO_3 + H_2O + CO_2.$$
$$\text{Sum: } CaSO_4 + 2CH_2O(\text{organic matter}) = CaCO_3 + H_2O + CO_2 + H_2S.$$
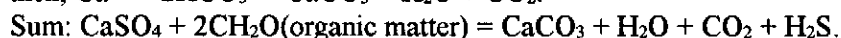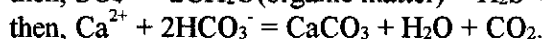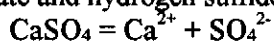
In the absence of solid calcium sulfate, this reaction can proceed using dissolved calcium and sulfate ions in seawater (Friedman and Sanders, 1978, p. 130). Seawater contains a large amount of dissolved sulfate which is used as the primary oxidant in the third, sulfate-reducing stage of organic matter oxidation (decomposition) with H_2S as a byproduct (Pedersen and Calvert, 1990, p. 458). Oxygenated seawater contains about 200 times as much oxygen in reducible sulfate as it does in dissolved O_2 (Pedersen and Calvert, 1990, p. 458). The reduction of gypsum or anhydrite by sulfate-reducing bacteria forms native sulfur, which occurs in modern salt lakes or playas or in caprock above salt diapirs (Friedman and Sanders, 1978, p. 131). In lakes and shallow- and deep-water marine environments, like the Black Sea, sulfate-reducing bacteria reduce sulfates to sulfides in the form of black, finely disseminated iron monosulfide, which colors the sediments black. Below the water-sediment interface the iron monosulfide changes to iron sulfide (pyrite or FeS_2) (Friedman and Sanders, 1978, p. 131). The black color of euxinic shales comes from finely dispersed pyrite or hydrotroilite, an hydrated iron sulfide (Keen, 1969, p. 89; Friedman and Sanders, 1978, p. 530). Sulfate-reducing bacteria are excluded in either an oxidizing environment, or where salinity reaches 400‰ (Friedman and Sanders, 1978, p. 245; Kirkland and Evans, 1981, p. 188), or where extremely high concentrations of H_2S are reached in near-surface bottom sediments lacking metallic reductants for S^{-2}, especially iron (Warren, 1986, p. 448-449).

Sulfur production by sulfate-reducing bacteria can occur: 1) in an anoxic water column (euxinic basin) using dissolved sulfates, 2) in the anoxic sediments underlying an anoxic water column utilizing either dissolved sulfates or gypsum, or 3) in the anoxic sediments underlying an oxic water column utilizing either dissolved sulfates or gypsum. Sulfur production by facultative anoxygenic photosynthetic cyanobacteria which utilizes H_2S and CO_2 as reactants, can occur, therefore, only in environments where sulfate-reducing bacteria have produced H_2S.

Bottom sediments in **oxic environments (oxygenated water column)** are commonly anoxic, but extensively bioturbated by oxygen-respiring invertebrates including polychaetes, holothurians, and bivalves (Demaison and Moore, 1980, p. 1183-1185). In both deep-sea and nearshore regions, bioturbation oxygenates a surface layer from 5 to 30 cm. deep (Demaison and Moore, 1980, p. 1184). Below this is a layer which is oxygen-depleted and undergoing bacterial sulfate reduction with the generation of H_2S and pyrite (iron sulfide or FeS_2) (Friedman and Sanders, 1978, p. 525). A third and deepest layer is sulfate-depleted and undergoing bacterial CO_2 reduction with the generation of CH_4. In **anoxic environments** only the lower two layers are present. Bacterial sulfate reduction occurs from within the water column, down through the upper layer of the bottom sediments, down to the sediment depth at which sulfate is depleted. A zero-Eh surface separates oxygenated waters or sediments from reducing waters or sediments (Friedman and Sanders, 1978, p. 524-525). Algal mats modify the sediment-water interface by decreasing vertical permeability to gas and liquids by a factor of ten or more (Bauld, 1981b, p. 312; Warren, 1986, p. 449). Dissolved oxygen, Eh, H_2S, and light intensity exhibit abrupt changes at, and steep gradients beneath the interface (Bauld, 1981, p. 312). In Laguna Madre of southern Texas, the zero-Eh surface occurs a few centimeters below the sediment surface in shoal areas associated with algal mat growth (Rusnak, 1960, p. 187-188).

Foree and McCarty (1970), Jewell and McCarty (1971), and Otsuki and Hanya (1972a, b) showed that rates of anaerobic degradation of algae by sulfate reduction are nearly identical to those of aerobic degradation. Thus if oxic sediments have three stages of oxidation (oxidative, denitrofying, and sulfate-reducing) prior to fermentation and anoxic sediments have only two stages (denitrofying, and sulfate-reducing), and if oxidation rates are the same for all stages, then 1.5 (or 3/2) times as much organic carbon should reach the fermentation stage in anoxic sediments than does in oxic sediments. This also assumes: 1) that the relative amounts of oxidants for the denitrofying and sulfate-reducing stages are equal in oxic and anoxic sediments, and 2) the supply of organic carbon is not completely consumed at any of the three stages prior to fermentation. Organic carbon reaching the fermentation stage would be available for hydrocarbon generation via methanogensis (Demaison and Moore, 1980, p. 1183-1185).

Additional factors which decrease the preservation of organic matter in oxic environments as compared to anoxic environments include: consumption by sediment-feeders; bioturbation by worms facilitating diffusion of oxidants (O_2, SO_4) in sediments; and less organic complexation with toxic metals in oxidizing environments (Demaison and Moore, 1980, p. 1184). Preservation of organic matter in anoxic environments is comparatively enhanced by the lack of the above factors and possibly by poorer utilization of lipids by anaerobic bacteria (Demaison and Moore, 1980, p. 1185). In anoxic environments lignolytic fungi cannot grow and lignin is preserved (Huc, 1980, p. 453).

Rather than stressing anoxic deposition as a primary control on the formation of source rocks as did Demaison and Moore (1980); Friedman (1980), Bauld (1981b, p. 314) and Warren (1986, p. 442, 449) stressed the high productivity of benthonic cyanobacterial mats deposited in updip, shallow, hypersaline (evaporitic) carbonate environments. This was also a different emphasis than that of Kirkland and Evans (1981), who stressed the plankton-derived, downdip, deep water source potential of carbonate-evaporite [hypersaline, especially mesohaline (salinity range 40-120‰)] deep-water barred evaporite basins. Bauld (1981b) compiled cyanobacterial productivity rates and total organic carbon percentages in modern lacustrine, geothermal, and intertidal and subtidal marginal marine settings which rank among the most productive aquatic photosynthetic ecosystems. Warren (1986) provided similar data from modern continental and coastal saline lakes (shallow water, subaqueous brine pans including salinas of South Australia and hypersaline lakes) and periodically exposed, brine-saturated salt flats (sabkhas and lagoons). Algal mats tend to preserve organic matter down to shallow burial depths of 1-3 m, for example algal mats and peats of the Arabian Gulf (Warren, 1986, p. 449). Preservation of organic matter is favored because cyanobacterial mats reduce vertical permeability to gas and liquids by a factor of 10 or more, which slows desiccation and the penetration of fresh, oxygenated rainwater into the saline pores of the mat during occasional periods of subaerial exposure (Bauld, 1981b, p. 312; Warren, 1986, p. 449). Warren (1986, p. 452) listed three factors favoring source rock preservation through catagenetic burial depths: 1) rapid emplacement in anoxic, high salinity pore fluids, 2) retention of this pore fluid system during burial without replacement by oxygenated waters, and 3) retention of this pore fluid system during burial without replacement by Mg-depleted waters, which would alter micrite to microspar and leach organic matter from the system prematurely. Warren (1986) proposed that two ancient settings met these criteria, namely: 1) deep basin, shallow water desiccating inland seas (saline giants) or the shelves of ancient epeiric seas, and 2) lacustrine basins in rift or foreland basin tectonic settings. Bauld (1981b, p. 313-314) also favored maximal organic preservation via a periodically completely desiccating lake model followed by an input of capping clays during flash flooding. Preservation is favored if periods of maximum organic productivity are followed by salinity increases beyond that of halite saturation which terminates all microbial activity, followed by burial under flood-borne sediment load. This rapid burial prevents flushing of hypersaline interstitial waters and also favors preservation through cementation and lithification. Friedman and Sanders (1978, p. 360-384) and Friedman (1980) developed an oxic epeiric sea model for the origin of petroleum source rocks described in "Model 12" of this report.

Brongersma-Sanders (1957, 1966, 1968) developed a model for shallow water, oxygen-depleted environments based on upwelling in which black shales are associated with high trace element content, with dry-climate deposits such as evaporites, and with evidence of mass mortality such as abundant fish remains

(Heckel, 1972, p. 262-264). The upwelling model has been extended by Parrish (1982) and Parrish and Curtis (1982).

Huc (1980, p. 453) identified four conditions which tend to protect organic matter from decomposition. These include: 1) anoxia such as occurs in deep embayments, oceanic trenches, and closed or semi-closed basins; 2) lack of nitrogen compounds; 3) presence of toxic metabolites such as H_2S and humic substances; and 4) physical conditions like low temperature and high pressure. He (1980, p. 462) identifed three "privileged zones" of the seabed containing high concentrations of organic matter including: 1) the rim of continents; 2) boreal zones; and 3) interior seas. Huc (1980, p. 466) also identified privileged organic matter depocenters occurring in low energy sedimentary environments, including: 1) deep parts of closed basins; 2) depressions in the continental shelf; 3) the base of the continental shelf; and 4) deltaic shales between channels. High organic matter concentrations also occur in high energy environments in the form of fecal pellets (Huc, 1980, p. 464, 466).

Pedersen and Calvert (1990) challenged the entire idea that water column anoxia and resulting enhanced preservation of organic matter is the first order control on carbon-rich sedimentation, concluding instead, that carbon-rich sedimentation is primarily the result of sporadic temporal and spatial increases in primary production, reflecting changes in the behavior and/or state of the ocean-atmosphere system. This contrasts with Demaison and Moore's (1980, p. 1180-1181) conclusion that "after exhaustive investigation, we could not find a systematic correlation between primary biologic productivity and organic carbon content of bottom sediments in the ocean". While the geological community continues to debate the origin of organic-rich shales, it is hoped that the range of possible origins for the Chuar Group is considered in the seven categories of euxinic basins and five oxic categories of organic-rich environments in Tables 4 and 5 and in the following discussion. Some of the points of debate will be noted below. In this report water salinity definitions will follow those of Murray (1973, p. 15): hyposaline = <32 per mille, normal marine = 32-37 per mille, and hypersaline = >37 per mille.

Euxinic Organic-rich Basin Models:

1) Large Euxinic, Permanently Stratified Tropical Lakes and Desiccating Isolated Seas (Table 4, IA)

The first category of euxinic basins includes lakes. Lakes in temperate zones experience seasonal overturn producing anoxic conditions in winter and summer due to temperature induced density stratification. Waters are oxygenated in spring and fall. Proglacial lakes may become anoxic in winter when they become frozen over and ice isolates them from atmospheric oxygen (Friedman and Sanders, 1978, p. 242-243).

Tropical lakes may become permanently stratified because the warm surface layer never cools enough to displace the subsurface water beneath the thermocline. Bottom waters become permanently stagnant. Modern examples of large anoxic, permanently stratified tropical lakes include Lake Tanganyika, Lake Kivu and the pre-1979 Dead Sea with organic carbon ranging from 0.4 to 15% in the sub-thermocline anoxic facies and from 1 to 2% in the oxic facies above the thermocline (Neev and Emery, 1976, p. 92; Demaison and Moore, 1980, p. 1187-1188; Warren, 1986, p. 446;).

Lake Tanganyika, which lacks evaporites, is an example of a large euxinic lake in a tropical humid climate moderated by extensive uplands, having 39 inches (1 m) of rainfall per year and a high evaporation rate equal to 90% of the total rainfall and river influx. (Trewartha, 1961, plate; Degens, et al., 1971, p. 230, 232; McHenry, 1992a, p. 669). The lake is the eighth largest in area and second deepest in the world with a maximum depth of 1500 m. Waters are anoxic, contain H_2S, and are toxic to fish and plankton below a depth of 100 to 150 m (Degens, et al., 1971, p. 229, 230; Rand McNally, 1973, p. 26-27). A stable, year-round thermocline is centered at 70 m. Below 400 m water temperature is uniform at 23.3 °C (Degens, et al., 1971, p. 230). Three rivers provide the lake with a small volume of inflow equal to one two thousandth of the volume of the lake. One river, the Lukuga River, drains it. The Lukuga River probably

acts as a spillway during periods of high lake level, but ceases flowing, leaving the lake with no outlet, during periods of low lake level, as was the case for a long period prior to 1876 (Degens, et al., 1971, p. 230). Water salinity of the lake is fresh to brackish with total dissolved solids of approximately 177 mg/l (Degens, et al., 1971, p. 232; McHenry, 1992, p. 541). Four sedimentary units have been described by Degens, et al. (1971, p. 232-235) from 3 m lake cores having ^{14}C age dates of 28,200 years B.P. and younger. The youngest (modern) layer, age dated as less than 3670 years B.P., is finely varved with fine-grained sediments consisting mainly of diatoms and organic matter. It contains pyrite and clays consisting of kaolinite, and some illite, chlorite, and sepiolite. Some calcium carbonate bands, either aragonite or calcite, occur in the upper half of the layer, which is less than 2000 years B.P. in age. The total organic carbon content of the layer ranges from 8 to 10%. Silty turbidites up to a few centimeters thick are found only in the deeper parts of the lake. No carbonate layers are found in any sediments older than 2000 years B.P. Diatoms, which are mostly marine and pelagic but do include several benthonic gerera, range in the geologic record from the Jurassic Period to the Recent (Jones, 1969, p. 21; Mintz, 1972, p. 148-149). Fresh water forms are known since the Miocene (Mintz, 1972, p. 148-149). It is not known if Proterozoic plankton played an equivalent role to Recent diatoms in creating anoxic lake conditions.

The Dead Sea, with evaporite deposition, occurs in a subtropical arid or desert climate with 2 to 2.5 (65 mm) inches of rainfall per year and an annual average evaporation rate of 55 inches (Trewartha, 1961, plate; McHenry, 1992b, p. 937). The salinity of the Dead Sea ranges from 285 to 330‰, one of the world's most hypersaline bodies of water (Friedman and Sanders, 1978, p. 244-245). For at least 300 years prior to 1979, the Dead Sea was a typical stable, long-term, density stratified, arid climate, tropical lake (Warren, 1986, p. 444). Above 50 m, the pre-1979 Dead Sea had surface waters with a salinity of about 288‰, a temperature range of 10 to 45 °C (mean of 19-36 °C), and contained a small amount of dissolved oxygen (1.5 ml/l). Below 50 m (thermocline) it was charged with hydrogen sulfide (10-11 ml/l), water temperature was uniformly about 22 °C, and salinity was 324‰ (Friedman and Sanders, 1978, p. 244-246). Because of its high salinity the pre-1979 Dead Sea precipitated evaporites ranging from aragonite to halite with gypsum being most common. In the upper 50 m of oxygenated waters gypsum was ubiquitous and aragonite was precipitated when surface water temperature exceeded 35 °C during periods of the most intense evaporation (about every fifth year) (Friedman and Sanders, 1978, p. 244-245, 255). Bottom sediments below 50 m contained small amounts of gypsum and consisted of dark layers of equal amounts of calcite and aragonite, and white layers in which aragonite was about four times as abundant as calcite. It is believed that anaerobic sulfate-reducing bacteria destroyed the gypsum and released calcium ions which combined with CO_2 to produce calcite. This implies gypsum will survive in the geologic record only where no anaerobic sulfate-reducing bacteria are present. These bacteria are excluded in either an oxidizing environment, or where salinity reaches 400‰ (Friedman and Sanders, 1978, p. 245; Kirkland and Evans, 1981, p. 188), or where extremely high concentrations of H_2S are reached in near-surface bottom sediments lacking metallic reductants for S^{-2}, especially iron (Warren, 1986, p. 448-449). The pre-1979 Dead Sea organic matter production did not significantly outpace organic matter destruction by sulfate-reducing bacteria, due to low levels of nutrients in inflowing surface waters from the surrounding desert (Warren, 1986, p. 449). Organic carbon in bottom sediments ranged from 0.4 to 2% TOC (Neev and Emery, 1976, p. 92; Warren, 1986, p. 446).

By February, 1979, river damming and water reclamation projects along the Jordan River destabilized the long-term, density stratification of the Dead Sea (Warren, 1986, p. 444). Lowered water levels and increased surface water salinities caused the Dead Sea waters to overturn, mixing anoxic bottom waters with surface water. As of 1985 the water column had not yet restratified. Since the 1979 overturn, gypsum, as well as halite and $CaCO_3$ has been settling to the deep basin floor of the Dead Sea (Warren, 1986, p. 444). Overturn may trigger deposition and preservation of bittern salts in ancient giant evaporite deposits (Warren, 1986, p. 444). During the Pleistocene Epoch, a 4000 m thick salt sequence was deposited under continental conditions in the Dead Sea graben (Friedman and Sanders, 1978, p. 205, fig. 8-11, p. 218).

If post-Pleistocene tectonics have not altered the morphology of the Red Sea portal, Pleistocene

glacial low sea-levels would have isolated the Red Sea as a saline lake, similar to the modern Dead Sea. This likelihood is supported by cores of Pleistocene sediments from the Red Sea which include calcite-rich muds and layers cemented by aragonite. The calcite-rich muds are inferred to be products of bacterial destruction of gypsum as in the modern-day Dead Sea (Friedman and Sanders, 1978, p. 536).

Ryan, et al. (1972), Hsu (1972), and Hsu, et al. (1973) advanced the hypothesis that the Late Miocene Messinian age Mediterranean Evaporite underlying the Mediterranean Sea was produced by the desiccation of the deep Mediterranean basin, which was at times completely isolated from the Atlantic, making it a large lake. "Evaporites were precipitated from desert playas or salt lakes whose water levels were dropped down to thousands of meters below the world wide sea level" (Hsu, 1972, p. 386). Hsu (1972) termed this the "desiccating deep-basin model" which he proposed as a model for the origin of giant evaporite deposits such as those of the European Permian Upper Zechstein, the western Canadian Devonian Muskeg Group, and the Silurian Salina Group of the Great Lakes region. The present-day Mediterranean Sea is approximately 2500 to 4000 m deep (Friedman and Sanders, 1978, p. 535, fig. D-15) and Hsu (1972, p. 392) stated that the Mediterranean brine pool at the start of gypsum deposition should have been more than 1000 m deep, i.e. far from entirely desiccated. The characteristic distribution pattern of evaporite facies for completely isolated basins is a bull's eye pattern. This is the same pattern as in modern playa deposits, where progressively higher grade evaporites (most soluble salts) are deposited in progressively deeper, more central parts of the salt pan as it desiccates (Hsu, 1972, p. 388-389, fig. 3). In this model euxinic shales and carbonates are temporally and spatially separated from gypsum and higher-grade evaporites (if present) by this bulls-eye depositional pattern of evaporite facies belts. If this is the depositional model for the Chuar Group, which lacks major gypsum and higher-grade evaporite deposits, the Chuar Group would either represent: 1) only the temporally early, non-evaporite, basin-margin portion of the bulls-eye depositional pattern produced by a subsequent, more basinward, lower lake level, evaporite basin stage , or 2) a tropical lacustrine deposit with a high enough water influx, from streams or a humid climate, to keep salinities below levels at which gypsum evaporite precipitation begins [70 to 72% for calcium carbonate, 124‰ for calcium sulfate (Copeland, 1967, p. 209; Scruton, 1953, p. 2503; Friedman and Sanders, 1978, p. 141; Kirkland and Evans, 1981, p. 186)].

In most modern coastal evaporite basins, such as Lake Macleod, Western Australia, there are salinity gradients such that carbonate precipitation will dominate in areas of water inflow, while gypsum or halite precipitation will dominate in areas of brine ponding (Warren and Kendall, 1985, p. 1018; Warren, 1986, p. 443). This produces an assymmetry to the more typical bulls-eye lithofacies pattern.

Large lakes, like the Great Lakes, experience similar tidal processes to oceans but with smaller tidal amplitudes (Shepard, 1963, p. 95; McHenry, 1992e, v.11, p. 760). Woolnough (1937, p. 1119, 1120, 1145) has pointed out that on the north end of Lake George, Australia there is evidence of a Pleistocene, lake-wide, transverse gravel bar ridge produced by waters which were banked against the north end of the lake by long duration southerly winds.

Evidence favoring tropical lake deposits as possible candidates for models of Chuar Group deposition are as follows.

1) Stromatolites are locally abundant in hypersaline lakes and salinas such as the Great Salt Lake of Utah and salinas of South Australia (Halley, 1976, p. 435, 437; Friedman and Sanders, 1978, p. 247; Kirkland and Evans, 1981, p. 182; Warren and Kendall, 1985, p. 1016, 1017, fig. 4).

2) Kirkland and Evans (1981, p. 182) noted that saline lakes and lagoons contain a cosmopolitan fauna (and flora) characterized by a paucity of species, but an abundance of individuals. Some, like Mono Lake, of east-central California, with a salinity of about 90‰ have "unlimited epilimnic phytoplankton productivity".

3) An arid, probably tropical climate and at least periodic isolation from the sea may be necessary to account for the evidence of desiccation, i.e. mudcracks, ripple marks (can be shallow marine), and questionable rain prints (intraclast impressions), and evidence of hypersalinity or sahbka conditions i.e., salt and gypsum or anhydrite pseudomorphs, casts of gypsum crystals, biomarker distributions, and heavy carbon isotope signatures. Dehler's ongoing work indicates the heavy carbon isotope signatures may also

34

be due to high productivity or high burial rates or diagenesis (many of the C-isotope values in Chuar carbonates are not primary). Other possible explanations of desiccation or hypersalinity/sahbka conditions involve eustatic sea-level fluctuations in a marine setting or climatic variations in rainfall. In addition James (1984, p. 216-219) has pointed out that desiccation features are typical of the intertidal (especially low energy intertidal) and supratidal zones of shallowing upward carbonate sequences, which would require no isolation from the sea.

Evidence against this being the only depositional setting involved includes the following.

1) Evidence of tidal influences in the Jupiter, Carbon Canyon (Dehler, et al. 2001), and Carbon Butte Members (Wiley, et al., 1998, p. 44, 55).

2) Stable carbon isotope ratios (del C13 Aromatic vs. del C13 Saturate) supporting a marine origin for the Tanner, Carbon Canyon, Awatubi, and Walcott Members. Demaison and Moore (1980, p. 1188) noted, however, that the carbon isotopes of recent organic matter in anoxic sedments of Lake Tanganyika are in a range normally associated with organic matter in marine sediments: -21 to -22‰ (Pedee belemnite-PDB).

3) Without at least an intermittent marine connection, what means of dispersal which would introduce an open water, cosmopolitan, eukaryotic planktonic biofacies into an entirely landlocked lake? Before the evolution of multicellular animals and plants as agents of dispersal, wind would be the sole means of dispersal across land, which appears unlikely. However, if the Chuar deposits were those of a saline/hypersaline coastal lake with a periodic surface connection to the sea (storm and spring tidal inflow), that might also allow the periodic introduction of this marine planktonic biofacies.

2) Restricted Normal Marine Euxinic Basin with Freshwater Outflow Blocking Silled Portal (Positive Water Balance) (Table 4, IIA1 and IIA3)

In restricted or semi-isolated normal marine basins with a greater freshwater input (rain, rivers, etc.) than evaporative loss, that is, with a positive water balance, euxinic conditions are created when the thickness of the outflowing surface freshwater lens occupies the full depth of the sill or threshold (Friedman and Sanders, 1978, p. 529). The freshwater and the sill isolate the denser underlying saltwater, preventing reventilation. Dissolved oxygen in the deep saltwater is consumed by first-cycle organic matter creating euxinic conditions. Periods of drought or lowered seasonal rainfall (e.g. winter) may allow occasional partial or complete reventilation of the basin (Friedman and Sanders, 1978, p. 530-531). Modern examples include the Black Sea; parts of the Baltic Sea; Lake Maricaibo; Kaoe Bay, on the coast of Halmahera, Indonesia; Saanich Inlet, British Columbia; and a few Norwegian fjords (Friedman and Sanders, 1978, p. 529; Demaison and Moore, 1980, p. 1189-1192). Organic carbon ranges from 1 to 16.75% (excluding 23.4% from Fjellangervag, Norway containing wood fiber from a saw mill on shore) in the anoxic facies (Strom, 1936, p. 61-66; Strom, 1937; Gripenberg, 1939, p. 304-306; Strom, 1939, p. 361; Trask, 1939, p. 447-450; Caspers, 1957, p. 823; Friedman and Sanders, 1978, p. 529; Demaison and Moore, 1980, p. 1189-1192; Pedersen and Calvert, 1990, p. 459) and is less than 1.4% (Friedman and Sanders, 1978, p. 529) or 4.1% (Gripenberg, 1939, p. 305) in the oxic facies. [In oxic restricted, normal marine basins with two way flow, i.e. the threshold is not blocked by outflowing freshwater, the oxic facies contains less than 6% dry weight organic carbon and the anoxic facies is absent (Pedersen and Calvert, 1990, p. 459, fig. 4)]. The salinity of the Baltic Sea decreases toward its innermost reaches to as low as 5‰ (Zenkevitch, 1963, p. 305; Wagner, 1970, p. 8). Zenkevitch (1963, p. 305) showed that the number of Baltic species decreased in direct relation to the reduction in salinity. Hallam (1965, p. 142, 150) pointed out that numerical abundance of specimens of restricted species is characteristic of waters of low salinity. This does not seem to be a model for Chuar depostion for two reasons:

1) It doesn't account for evidence of hypersalinity and desiccation which require a negative, not a positive, water balance.

2) In basins with a positive water balance with a freshwater surface lens completely blocking the threshold, how would a cosmopolitan marine planktonic biofacies be introduced and how would a marine

microflora survive in fresh surface waters?

3) Restricted Hypersaline Euxinic Basin - Portals with Two-way Flow (Negative Water Balance) (Table 4, IIB1a)

Restricted basins in hot, arid climates lose more water by evaporation than river and rainfall influx. Consequently water level drops and surface seawater flows into the basin. Basins having portals with a deep sill (threshold) allow two-way flow of water: a surface influx of normal marine water and a reflux (outflow, backflow, or counter-current) of dense hypersaline brine at depth. This circulation pattern is termed antiestuarine circulation (Brongersma-Sanders and Groen, 1970; Kirkland and Evans, 1981, p. 187). The inflowing normal marine water forms a wedge which thins to zero thickness at the innermost reaches of the basin. Salinity of the surface wedge becomes progressively higher toward the innermost portions of the basin, and consequently the highest grade evaporites, if present, are deposited in the innermost portions of the basin forming a "teardrop" pattern of evaporite facies belts (Hsu, 1972, p. 388-389, fig. 3). Both "deep water, deep basin" and "shallow water, shallow basin" evaporite depositional models are characterized by the "teardrop" pattern of evaporite facies belts (Hsu, 1972, p. 385-388; Hsu, et al., 1973, p. 240-243). At the innermost portions of the basin, surface water reaches its highest salinity and density due to evaporation and a salinity stratification does not exist. Downwelling occurs creating the dense outflowing reflux current. The amount of oxygen carried to depth depends on the salinity of the downwelling water, as the solubility of oxygen decreases rapidly with increasing salinity. The inflowing surface waters bring in nutrients and are high in organic productivity, rivaling upwelling zones (Kirkland and Evans, 1981, p. 186-188). Wave mixing and oxygenation is confined to the normal marine surface wedge, unless the basin is extremely shallow (Kirkland and Evans, 1981, p. 186-187).

Most deep-water, barred evaporite basin models (Scruton, 1953, p. 146, fig. 4; Hite, 1972, p. 331, fig. 1; Shaw, 1977, p. 7-10, figs. 3, 6; Friedman and Sanders, 1978, p. 535, fig. D-16; Kirkland and Evans, 1981, p. 186, fig. 4) include an inflowing surface wedge with a horizontal gradient of increasing salinity landward along the water surface. Isohalines and isopycnals within the surface wedge vary in different models from subhorizontal to subvertical. The sub-wave base, reflux current occurs in the deep, dense, high-salinity brine pool. The top of the brine pool approximates the sill (threshold) depth at the portal and rises to the water suface at the inner reaches of the basin. These models propose that the salinity gradient of the surface wedge, combined with the salinity range at which different evaporites precipitate, determine the teardrop-shaped distribution of evaporite lithofacies belts. This surface layer of superheated, increasingly hypersaline water precipitates a rain of evaporite particles through the underlying brine pool and onto the basin floor (Shaw, 1977, p. 7-10, fig. 3, 6). It should be stressed that according to this model, gypsum and higher grade evaporite deposition (if present, salinity $\geq 124‰$), and carbonate and euxinic shale deposition of the mesohaline environment (salinity range from 40 to 120‰) are spatially separated in teardrop-shaped lithofacies belts (Kirkland and Evans, 1981, p. 181, 186-187, fig. 4). Carbonates [precipitation salinity range = 72-199‰ (Scruton, 1953, p. 2503)] and organic-rich shales are deposited proximal to the portal. Gypsum [precipitation salinity range = 124-427‰ (Friedman and Sanders, 1978, p. 141; Scruton, 1953, p. 2503)] and higher grade evaporites are increasingly distal to the portal. Kirkland and Evans (1981, p. 181, 188) considered calcium carbonate precipitating in the mesohaline environment (40-120‰) to be an evaporite. One problem with this model is that it is not clear why the deep refluxing brine pool would not precipitate evaporites (if the basin reaches evaporite range salinities), of the maximum surface salinity range, all across the basin floor while refluxing out of the basin. Contrary to the models, therefore, in areas underlying the mesohaline portion of the surface wedge, gypsum and higher grade evaporites precipitating from the deep brine pool would be expected to mix with carbonates precipitating from the surface wedge.

Kirkland and Evans (1981, p. 186-188, fig. 4) postulated anoxic bottom conditions for negative water balance basins in which gypsum or higher grade evaporites are precipitating, which would require

sub-threshold (deep brine pool) salinities greater than or equal to 124‰ NaCl (Friedman and Sanders, 1978, p. 141; Kirkland and Evans, 1981, p. 186) or 199‰ NaCl (Scruton, 1953, p. 2503, Table 1). Brines at a temperature between 20 and 40°C and in the salinity range of gypsum precipitation contain between 2.0 and 4.5 mg dissolved oxygen per kg of water (or ppm or mg/l) (Kinsman, et al., 1973, p. 326, fig. 4). Halite precipitation begins at a salinity between 290‰ (Copeland, 1967, p. 209; Shaw, 1977, p. 2) or 353‰ (Scruton, 1953, p. 2503, Table 1; Kirkland and Evans, 1981, p. 187). Brines at a temperature between 20 and 40°C in the salinity range of halite precipitation contain between 1.4 and 2.3 mg/kg dissolved oxygen (Kinsman, et al., 1973, p. 326, fig. 4). These low oxygen levels are close to the begining of dysaerobic conditions (1 to 0.5 ml/l O_2) as defined in this report and the 1 to 2 ml/l threshold levels above which aerobic oxidative metabolism occurs and below which anaerobic oxidative metabolism occurs (Kinsman, et al., 1973, p. 325). Kirkland and Evans (1981, p. 188) postulated that in basins precipitating gypsum or higher-grade evaporites the refluxing current carries only these relatively small amounts of oxygen to depth and that these small amounts are depleted rapidly by oxidation of abundant organic matter and by oxidation of hydrogen sulfide. A second problem with this model is that the deep brine pool should contain the anoxic facies, if present, but only if the basin is precipitating gypsum or higher-grade evaporites. As with the first problem, in that part of the basin underlying the mesohaline portion of the surface wedge, it is not clear why refluxing brine pool evaporites would not mix with the organic-rich planktic deposits settling into the anoxic brine pool. If we accept this model and disregard these two objections, since major gypsum and higher-grade evaporite deposits are not present in the Chuar Group, the Chuar Group, if deposited according to this model, would only represent the mesohaline portion of the teardrop depositional pattern, which is located proximal to the portal.

Debate exists as to whether these basins can become euxinic and whether they can reach salinities high enough for evaporite deposition. Demaison and Moore (1980, p. 1190, fig. 6, p. 1192) considered all negative water balance basins to be oxic due to bottom oxygenation by the downwelling which creates the reflux current. The modern Mediterranean is experiencing two-way flow through its portal at Gibraltar, but no evaporites are currently being deposited and bottom sediments are not euxinic (Friedman and Sanders, 1978, p. 528, 533; Demaison and Moore, 1980, p. 1192). Its sediments contain 1- 3% organic matter (Trask, 1939, p. 447). The Mediterranean currently has a surface salinity of 36‰ at the Straits of Gibraltar (portal) and 38.5‰ to 39‰ at its distal eastern end (Friedman and Sanders, 1978, p. 533).

The Red Sea, as a whole, is another basin with two-way flow and high evaporative loss and it is also neither an evaporite nor a euxinic basin (Shaw, 1977, p. 7-9; Friedman and Sanders, 1978, p. 536; Demaison and Moore, 1980, p. 1192). The Red Sea does, however, contain localized anoxic areas, both adjacent to the portal to the Gulf of Aden and in isolated deeps (Watson and Waterbury, 1969, p. 272; Demaison and Moore, 1980, p. 1192). The oxygen content in general is very low and the bottom is remarkably barren of animal life (Strom, 1939, p. 365; Dubar and Rodgers, 1957, p. 61). The Red Sea has a maximum salinity at its northwest end and below the sill of 40 to 41% (Friedman and Sanders, 1978, p. 536). Gypsum and halite are precipitated in shallow salinas around the margins of the sea which reach salinities of 300‰ or more, but they are not precipitated in the deep parts of the Red Sea (Shaw, 1977, p. 8).

On the basis of evaporation rates, water balance, diffusion, and salinities, Shaw (1977) concluded that no deposition of evaporites is possible in deep water (1000 ft or more deep) of a semi-isolated basin and that all evaporites must be products of shallow-water deposition. In essence Shaw argued against the possibility of a "deep water, deep semi-isolated basin" model for evaporite deposition. He noted that although the Red Sea has the physical configuration, water balance, and climate matching the classical barred evaporite basin model, it fails to behave as the model hypothesizes in several respects. It is not precipitating evaporites in either a shallow lens or a deep, high-salinity brine pool. There is no deep, high-salinity brine pool below the sill depth. There is no salinity-density stratification below the sill. Waters below the sill are less than 1‰ more saline than the maximum salinity of waters inflowing over the sill.

Lucia (1972) showed that for arid climates, the salinity reached in a restricted or barred-basin is related to the ratio of the surface area of the basin (Ao) to the cross-sectional area of the inlet's inflow (Ai).

37

A plot of this ratio (Ao/Ai) against the salinity of bodies of water with an average depth of 10 m or less in a dry climate, showed a rapid increase in salinity when the ratio reached 10^6 (Lucia, 1972, p. 164-167, figs. 4 and 5, Table 2). The initiation of gypsum precipitation (salinity = 100‰) also intersects this plot at the same ratio. Lucia (1972, p. 165) concluded that gypsum deposition means "restriction" to an Ao/Ai ratio on the order of 10^6 or higher in an arid or semiarid climate. Bedded gypsum can be deposited either in hypersaline lakes or in standing bodies of water with a minor connection to the ocean, meaning the channel would generally be so small as to be geographically insignificant. The Ao/Ai ratios for the modern Red Sea and Persian Gulf, which are not precipitating gypsum (salinites are 37-41‰ and 39-41% o respectively), are 3×10^5 and 1×10^5 respectively. The Mediterranean Sea has surface area of 970,000 square miles and a portal, the Strait of Gibraltar, which is 8 miles wide by 286 m (938.3 ft) deep, which gives an Ao/Ai ratio of 6.8×10^5 (Friedman and Sanders, 1978, p. 533; McHenry, 1992c, p. 1008). Lucia (1972, p. 167) further concluded that salt deposition must indicate complete surface disconnection from the ocean, with salt water supplied from ground water, sea water springs, or periodic marine flooding. In the modern salt deposits of Ojo de Liebre Lagoon, in Baja California, 2-3 m of salt have been deposited in a salt basin flooded by the ocean every 20 years. Lucia's (1972) conclusions, where salinity is not depth dependent, may be less comprehensive than and inconsistent with those of Shaw (1977, p. 15), where shallower depths promote increased evaporation and salinity.

In shallow open-marine coastal areas tidal ranges of 15 to 30 ft are common (Holmes, 1965, p. 787; Bickford, et al, 1973, p. 331). Long bays, like the Bay of Fundy (world maximum tides of 60 ft) or the English Channel (tides to 42 ft in the Bristol Channel), which have natural periods nearly in resonance with the tidal period have enormous tidal ranges. By comparison, most inland seas, like the Gulf of Mexico and the Mediterranean, have very small tides, with a normal range of not more than 1 or 2 ft, because of their restricted entrances (Holmes, 1965, p. 788; Shepard, 1963, p. 95; Shepard, 1969, p. 21, 56). Tides in the Black Sea have a normal range of only 4 inches (Holmes, 1965, p. 787). However, large tidal currents exist locally in inland seas where there is a narrow strait between two sizable bodies of water, for example at the entrance to Barataria and Terrebonne Bays, Louisiana or the Straits of Messina, Italy (Shepard, 1963, p. 95-96).

Woolnough (1937, p. 1132, 1133, 1136) pointed out three significant reasons why the bar or portal responsible for restricted basins, may not itself be preserved or recognized in the geologic record. These include: 1) the small area of the bar relative to the area of the basin; 2) the weak and temporary nature of many bars/portals make them subject to contemporaneous erosion and subsequent erosional removal by slight uplift since many probably formed on peneplained, continental margins near base-level; and 3) lack of explicit search for them or anticipation of finding them in the field.

Evidence favoring this model for Chuar deposition includes the following:

1) The antiestuarine circulation pattern explains the introduction of a cosmopolitan marine planktonic biofacies into the basin and provides a nutrient supply which can sustain high organic productivity.

2) The negative water balance is consistent with high evaporation rates and evidence of hypersalinity and possibly for desiccation, although there is not evidence in the Chuar Group for sahbka facies.

3) Hypersaline marine environments are known to support domal and columnar stromatolites (Hamelin Pool, Shark Bay, Australia).

4) It provides a restricted basin setting favorable for dolomitizing brine formation.

5) It allows for marine stable carbon isotope signatures and evidence of marine tidal influences.

This model faces three problems as a model for Chuar Group deposition.

1) Can such basins can actually become anoxic? In the modern negative water balance basins with two way portal flow, the anoxic facies is absent and the oxic facies of the Persian Gulf, for example, reaches a maximum organic carbon content of 2.5% (Demaison and Moore, 1980, p. 1192). The Mediterrean has a maximum organic carbon content of 1.7% (Trask, 1939, p. 447). While these values are close to average Walcott TOCs, they are less than maximum Walcott Member values.

2) If these basins do become anoxic in the deep brine pool due to gypsum or higher-grade evaporite deposition distal to the portal, and if the Chuar Group represents the mesohaline portion of the basin

proximal to the portal, then why wouldn't refluxing brine pool evaporites be mixed with the planktic organic-rich deposits settling to the euxinic brine pool.

3) Similarly, if these basins do become anoxic in the deep brine pool due to gypsum or higher-grade evaporite deposition distal to the portal, and if the Chuar Group represents the mesohaline portion of the basin proximal to the portal, then why wouldn't refluxing brine pool evaporites mix with carbonates precipitating from the surface wedge. Destruction of gypsum by sulfate-reducing bacteria producing calcium carbonate is a possibility, however the carbonate members of the Chuar Group are generally associated with benthonic microfossils indicative of oxic, not anoxic, conditions. Sulfate-reducing bacteria are excluded by oxic conditions. Furthermore, bedded gypsum or salt are unknown from the Chuar Group.

4) Restricted Hypersaline Euxinic Basin - Portals with One-way Flow (Negative Water Balance) (Table 4, IIB2A)

This model is similar to the previous one except that the portal is shallower, permitting only normal marine inflow and blocking reflux (outflow). Inflowing surface marine water again flows to the most distal region from the portal, becoming progressively denser by evaporation. Eventually it sinks, carrying an amount of dissolved oxygen to the basin floor which is dependent on the salinity of the water when it leaves the surface as described in the previous model. In these basins the densest brine accumulates in the deepest part of the basin and the most saline evaporites, if present, are deposited in the deepest central portions of the basin [bullseye pattern of Hsu (1972, p. 388-389, fig. 3)]. No modern examples of this type of basin are known either (Friedman and Sanders, 1978, p. 536). As in the previous model non-evaporite deposition is spatially separated from evaporite deposition (if present) by the bulls-eye depositional pattern of evaporite facies belts. The Chuar Group, lacking major evaporite deposits, would represent the shallowest portion of such a basin, lacking gypsum or higher grade evaporites..

The Gulf of Karabugas on the Caspian Sea, which has been taken as the example for Ochsenius's (1877; 1888) barred evaporite basin model, is experiencing only inflow and no reflux (outflow) and is extremely shallow (Hsu, 1972, p. 374-375). It is an evaporite basin, with the most saline evaporites currently being potash salts, but only reaching gypsum in the 1800's when the Gulf was deeper. Its maximum depth was 13 m in the 1800's and is currently only 3.1 m due to fall in water level of the Caspian Sea in the 1930's (Hsu, 1972, p. 374-375).

The Hamelin Pool Basin of Shark Bay, western Australia may be an example of this basin type, however it is not euxinic and it is not precipitating subaqueous gypsum, although Warren and Kendall (1985, p. 1013) reported supratidal evaporites in Shark Bay. It exhibits vertical salinity boundaries, becoming more saline toward the innermost reaches of the bay and reaching a maximum of 65,000 ppm (Friedman and Sanders, 1978, p. 526). Horizontal stratification of water masses was not found and no seaward hypersaline bottom reflux was seen (Friedman and Sanders, 1978, p. 526). As salinity increases, the numbers of species decreases, but the number of individuals of surviving species increases (Kirkland and Evans, 1981, p. 183). Salinities at Hamelin Pool, however, do not reach the minimum necessary for the subaqueous precipitation of gypsum, i.e. 124,000 ppm (Friedman and Sanders, 1978, p. 141; Kirkland and Evans, 1981, p. 186).

As a candidate for a Chuar Group depositional model this model has all the advantages of the previous model, but may avoid its disadvantages. Without a reflux current it it is more probable that in these basins the the subsill water layer would become anoxic and reach a high enough salinity to begin precipitating evaporites. Such a basin would be similar to the Dead Sea which is fed by the Jordan River and smaller streams except that, in this case the marine inflow would be more saline to start with. Anoxia could explain the high TOC values in the Walcott Member as well as evidence of sulphur products. Salinities sufficient for gypsum (anhydrite) deposition could explain the sulphur products as a result of sulphate reducing bacteria.

There are two possible problems with this model:

1) Depending on the salt balance of the basin, which in turn depends on rates of evaporation, marine inflow (dilution), evaporite precipitation, and diffusion, a progressive salinity increase could lead to such a basin becoming predominantly an evaporite basin. Since bedded gypsum or higher grade evaporites are not present in the Chuar Group, the Chuar Group would only represent deposits of the shallow, non-evaporite portion of the bulls-eye depositional pattern characterizing this basin model.

2) This model does not easily account for desiccation since inflowing seawater maintains basin water level close to sea-level, **unless** the basin is periodically isolated from the sea (becoming a lake) by (glacio-) eustatic sea level changes or tectonic alterations of sill depth. Alternatively, the basin could remain connected to a sea experiencing (glacio-) eustatic sea level changes. Evidence for glacio-eustatic sea level changes during Chuar Group deposition is presented by Dehler, et al. (2001). Isolation would be more easily accomplished with this model than the previous model because of this model's shallower portal (sill).

5) Anoxic Depressions (Basins) in the Oxic Open-ocean (Table 4, III)

Euxinic conditions may occur in open-ocean closed bathymetric lows (basins) bordering the continents. In the deep sea, water temperature decreases with depth. An open-ocean, closed bathymetric low (basin) will fill with water of a uniform temperature determined by the depth of the highest closed contour and can become euxinic. This is especially true if the water filling the depression derives from an oxygen minimum layer described in Category 7, below, as in the case of the southern California continental borderland. Modern examples occur in the Moluccas, Indonesian Archipelago; the southern California continental borderland; the Orca Basin, N.W. Gulf of Mexico; and the Cariaco Basin, off northern Venezuela (Friedman and Sanders, 1978, p. 531; Demaison and Moore, 1980, p. 1192-1193). Organic carbon content ranges from 0.8 to 6% in the anoxic facies and averages 0.8% in the oxic facies of these basins (Trask, 1939, p. 446; Demaison and Moore, 1980, p. 1192-1193).

This model does not appear to be a likely one for Chuar Group deposition for two reasons.

1) The sill depths controlling such basins are far deeper, ranging from about 200 m for the Santa Barbara Basin (Friedman and Sanders, 1978, p. 532) to 2200 m for the Orca Basin (Demaison and Moore, 1980, p. 1193), than the likely depositional depths for the Chuar Group. The likely maximum depth for domal and columnal stromatolite deposition is not much deeper than 10 m (Dill, et al., 1986). A maximum depth for stromatolite deposition may be 150 ft (46 m) as proposed by Playford and Cockbain (1969) for the Devonian of Western Australia. The Carbon Butte Member was deposited under shallow marine tidal influences.

2) It would be very unlikely that these submarine basins with such deep sills would become desiccated or hypersaline.

6) Anoxic Layers Caused by Upwelling (Table 4, IVA)

Upwelling occurs when the net transport of water is offshore, and the water moved away from the shore is replaced by water from as much as 300 meters below (Turekian, 1968, p. 79; Parrish, 1982, p. 755). Upwelling occurs when prevailing winds, associated with permanent atmospheric latitudinal pressure cells, blow parallel to the coast (Parrish, 1982, p. 755). Parrish (1982, p. 755) identified two major categories of upwelling in the present-day oceans: **coastal upwelling** and **open-ocean divergences**. There are seven major present-day areas of **coastal upwelling** which she grouped in three categories:

1) Meridional upwelling is asssociated with subtropical high pressure cells and occurs on west-facing, longitudinally oriented oceanic shelves at about 30° (i.e. low) latitude. Examples occur west sides of continents, i.e. off western North America, western South America, and northwestern and southwestern Africa. These are the predominant type of upwelling in the modern world because of the preponderance of present-day meridionally oriented coastlines.

2) Zonal upwelling is driven by zonal winds and occurs on north- or south-facing coastlines that are

situated at the proper latitude relative to the major zonal wind system. The major present-day example occurs off northern South America and Yucatan.

3) Monsoonal upwelling is seasonal and driven by cross-equatorial winds associated with monsoons and occurs when monsoonal winds blow parallel to a coastline. Present-day examples occur off Somalia and possibly western India.

Open-ocean Divergences include three types which are associated with divergence under stable atmospheric low-pressure systems and include:

1) Symmetrical divergence at the equator.

2) Symmetrical divergence in wide oceans at about 60° latitude (e.g. around Antarctica).

3) Radial divergence in more restricted oceans at about 60° latitude (e.g. around the southern tip of Greenland).

Upwelling water is rich in nutrients, especially nitrates and phosphates, and results in high biologic productivity (Demaison and Moore, 1981, p. 1195). This high productivity can result in anoxia in the underlying sediments as occurs on the southwest African shelf off Namibia below the Benguela Current and along Peru below the Humbolt Current (Demaison and Moore, 1981, p. 1194-1200). As shown in Table 4, the anoxic facies of upwelling zones can contain between 3 and 26% organic carbon, whereas the oxic facies contains between 0.5 and 3% organic carbon (Demaison and Moore, 1981, p. 1194-1200). The anoxic facies are associated with phosphorites, diatomites, and glauconites (Demaison and Moore, 1981, p. 1205, 1206; Parrish, 1982, p. 756). By comparison organic carbon in the oxic facies of upwelling zones without anoxic layers ranges from 0.10 to 2.8% (Table 4). The depth range of the anoxic facies is from 100 (or less?) to 500 m (Table 4).

As a model for the Chuar group, this model shares the same two weaknesses of the previous model. The organic matter of the Benguela Current sediments are mostly planktonic and the sediments of the Peru Current are silty clays and laminated diatomaceous oozes (Demaison and Moore, 1981, p. 1194-1200) indicative of deeper water deposition than is likely for the Chuar Group. For the Chuar Group, this model does not account for the nearshore, shallow water, benthonic biofacies and shallow water stromatolites.

7) Anoxic Open Ocean Water Masses (Oxygen Minimum Zones) (Table 4, VA)

The deep (below 1500 meters) and intermediate depth circulation of the oceans is driven by density differences created by variations in temperature and salinity and is termed thermohaline circulation (Turekian, 1968, p. 76-80). Differences in salinity and temperature are caused by chilling, evaporation, freezing, or dilution by rain or meltwater (Turekian, 1968, p. 79). Water masses with a distinctive range of salinities and temperatures are termed deep or bottom water below 1500 meters and are termed intermediate water masses from about 100 to 1500 meters (Turekian, 1968, p. 78-80). All deep and bottom water masses, and some intermediate water masses, have their origin in high latitudes, i.e. the North Atlantic and around Antarctica, where cold oxygenated surface water is chilled, increasing in density until it sinks to abyssal depths (Turekian, 1968, p. 76-80; Demaison and Moore, 1980, p. 1200). From the pole of origin, water within these water masses flows toward the opposite pole. With increasing distance from the pole of origin, and with increasing time from contact with the atmosphere, there is a gradual decrease in oxygen concentration within each water mass due to biochemical oxygen demand over time (Demaison and Moore, 1980, p. 1200; Pedersen and Calvert, 1990, p. 459). A water mass containing only marginal amounts of dissolved oxygen (0.1 - 0.5 ml/l) due to oxidation of organic debris derived from high productivity in the overlying photic zone is termed an oxygen minimum zone (Richards, 1957). Present-day oxygen minimum zones exist in the northeastern Pacific Basin and the northern Indian Ocean (Demaison and Moore, 1980, p. 1200-1204), the western Gulf of Mexico (Friedman and Sanders, 1978, p. 524) and off the southern California continental borderland (Demaison and Moore, 1980, p. 1201-1203; Ingle, 1980). Oxygen-depleted areas in the Pacific and Indian oceans tend to occur in cul-de-sacs or in the lea of sources of oxyenated bottom water (Demaison and Moore, 1980, p. 1200). The preferential distribution of

oxygen-minimum layers in the world ocean is at low latitudes and on the eastern sides of oceanic basins, reflecting the effects of the Coriolis force upon deep circulation of oxygenated bottom water (Demaison and Moore, 1980, p. 1200 and 1205). The present-day Atlantic Ocean, forming an open corridor between polar oxygen sources, does contain an oxygen-minimum layer, but only the Angola Basin reaches the anoxic level of less than 0.5 ml/l (Demaison and Moore, 1980, p. 1202). Table 4 indicates that the anoxic facies of oxygen minimum zones contain from 1 to 11% organic carbon, while the oxic facies ranges from less than 0.5 to <2% organic carbon. By comparison the oxic facies of the oxic open ocean has an organic carbon range of 0.5 to 5% (Table 4). The depth range for the organic-rich, anoxic facies is 100 to 1500 m (Table 4).

Ingle (1980) used the top and base of important water mass boundaries, including the oxygen minumum zone, to interpret the Cenozoic paleobathymetry and depositional history of the southern California continental borderland. He (1980, p. 167, 177) gave an upper boundary of 200 to 500 m and a lower boundary of 1000 to 1500 m, for the oxygen minimum zone off present-day southern California, which approximates the upper middle bathyal depth zone (upper middle continental slope). Anaerobic conditions in the oxygen minimum zone occur where oxygen content is less than 0.2 ml/l (Ingle, 1980, p. 173). Presently the Santa Barbara Basin and Gulf of California are euxinic basins (Ingle, 1980, p. 186-187). "Intersection of this unique water mass (oxygen minimum zone) with the continental slope and/or basin sills leads to a reduction or exclusion of macrofaunal invertebrates and minimal bioturbation of sediments, resulting in preservation of conspicuously thin bedded or laminated sediment enriched in organic matter" (Ingle, 1980, p. 168). Ingle proposed that the laminated diatomites and siliceous siltstones and mudstones of the Miocene Monterrey Formation were deposited in the oxygen minimum zone of marginal marine closed basins.

Because this model is a relatively deep-water model, as a potential Chuar depositional model, it faces the same two objections as the two previous models.

Oxic Organic-rich Basin Models

8) Shallow, Saline/Hypersaline, Coastal and Continental Oxic Lakes (Table 4, VIA)

Shallow, saline or hypersaline coastal and continental oxic lakes are one of the two evaporitic depositional settings with hydrocarbon source-rock potential favored by Friedman (1980), Bauld (1981a, 1981b), and Warren (1986). The second of these is the lagoon (10) environment, considered in the following section (9-10). These authors identified cyanobacterial mats as the source of high organic carbon found in these two modern settings. As seen in Table 4, organic carbon in present-day saline/hypersaline coastal and continental lakes ranges from 1.2% to 29.6%.

Warren (1986, p. 442-445) noted four ways by which evaporating brine bodies are connected to their water sources, involving the combinations of continuous or periodic and surface or subsurface influx. The resulting evaporite basins range from: 1) basins with a stable water level, with stable depositional lithologies, and favoring early preservation of organic matter in saline, anoxic pore waters, to 2) basins with unstable water levels, complex evaporite lithologies, penecontemporaneous diagenetic overprints, and destruction of organic matter due to influx of fresh, meteoric, oxygenated pore waters. Warren (1986) believed that desiccating inland seas or lakes (Model 1) and rift basin lakes (Model 1) would experience continual saline, anoxic, water saturation and rapid burial to preserve the high organic content found in these settings. Bauld (1981b, p. 314) similarly believed that shallow saline lakes undergoing total evaporation, with subsequent flash flooding resulting in a clay cap, would result in maximum preservation of organic matter. Both authors believe organic matter forms in oxic conditions (Model 8), whereas preservation results from subsequent extreme salinity and anoxia (Model 1) due to further evaporation and rapid burial.

As a model for Chuar deposition, this model explains the benthonic biofacies of the cherty

carbonate lithofacies, but it does not explain the absence of a benthonic biofacies in the planktonic biofacies of the clastic and shale lithofacies.

9-10) Other Non-Euxinic (Oxic) Categories: (9) Deltas, (10) Lagoons, (Table 4, VIB, C)

As shown in Tables 4 and 5, other non-euxinic environments including deltas and lagoons, can reach significant levels of organic carbon enrichment up to 32%. The organic carbon content of lagoons ranges from 0.1 to 32‰. Modern examples of lagoons include the bays of Texas, Laguna Mormona of Baja California, Mexico, Pamlico Sound on the east coast of the United States, and Abidjan Lagoon of Ivory Coast (Table 4).

Laguna Madre of southern Texas is the only large hypersaline lagoon in the United States. Its salinity varies from about 35‰ at the the inlets (passes) to the Gulf of Mexico up to 75‰, although it reached as much as 113.9‰ prior to the completion of the Intercoastal Waterway in 1946 (Kirkland and Evans, 1981, p. 183-184). Laguna Madre is one of the most biologically productive areas in the world, with exceptionally large fish, zooplankton (primarily copepods), mollusk, and phytoplankton (blooms of red-pigmented green algae) populations (Kirkland and Evans, 1981, p. 184). The northern and southern Laguna Madre has sandy bottom sediments with water depths less than 2.5 ft deep (Rusnak, 1960, p. 194). Slightly deeper parts of the lagoon act as wave protected fine-grained sediment traps and settling basins for clays, such as, along its western edge with depths up to 7 ft and in Baffin Bay with depths up to 8 and 10 ft. In parts of Laguna Madre with bottoms consisting of soft fluid clay, such as the central part of Baffin Bay, free-swimming organisms are present, while bottom-dwelling organisms (fauna) are strikingly absent. Bottom-dwelling organisms are absent because the soft fluid clay does not prevent them from sinking below the zero Eh surface and perishing in the anaerobic near-surface sediment. Recently deposited, soupy muds may include up to 90% or more water and have practically no mechanical strength before compaction (Dunbar and Rodgers, 1957, p. 24). Baffin Bay is barren of marine vegetation except for a blue-green algal mat along the sandy shore. Also found in its sandy margins are four species of macro-invertebrates (Rusnak, 1960, p. 185, Table IV). Water depths in Baffin Bay average 5 ft and salinity is consistently very high with a chlorinity of 30‰ (Rusnak, 1960, p. 187, Table V) [equaling a salinity of 54.45‰ by the formula (salinity = 0.03 + 1.805 x chlorinity) of Zenkevitch, 1963, p. 529; or 49.35‰ by the formula (salinity = 1.645 x chlorinity) of Dresser Atlas, 1979, p. 6]. To summarize, the central portion of Baffin Bay has a soft fluid clay bottom, is up to 8 to 10 ft deep, and lacks both a benthonic fauna and marine vegetation. Its sandy margins support four species of benthonic macro-invertebrates and blue-green algal mats.

Rusnak (1960, p. 187, Table V) also noted blue-green algal mats in Laguna Madre in barrier flats of the southern Laguna, with water depths of less than one foot and a highly variable salinity, ranging from 22‰ to 45‰. These areas have a sand bottom and are barren of marine vegetation except for blue-green algal mats.

Shepard (1963, p. 475-476; 1969, p. 222) noted that black muds with unburrowed, laminated bedding are found in the Laguna Madre where lack of oxygen exists under an algal mat coating of the sediments. Rusnak (1960, p. 187-188) noted that in the semi-arid, hypersaline Laguna Madre, fine-grained sediments in shoal areas associated with algal mat growth change from akaline-oxidizing at the sediment surface to acid-reducing conditions a few centimeters below the surface. The acid-reducing conditions are associated with organic matter decomposition and strong H_2S odors. The overlying waters are well oxygenated and alkaline.

Goldman (1924) reported that two areas of the Chesapeake Bay contained organic-rich black muds associated with the mortality of fish and oysters. The site of the fish mortality occurred in a depression in the bottom of the Potomac River near its mouth where sediments contained hydrogen sulfide. The oyster mortality occurred along the west side of the Chesapeake Bay in black muds located between the sandy, near-shore deposits and the better-scoured central channel.

A lagoonal depositional environment is a possible model for the Chuar Group. Periods of low sediment influx allowing the periodic establishment of benthonic carbonate stromatolites containing a benthonic biofacies may have alternated with periods of higher clay sediment influx with soft fluid bottom conditions and anoxic conditions in the near-surface sediment. The soft fluid (soupy or watery) clays with anoxic conditions slightly below the water-sediment interface could have eliminated the benthonic and carbonate biofacies, while entombing a planktonic biofacies derived from the overlying oxygenated water column of the lagoon. The anoxic sediment column would be laminated due to a lack of bioturbation and anoxic sediments would allow sulfate-reducing bacteria to produce sulfur products. Periods of stromatolite growth would allow establishment of algal mats which could also produce underlying anoxic conditions promoting organic matter preservation. Alternatively slight eustatic or tectonic changes in these shallow lagoons could transform large areas from shore-margin flats supporting cyanobacterial mats to slightly deeper clay and clastic sediment traps. A similar suggestion is made by Dehler, et al. (2001). Klemme and Ulmishek (1991, p. 1839) suggested that scarcity of fossils in lower-middle Paleozoic organic-rich black shales "probably does not suggest anoxia, but rather indicates semi-liquid substrates unfavorable for sessile animals". Similar semi-liquid substrates are seen in modern anoxic basins. Gripenberg (1939, p. 300, 305) noted that the post-glacial black muds of the Baltic Sea have a gelatinous appearance if the percentage of colloid is high, but the muds seem almost liquid if the mineral components are sandy or silty. Strom (1936, p. 65) described "black, putrid, very loose deposits" in fjords of Norway.

11) Other Non-Euxinic (Oxic) Categories: Areas of Limestone Deposition (Table 4, VID)

Areas of Limestone deposition can contain from 0.6 to 16% organic carbon (Tables 4 and 5). In the Bahamas and Florida, organic matter ranges from 3 to 6% in shallow marl banks in 0.3 to 1 m of water, and ranges from 1 to 6% in adjacent deeper oceanic water (Trask, 1939, p. 450). Organic carbon content in the Bahamian shallow marine platform oolite ranges from 3 to 5% (Warren, 1986, p. 446, Table 2). Organic carbon in the Gulf of Batabano, on the southern Cuban shelf ranges up to 16% (Warren, 1986, p. 446, Table 2). Friedman and Sanders (1978, p. 369) considered this to be a small-scale reef-fringed, shelf lagoon. Carbonates of the Gulf lack iron to reduce S^{-2}, allowing the buildup of H_2S in the near surface sediment to levels sufficient to kill sulfate reducing bacteria and resulting in the high total organic carbon content. Surface waters are oxygenated and salinity ranges from 37‰ at the seaward southern margin to 28‰ in the Bay of Pigs due to high rainfall and the high freshwater discharge of the Rio Hatiguanico (Friedman and Sanders, 1978, p. 369; Warren, 1986, p. 448).

Klemme and Ulmishek (1991, p. 1839) proposed that late Proterozoic through Cambrian shallow-water marine, organic-rich stromatolitic carbonate rocks formed under anoxic, dysoxic, and even oxic (including reefal) conditions. Stromatolitic dolomites of the Turkut Formation of the northern Siberian craton contain 2% total organic carbon (Klubov, 1983). Stromatolitic carbonates are the source rocks for oil and gas fields and shows and for bitumen deposits in the Sichuan basin of China (Tang Zeyao and Zhan Shenyu, 1984), on the northern Siberian Craton (Klubov, 1983), and on the eastern Russian craton (Lagutenkova and Chepikova, 1982).

12) Other Non-Euxinic (Oxic) Categories: Epeiric Seas

Freidman and Sanders (1978, p. 360-384) and Friedman (1980) proposed a model for hydrocarbon source rocks and evaporites related to vast epeiric seas having the following elements. The model considers ancient epicontinental seas having great widths (thousands of km) and shallow depths (less than 30 m) which dampen periodic lunar tides and extensive wave action. Citing the Red Sea, Persian Gulf, Mediterranean Sea, and Baltic Sea as examples, Hayes (1967, p. 120) noted that "the hydrologic energy of many inland seas, which are not exposed to normal oceanic waves, currents, and tides, is not directly correlative with that of the open ocean". Epeiric sea water level fluctuation would be irregular and in

response to wind effects rather than tides (Friedman and Sanders, 1978, p. 361). Circulation would result from wind-driven unidirectional surface currents rather than deep thermohaline circulation (Friedman and Sanders, 1978, p. 361, 373, 374). Waters 30 m deep could accomodate large sea waves but would dampen long period swells (Friedman and Sanders, 1978, p. 373-374). If, as in the modern oceans, evaporation exceeded precipitation, hypersalinity would increase away from the open ocean. Epeiric seas within 40 degress of the equator would tend to be hypersaline (Friedman and Sanders, 1978, p. 374). Evaporites would precipitate on vast stretches of the sea floor. In inland flats evaporation would produce periodic emergence and desiccation. The model needs no semi-isolated or isolated morphologic basin having a portal or sill to restrict passage of sea water. Evaporites accumulate due to hypersalinity developed over thousands of kilometers of shallow water in a tropical arid setting. There is no need for brines exhibiting density stratification or pycnoclines. Waters of the shallow epeiric seas would be wind mixed throughout (Friedman and Sanders, 1978, p. 374). Abundant mat-forming algae, exhibiting wide tolerance to salinity variations and desiccation, carpeted the vast evaporite shallows and flats. These same conditions eliminated less tolerant invertebrate algal-mat consumers. Dolomite formation was promoted by hypersaline interstitial fluids and interstitial precipitation of evaporites. On large epeiric flats evaporites precipitated subaqueously in marginal playa lakes forming fine laminae, and precipitated interstitially in marginal sabkhas forming nodular gypsum or anhydrite. Sheet or flash floods of fresh-water runoff spread seasonally across the flats filling the playa lakes. This model blurs the distinction between marine and non-marine evaporites. On the epeiric flats hypersalinity alternated with emergence, desiccation, and fresh-water flooding. Hypersalinity resulted in dolomitization. Leaching fresh-waters resulted in the dissolution of non-dolomitzed calcium carbonate and produced intercrystalline and moldic porosity. Fresh waters may have removed evaporites after deposition producing pseudomorphs of evaporites, solution collapse breccias, fracture porosity, and other features. The model postulates hydrocarbon traps formed in regressive sequences with the following three components. Stromatolitic algal mats form the source rocks. Reservoirs are formed by hypersalinity-induced dolomitization, followed by fresh-water leaching, solution collapse, and fracturing. Non-porous nodular or bedded anhydrite or halite form the caprock or seal facies.

Friedman and Sanders (1978, p. 373) and Sanders (1980, p. 599) noted that epeiric seas on a continent-wide scale as inferred to have existed in the past are not found in the modern world. Six modern examples on a smaller scale are listed by Heckel (1972, p. 268-270) and include: 1) Hudson Bay, 2) the Baltic-North Sea system, 3) the Persian Gulf, 4) the Sunda Shelf comprising the Gulf of Siam, the Java Sea, and the southwestern part of the South China Sea, 5) the Yellow Sea, and 6) the Arafura Sea, Gulf of Carpenteria, and Sahul Shelf (part of the Timor Sea) between Australia and New Guinea. Terrigenous clastics are the dominant sediments of all but the third example, with sediments of the first example, Hudson Bay, being largely unstudied (Heckel, 1972, p. 268-270). Areas of carbonate deposition are also important in the sixth example.

Keulegan and Krumbein (1949) showed that the gently shelving sea floor of the western Yellow Sea effectively dampens storm waves such that they do not break at shore. In the Gulf of Chihili (Pechili or Po Hai) off the northern Yellow Sea sandy beaches and barrier islands are notably absent (Dunbar and Rodgers, 1957, p. 84). Sediments of the Gulf of Chihili are mud and sand (Heckel, 1972, p. 261). Fresh water influx from the Hwang Ho River reduces salinity of the Gulf to about 25 ppt. NaCl is reduced to 52.16% as compared to a normal value of 77.76%, and MgCl2 is increased to 32.59% as compared to a normal value of 10.88%, and MgSO4 is increased to 9.46% as compared to a normal value of 4.74% (Dunbar and Rodgers, 1957, p. 84). Faunas of the Gulf exhibit a reduction in diversity and dwarfing (Heckel, 1972, p. 261).

Since evaporites are not found in the Chuar Group, if the Chuar Group were deposited according to this model, the Chuar Group would likely have formed in an epeiric sea near enough to its marine origin that its salinity had not risen to the range of gypsum precipitation. Alternatively Chuar deposition may have occured pole-ward of 40 degrees from the equator where lower evaporation rates may not have been sufficient to produce gypsum-precipitating hypersalinity (see Friedman and Sanders, 1978, p. 373-374).

Alternation of Environments and Cyclicity

Scruton (1953, p. 2509-2510) and Demaison and Moore (1980, p. 1192) have both suggested that a change in the precipitation-evaporation budget could convert a negative water balance, oxygenated evaporite basin into a positive water balance, euxinic basin. Demaison and Moore (1980, p. 1192) suggested this alternation model for the Pleistocene of the eastern Mediterranean. There, anoxic, laminated muds (sapropels) of the upper Pleistocene contain 2 to 8% organic carbon and are devoid of benthic fauna. By contrast oxidized Pleistocene sediments contain less than 0.5% organic carbon. The anoxic sediments may have occurred when a sudden influx of freshwater, due to increased precipitation or deglaciation converted the Mediterranean into a positive water balance basin. Friedman and Sanders (1978, p. 531) described an alternative explanation involving the influx of relatively dense aerated saltwater from the Mediterranean into the Black Sea during periods of rising, but lower, sea levels. Displaced fresh water from the Black Sea spread across the eastern Mediterranean causing stagnation and euxinic conditions beneath it.

Pedersen and Calvert (1990, p. 460-461) suggested that Pleistocene organic carbon enrichments during glacial stages which are seen in cores from both the Atlantic and Pacific oceans are a result of increased productivity, driven by enhanced atmospheric circulation and upwelling during glacial stages.

As previously described (Model 1) the negative water balance marine Red Sea may have been converted to a hypersaline lake during Pleistocene glacial stage lower sea-levels (Friedman and Sanders, 1978, p. 536).

Strom (1936, p. 66) pointed out that due to post-glacial rebound, a number of present-day Norwegian lakes have gone through stages of being: 1) well-ventilated saltwater fjords, then 2) badly ventilated, euxinic, land-locked fjords, 3) afterwards a transitionsal stage with occasional invasions of saltwater, 4) then true lakes with diminishing quantities of saltwater at the bottom (still unventilated), and finally 5) well ventilated freshwater lakes. Strom (1936, p. 81) also pointed out that "the state of relative equilibrium in the bottom waters of badly-ventilated basins is a delicately adjusted mechanism. Through long-time changes in climate or relative water level we may easily get a primary alternation between black shales and "ventilated" deposits, which in warm waters are mainly limestones".

Bauld (1981b) and Warren (1986) postulated that cyanobacterial derived organic-rich sediments deposited in shallow, saline, oxic coastal or continental lakes (Model 8 or Model 1) are preserved by progressive desiccation producing anoxic and extreme hypersaline conditions (Model 1).

Chuar Group Cyclicity

The foregoing review of possible depositional and basin circulation models for the Chuar Group implies that there are many possible secondary mechanisms which could produce the cyclical alternation of Chuar Group carbonates and shales. The primary driving mechanism for this cyclicity is most likely either episodic tectonism or glacioeustacy. Dehler, et al. (2001) concluded these two factors in combination with short-term wet/dry cycles controlled short and long term Chuar Group cyclicity. Timmons, et al. (2001) document movement within the Butte fault system throughout Chuar Group deposition, which could have caused periodic fluctuations in water depth and/or altered the degree of restriction of the Chuar Group depositional basin.

A second possible primary driving mechanism for lithologic cyclicity is glacioeustacy. Hoffman, et al. (1998, p. 1345) dated the Neoproterozoic [1000-543 Ma (Dehler, et al., 2001)] Sturtian glaciation at approximately 760 to 700 Ma and dated the Varangian glaciation at approximately 620 to 550 Ma. Two discrete glacial units of Sturtian age, the Chuos and Ghaub formations occur in the Otavi Group of northern Namibia (Hoffman, et al., 1998, p. 1342). Hoffman, et al. (1998) and Hoffman and Schrag (2000) postulate that the Earth's climate has alternated between global glaciation (a snowball Earth) and extreme greenhouse conditions (a hothouse Earth) as many as four times between 750 Ma and 580 Ma. The age of the Chuar Group is constrained by Rb-Sr age dates of 1070 +/- 70 Ma for flows of the underlying

Cardenas Basalt (Elston, 1989, p. 97, 104) and by an U-Pb age date of 742 +/- 6 Ma for an ash at the top of the Walcott Member (Dehler, et al., 1999; Karlstrom, et al., 2000; Dehler, et al, 2001). Estimates of the age of the base of the Chuar Group range from 900 Ma (Elston, 1989, p. 97, 104), to 850 Ma (Weil, et al., 1999), to 800 Ma (Karlstrom, et al., 2000, p. 620). The overlap (760-742 Ma) of the dates of the Chuar Group (900-742 Ma) with those of the Sturtian glalciation (760-700 Ma) indicate that the Sturtian glaciation may have been in progress during the deposition of the upper Chuar Group. Dehler, et al. (2001) suggested that "Chuar Group cycles and sequences may record glacioeustatic fluctuations during the climatic *transition* into (even before) the Sturtian Ice Age (~750-700 Ma)".

Flint (1971, p. 6) stated that the Miocene sea level, prior to the formation of the Antarctic continental ice sheet, is estimated to have been 65 m (213 ft) higher than present and that at maximum Pleistocene glaciation sea level is estimated at between less than 100 m (328 ft) and about 140 m (459 ft) below present sea level. The difference in sea level between total deglaciation and maximum glaciation is thus between 165 m (541 ft) and 205 m (673 ft). This range could easily shift Chuar Group water depths between the three oxygen-based water zones (aerobic = 0-50 m; dysaerobic = 50-150 m; anaerobic = below 150 m) of a restricted basin, or between the upper two of the three bathymetric water layers of the open ocean [seasonal or surface or mixed layer = 0 to 100 or 150 m; permanent thermocline = 100 or 150 to 1000 or 1500 m; deep (and bottom) waters = below 1000 or 1500 m].

Possible secondary mechanisms producing cyclical sedimentation, can be grouped into models postulating carbonate deposition during lowstand sea level and shale deposition during highstands, in contrast to models postulating the opposite lithologic-sea level association. Secondary mechanisms may involve an interplay of arid/humid climate cyclicity, sea level highstand/lowstand cyclicity, and anoxic/oxic basin cyclicity. The choice of secondary mechanisms for Chuar Group cyclical sedimentation is intimately tied to the choice(s) of its basin circulation and depositional models. Because the present study concludes five basin models alone or in alternation are most probable for the Chuar Group, only a range of possible secondary mechanisms for cyclical sedimentation can be suggested herein.

Models Postulating Lowstand Sea Level Carbonates and Highstand Sea Level Shales

Dehler, et al. (2001) interpreted glacioeustacy as a mechanism which controlled meter-scale cyclicity and possibly hundred meter-scale lithologic cyclicity. Dehler, et al. (2001) further interpreted long- and short-term humid/arid cycles and associated mudrock deposition with more humid climate, interglacial phases, and transgression. Carbonate deposition was associated with more arid climate, glacial phases, and regression. Imbrie and Imbrie (1986, p. 153) summarized work done in 1961 by Kukla and Lozek, indicating that when Pleistocene ice sheets were large, Central Europe, including non-glaciated Czechoslovakia and Austria, was a dry, treeless, polar desert swept by bitter winds which deposited layers of loess. Interglacial stages, by contrast, were warmer and wetter than today with temperate forests, broadleafed trees, and fertile soils.

Similar lithologic-sea level associations are suggested herein for deposition under the oxic lagoon (model 10) and oxic epeiric sea (model 12) models. Chuar Group shales are interpreted to reflect increased water depth (highstands, possibly during interglacial stages) and/or sediment influx, while carbonates reflect decreased water depth (lowstands, possibly during glacial stages) and/or sediment influx.

By analogy with the Pleistocene Mediterranean cyclical sapropels described above, Chuar Group oxic carbonate environments may correspond to a restricted, arid, negative water balance basin (model 3) and sea level lowstands during glacial stages. Anoxic shales may correspond to a humid climate and/or warming-induced, deglaciation meltwaters producing a positive water balance basin (model 2) during interglacial stages.

An alternative explanation of the Pleistocene Mediterranean cyclical sapropels (Friedman and Sanders, 1978, p. 531) is that rising sea levels (interglacials) in the Mediterranean flooded the Black Sea with dense marine water and displaced bouyant fresh water from the Black Sea out across the eastern Mediterranean, trapping and isolating stagnant marine water beneath. This in turn created anoxia and

sapropel deposition. By analogy the anoxic Chuar Group organic shales (sapropels) would correspond to interglacial highstands and the oxic Chuar Group carbonates would correspond to glacial lowstands.

Another possibility, based on the euxinic basin model (model 2) of Byers (1977), is that the Chuar Group basin was restricted at all times with a persistent tripartite water column (aerobic in the upper 50 m, dysaerobic at 50-150 m, anaerobic below 150 m). Sea level fluctuations may have merely shifted the water depth of Chuar deposition, and thus the portion of the water column intersecting the bottom at the site of Chuar Group deposition. Thus by this view, carbonate deposition occurred during low sea level stands (glacials) when the bottom was within 50 m of the surface, i.e. within the aerobic water column. Organic shale deposition occurred during high sea level stands (interglacials) when the bottom was deeper than 50 m from the surface, placing it within the dysaerobic or anaerobic water column.

Models Postulating Highstand Sea Level Carbonates and Lowstand Sea Level Shales

A possible cyclical model proposed by Pedersen and Calvert (1990) involves enhanced wind circulation which produced greater upwelling and productivity (anoxic organic shales) during glacial stages and less upwelling and productivity (oxic carbonates) during interglacials.

Another possibility is based on the Pleistocene Red Sea. During Pleistocene glaciation the Red Sea was an isolated tropical lake (model 1) which became anoxic supporting sulfate-reducing bacteria, which converted gypsum to calcite and released sulfur. During Holocene deglaciation the Red Sea became an oxic negative water balance basin (model 3). By analogy the Chuar Group basin may have been a totally isolated lake during glacial sea level lowstand which would produce anoxic shale deposition with hypersaline waters and sulfate-reducing bacteria converting sulfates to sulfur and calcite. Deglaciation and rising sea level would reestablish a connection to the sea producing an oxic negative water balance basin and allowing tropical marine carbonate deposition.

In the Sturtian and Varangerian icehouse-hothouse climatic cycles described by Hoffman, et al. (1998) and Hoffman and Schrag (2000), interglacial or non-glacial platform carbonates preceeded glacial deposits. Glacial deposits consist of mudstones containing ice-rafted dropstone clasts and banded iron deposits, indicative of anoxic oceans. The subsequent hothouse deposits consist of capping carbonates with rapidly precipitated, large-crystal aragonite fans. If the Chuar Group was deposited during earlier, less severe glaciation, and possibly in part during the early part of the global Sturtian glaciation, Chuar Group cyclicity patterns would be expected to follow this same pattern, with carbonates representing the sea level highstand interglacials, and with shales representing the sea level lowstand glacial stages. The lack of dropstones in the Chuar Group shales suggests that if these were deposited during glacial stages, the scale of that glaciation was not global, and did not reach the tropics. Paleomagnetic data (Weil, et al., 1999; Karlstrom, et al., 2000) indicates the Chuar Group was deposited in the tropics, between 10 and 20 degrees of the equator.

In this Sturtian and Varangerian snowball Earth proposal, the timing of sea level fluctuations differs somewhat from that of the Pleistocene glaciations. Because Neoproterozoic continents are thought to have been clustered near the equator (Hoffman and Schrag, 2000, p. 70), the early and main, prolonged period of global-wide glaciation and resulting anoxic oceans, involved mainly sea-ice, and limited continental glaciation compared to Pleistocene continental ice sheets. Frozen world oceans terminated the hydrologic cycle and arrested growth of continental glaciation, creating vast deserts of windblown sand. Sea level at this stage was not yet at maximum lowstand. It was only as the snowball Earth began thawing that continental glaciation reached its maximum and consequently sea level reached its minimum (Hoffman, et al., 1998, p. 1342; Hoffman and Schrag, 2000, p. 73).

Depositional Environment of the Chuar Group

<u>Black Shales</u>

The thin-bedded, black, highly organic shales, found primarily in thin beds of the Tanner and Carbon Canyon Members, in the upper portion of the Awatubi Member, and in most of the Walcott Member, indicate deposition in the dysaerobic to anaerobic water zones. The typical depths of 50-150 m for the dysaerobic zone, and greater than 150 m for the anaerobic zone given by Byers (1977) are probably maximum limits for the Chuar, because: 1) there is evidence of hypersaline conditions in the Jupiter, Carbon Canyon, Awatubi, and Walcott Members (Ford and Breed, 1973; Bloeser, et al., 1988), and 2) the black shales are intimately interbedded with peritidal carbonates (Dehler, Ph.D., in prep.). As Byers (1977) noted, hypersaline conditions increase the density of bottom waters resulting in a rapid density increase with depth and a thinner than typical pycnocline (dysaerobic zone). Increased salinity also decreases the solubility of oxygen. The presence of sulfur in the Tanner, Awatubi, and Walcott Members (Wiley, et al., 1998) is indicative of either euxinic basin depositional conditions, i.e. hydrogen sulfide in bottom waters and/or sediments and no oxygen, or anoxic sediments in an oxic basin. The sulfur is a product of the sulfide-reducing, anaerobic bacterial decay of organic matter in the presence of the sulfate radical (Friedman and Sanders, 1978, p. 130-131, 217, 245, 524, 536; Kirkland and Evans, 1981, p. 188). The sulfate radical could be derived from the destruction of gypsum precipitated under hypersaline conditions as in the case of the modern-day Dead Sea and Pleistocene Red Sea, although this does not appear to be the case for the Chuar black shales for the following reason. Friedman and Sanders (1978, p. 245) observed that gypsum may not be preserved in the geological record if anaerobic sulfate reducing bacteria are present. Bacterial destruction of gypsum, however, would be expected to free calcium ions, resulting in layers of calcite and aragonite as in the modern Dead Sea and Pleistocene Red Sea examples (Friedman and Sanders, 1978, p. 245, 536). Carbonate layers are not abundant in the clastic members of the Chuar Group, and when present they generally are associated with benthonic microfossils indicative of the aerobic portion of the water column. Dissolved sulfate in the water column is another potential source of the sulfate radical for sulfur produced by bacterial sulfate reduction. Sulfate-reducing bacteria require anoxic waters in euxinic basins or anoxic sediments in either euxinic or oxic basins. Facultative anoxygenic photosynthetic cyanobacteria utilize H_2S and CO_2 as reactants to produce sulfur, which therefore can occur only in environments where sulfate-reducing bacteria have produced H_2S.

The microfossils reported from the shaly or clastic facies lend further support to deposition in a euxinic basin. They are a cosmopolitan planktonic biofacies which could flourish in the shallow, overlying aerobic water column, and settle to the bottom to be preserved in the anoxic bottom waters upon death. The anoxic bottom waters were anaerobic and toxic to any benthos and benthonic microfossils are absent in the Chuar Group black shales.

Chuar Group Shales, largely lacking sands and storm rip-ups (with the notable exception of the contorted, basal Walcott Member Flaky Dolomite bed, by this interpretation), suggest deposition at least below fairweather wave base (5-20 m; 16-66 ft), and possibly at mid to outer shelf depths [approximately 50 to 150 m (164 to 492 ft) following Ingle (1980, p. 167, 177)] below the inner shelf depths dominated by storm wave processes. (See discussion of alternatives in the "Nearshore and Shelf Sands and Wave Base, Implications for the Chuar Group Shales" section).

An alternative model is deposition in the deeper parts of a shallow saline or hypersaline oxic lagoon or epeiric sea with a soft fluid (soupy or watery) clay or semi-liquid bottom and anoxic near-bottom sediments.

The fact that the organically-rich facies of the Awatubi and Walcott Members are thicker in the Sixtymile Canyon section than in the neighboring Carbon Canyon (Walcott Member thin and not sampled) and Nankoweap Canyon sections (fig. 6), suggests that the Sixtymile Canyon section was deposited in a deeper portion of the Chuar Basin [perhaps nearer its center or axis (more basinward)], with more

deposition below the anaerobic portion of the water column than the neighboring sections.

Stromatolite and Algal-bearing Units

The Flaky Dolomite Bed at the base of the Walcott Member may have been deposited by flocculose cyanobacterial mats. Bauld (1981a, p. 95-97) describes flocculose cyanobacterial mats as loose and continually shifting, benthic, crumbly gelatinous aggregates that cover much of the bottom sediments of Lake Lenore and Soap Lake, Washington. This description is similar to Ford and Breed's (1973, p. 1252) description of the Flaky Dolomite Bed consisting of wildly disoriented, irregularly heaped, silicified algal flakes. Modern flocculose mats also form during winter stratification on the bottom of Solar Lake, Israel during high H_2S concentrations and very low light intensities (Bauld, 1981a, p. 101). The flocculose mat-forming cyanobacteria are capable of facultative anoxygenic photosynthesis using H_2S as an electron donor. After summer lake-overturn and mixing, these cyanobacteria switch from anoxygenic to oxygenic photosynthesis, initiating oxygen evolution, and the mat condenses to a layer 0.5 to 1 cm. thick. Entrapment of oxygen bubbles causes large patches of the mat to become detached and float to the water surface. This process may in part explain the contorted bedding seen in the Flaky Dolomite Bed, and that the beds above and below are unaffected and have great lateral continuity (Ford and Breed, 1973, p. 1252). Other possible origins for the contorted bedding of the Flaky Dolomite Bed include slumping, storm rip-up, or deposition in desiccation-flooding-desiccation cycles. Eugster and Hardie (1975) postulated that organic-rich dolomitic laminate facies of the Green River Formation oil shale deposits were produced by the accumulation of flocculent mats of gelatinous cyanobacteria (Bauld, 1981b, p. 314-315). A second Green River Formation oil shale facies, lenses of oil shale breccias, was believed to originate when marginal mats, dried and polygonally cracked during periods of desiccation, were subsequently transported and concentrated in lows during periods of flooding (Eugster and Hardie, 1975).

Five lines of evidence [(1)-(5)] indicate the stromatolitic and algal beds were deposited under generally oxygenated conditions in the photic zone at depths less than 50 m. (1) They are associated with a benthonic biofacies indicating oxygenated bottom waters (Bloeser, et al., 1977; Vidal and Knoll, 1983; Vidal and Ford, 1985; and Vidal, 1986). In isolated basins like the Dead Sea (Friedman and Sanders, 1978, p. 244-246) and semi-isolated basins like the Black Sea (Byers, 1977, p. 98) the aerobic zone is commonly shallower than 50 m. Since algae and stromatolitic cyanobacteria are photosynthetic, they require deposition in the photic zone which has a maximum base of 80 to 200 m (see "The Photic Zone" references). (2) In nearshore areas most photosynthesis occurs at depths less than 50 m (Phleger, 1960, p. 9; Huc, 1980, p. 448-449). (3) In the Bahamas, algal mats have been observed to depths of 50 m (Gebelein, 1976, p. 381). Modern domal and columnar stromatolites of Hamelin Cove, Australia and the Bahamas are intertidal to shallow subtidal (to 8 m), but their Precambrian distribution may have been more widespread because herbivorous and sediment-feeding invertebrates had not yet evolved. (4) For example, Playford and Cockbain (1969) suggested that deepwater marine stromatolites of the Devonian of Western Australia lived at water depths of up to 150 ft (46 m). (5) Shelf waters shallower than a few hundred feet (60-90 m?) are well mixed and isothermal at all seasons and at all latitudes (Phleger, 1960, p. 5-9; 17-18).

The stromatolitic and algal beds may record periods of basin shallowing (perhaps not by much if the tripartite oxygen zonation of the water column was compressed by hypersaline conditions) to within the aerobic zone (0-50 m). Dolomite composition suggests restricted hypersaline or evaporitic conditions or supratidal sabkha conditions creating dolomitizing magnesium enriched brines. Alternatively dolomite may result from early diagenesis as suggested by $d^{18}O$ data (Dehler, Ph.D, in prep., which see for additional discussion).

Alternative models for the deposition of stromatolite and algal-bearing units includes 1) deposition in a shallow saline or hypersaline oxic lagoon setting (Model 9), perhaps along its margins or during periods of decreased water depth and/or sediment influx, or 2) in an epeiric sea (Model 12).

Carbon Butte Member

Sandstones of the Carbon Butte Member contain sigmoidal crossbeds and bimodal crossbeds indicating reverse-flow, and other evidence of deposition under shallow marine tidal influences as reported by Wiley, et al. (1998, p. 44, 55, 80), and Dehler, et al. (2001). Utilizing Walther's law, the Carbon Butte Member could represent: 1) a barrier bar which has moved landward over normally lagoonal Chuar Group shales during a sea level highstand, or 2) the nearshore sand wedge moved seaward over normally basinal Chuar Group shales during a sea level lowstand.

Green, Gray, and Red Shales

The green, gray, and red shales with a low organic content and found primarily in the Jupiter, Carbon Canyon, and Duppa Members indicate deposition under oxidizing conditions as suggested by low total organic carbon values. Such conditions could have occurred due to shallowing of the basin to within the aerobic portion of the water column, or due to ventilation of the basin caused by a deepening of the portal or rise in sea level. The shallowing alternative is favored by the evidence of emergence and desiccation in the Tanner, Jupiter, Carbon Canyon, Carbon Butte, and Awatubi Member from Ford and Breed (1973) (see "Key Evidence"). It is significant that the Carbon Canyon Member consists of green and red sandstones and mudstones alternating with carbonate beds, some of which contain algae and are therefore also of relatively shallow water (<50 m) origin. Some of the variegation may be due to weathering or diagenesis, based on observations by Dehler of color changing laterally in many intervals and of variegated shales in outcrop which are gray to black on freshly exposed surfaces. Dehler has also observed mudcracked black shales in the Carbon Canyon Member and stromatolites interbedded with black shales. These observations suggest that some of the gray or black shales of low organic content are of an oxic shallow water origin.

Chuar Group Basin Models

The range of possible basin models proposed for the Chuar Group include three euxinic models (1, 3, or 4) and two oxic models (10 or 12), all of which have some degree of restriction. The euxinic models include the restricted hypersaline euxinic marine basin models with two-way (model 3) or one-way (model 4) flow through the portal, or the isolated tropical humid climate euxinic lake model (model 1). Stable carbon isotope ratios (del C13 Aromatic vs. del C13 Saturate) indicate the lacustrine model is less likely, at least for the Tanner, Carbon Canyon, Awatubi, and Walcott Members (Wiley, et al., 1988). Two oxic, restricted marine models, the shallow saline/hypersaline lagoon (model 10), or an epeiric sea model (model 12) are also possibilities. Some alternation of these five models is also possible. The lack of bedded gypsum or higher grade evaporites in the Chuar Group implies that for any of the restricted basin depositional models under consideration, the degree of restriction was less than that necessary to concentrate seawater to a salinity of 124‰ at which gypsum precipitation begins. Lucia (1972) has shown that gypsum is not deposited when the ratio (Ao/At) of the surface area of the restricted basin (Ao) to the cross-sectional area of the inlet (At) is less than 10^6.

The restricted hypersaline euxinic basin models (3 or 4) or the lagoon model (10) or the epeiric sea model (12) would each allow marine inflow, nutrient concentration, and blooms of cosmopolitan marine phytoplankton in normal marine, oxygenated surface water. High phytoplankton productivity would result in high amounts of organic matter settling to anoxic bottom waters (models 3 or 4) or soft fluid (soupy or watery) clays or semi-liquid bottom conditions with anoxic sediments (models 10 or 12) upon their death. These anoxic bottom waters or semi-liquid anoxic sediments containing hydrogen sulfide would be toxic to any benthos, would preserve the organic sedimentary component, and would account for the sulphur reported by Wiley, et al. (1998) and in this report. The black, organically rich shales of thin beds of the Tanner and Carbon Canyon Members, the upper portion of the Awatubi Member, and most of the Walcott

Members represent deposition under these conditions.

The algal, and stromatolitic carbonates containing a benthos indicates basin shallowing to within the aerobic zone and water depths of 50 m or less. Photosynthesis limits depth to a maximum of 80-200 m, or if in shelf waters 50 m or less, but would more likely have been intertidal to shallow subtidal where modern domal and columnar stromatolites flourish in Hamelin Pool of Shark Bay, Australia and the Bahamas. Alternatively, these carbonate units could represent shallow saline/hypersaline lagoonal deposition during periods of decreased water depth (shallowing) and/or sediment influx. Another possibility is deposition in epeiric seas, which are thought to have been shallower than 30 m when widespread sheets of carbonate were being deposited (Friedman and Sanders, 1978, p. 373; Friedman, 1980, p. 600). Extensive algal mats may also have promoted anoxia in near-surface sediments.

While any of models 3 or 4 or 10 or 12 alone may be sufficient, one or more may have alternated cyclically with periods in which the basin became completely isolated from the open sea, producing a hypersaline lake or desiccating sea (model 1), much as Hsu (1972) proposed for the Miocene Messinian Mediterranean Evaporite. Basin isolation may be required to account for the gypsum and salt deposition reported by Bloeser, et al. (1977) and Ford and Breed (1973) and also for the evidence of emergence and desiccation reported by Ford and Breed (1973). Authors such as Hsu (1972) and Shaw (1977) argue that widespread gypsum deposition (not seen in the Chuar Group) requires shallow, desiccating conditions in isolated basins. Such hypersaline lakes are known to be anoxic at depth (e.g. Dead Sea), and contain some oxygen in shallow water supporting a benthos, with widespread stromatolitic calcareous biohermal deposition in shallow water (e.g. Great Salt Lake), support a cosmopolitan phytoplankton flora, and are often highly organically productive (Kirkland and Evans, 1981). Since evaporites are not known from the Chuar Group, if it was (partially) deposited in a tropical lake, it would most likely have occurred in a humid climate, like Lake Tanganyika which lacks evaporites.

Both Model 4 and Model 1 exhibit a bullseye depositional pattern of evaporite facies belts, if present. Model 3 exhibits a teardrop evaporite facies depositional pattern, if present. The Chuar Group, which lacks major evaporite beds, could represent the non-evaporite temporal or spatial portions of the basin in the event unpreserved or unexposed portions of the basin ever reached salinities sufficient to deposit evaporites. Perhaps evaporite-grade salinities were only reached during the late desiccation stage of model 1 (isolated hypersaline lake model), and the part of the basin represented by the Chuar Group during this period is only represented by the evidence of desiccation. More likely, the ratio of the surface area of the restricted basin (Ao) to the cross-sectional area of the inlet (At) was less than 10^6, or the minimum necessary for the precipitation of gypsum (Lucia, 1972, p. 165-167).

Most of the lower Chuar Group (excepting thin organic-rich beds of the Tanner and Carbon Canyon Members) was deposited under conditions which remained shallow enough (<50 m) for continuous mixing, oxygenation, and periodic emergence and desiccation. The organically rich upper Awatubi and Walcott Members record a deepening episode, perhaps associated with the initiation or acceleration of movement on the Butte Fault, which initiated prolonged euxinic conditions, and deposition in the deeper dysaerobic and anaerobic zones (>50 m). Timmons, et al. (2001) report that the Butte Fault zone was intermittently active throughout Chuar Group deposition. Dehler, et al. (2001) report that this deepening is partly climate controlled. The contorted bedding and carbonate clasts noted in the Flaky Dolomite Bed of the Walcott Member (Ford and Breed, 1973, p. 1252; Cook, 1991; field notes, this report) could indicate possible slumping following basal Walcott Member deposition. Alternatively the Flaky Dolomite Bed may have been deposited: 1) by flocculose cyanobacterial mats, with the contorted bedding resulting from bouyant, entrapped, oxygen produced by mat photosynthesis, or 2) as a result of storm rip-up, or 3) in desiccation-flooding-desiccation cycles. Alternating with this euxinic episode, intermittent basin ventilation accompanying carbonate deposition occurred up to 8 times (stratigraphic column, Plate 1).

Conclusions

1) Measured Section: In the Sixtymile Canyon section, the Awatubi Member of the Kwagunt Formation is

653 ft (199 m) thick, and the Walcott Member of the Kwagunt Formation is 827 ft (252 m) thick. The traverses and samples were plotted on the Cape Solitude 7.5' U.S. Geological Survey Topographic Quadrangle, Coconino County, Arizona.

2) Sampling: Nine samples were collected from the Awatubi Member and 21 samples were collected from the Walcott Member. These are deposited with the Arizona Geological Survey and are available for future study.

3) Awatubi Organic Richness: For the Sixtymile Canyon section Awatubi Member, a wide variance is seen in the amount of section rated as potential source rock by different geochemical indices of organic richness. The lowest estimate, based on genetic potential, was that the uppermost 10 ft (2%) had moderate oil source rock potential, with the basal 98% rated as non oil/some gas potential. Hydrogen Index indicated that the upper 37 ft (8%) was gas prone, with the basal 92% having no hydrocarbon potential. The S2/S3 ratio indicated 100 ft (22%) was gas prone, with the remaining section having no hydrocarbon potential. The highest estimate, based on total organic carbon (TOC), was that 355 ft (78%) of the 456 ft sampled was fair or better in richness, i.e. potential source rock. Three hundred thirty-eight feet (74%) rated good or better, and 100 ft (22%) rated very good. In summary, for the Awatubi Member, a minimum of 10 ft (2%) and a maximum of 355 ft (78%) of the 456 ft of measured Awatubi is potential source rock.

4) Walcott Organic Richness: Again for the Walcott Member of Sixtymile Canyon, a variance is seen in the amount of section rated as potential source rock by different indices. On the basis of total organic carbon (TOC) the entire 814 ft (100%) of the sampled Walcott Member was fair or higher in richness, i.e. potential source rock. On the basis of genetic potential, however, only 60% (489 ft of the 814 ft sampled) of the section rated as moderate or higher (oil) potential. For the Walcott Member, a minimum of 489 ft (60%) and a maximum of 814 ft (100%) of the 814 ft of sampled Walcott section is potential source rock.

5) Awatubi Organic Maturity: In the Sixtymile Canyon section, organic maturity of the Awatubi Member based on Tmax is lower than that based on productivity index (transformation ratio). Based on productiviy index, 434 ft (95%) of the 456 ft of the sampled Awatubi section is early oil or higher maturity and 182 ft (40%) of the 456 ft of sampled Awatubi section ranges up to late oil and postmature (gas windows).

The Awatubi maturity based on Tmax, however, was much lower, with an average value in the immature window. The Awatubi Member Tmax gradient was entirely within the early oil window.

The Tmax values for all the Awatubi Member samples are unreliable due to low kerogen S2 values. The productivity index values also have relatively large errors due to the very small S1 and S2 values, but they may be a more reliable indicator of the thermal maturity of the samples. Based on the maturity of the Walcott Member, the Awatubi Member is likely to be in the peak to late oil generation window.

6) Walcott Organic Maturity: In the Sixtymile Canyon section Walcott Member the two measures of maturity, Tmax and productivity index, are fairly consistent in the upper part of the member, but in the lower part of the member the maturity indicated by productivity index is generally higher than that indicated by Tmax. The Tmax gradient for the upper 420 ft (51%) of the 827 ft of total Walcott section is in the immature window and the gradient of the lower 407 ft (49%) of the total Walcott section is in the early oil window.

Based on productivity index, 358 ft (44%) of the 814 ft of sampled Walcott section is immature, and 456 ft (56%) is early oil or higher. Three hundred seventeen feet (39%) is early oil-peak oil gap or higher, 112 ft (14%) rated peak oil or higher, and 20 ft (2%) rated late oil and postmature (gas) windows.

Both measures rate much of the upper part of the member as immature. For the basal part of the section, the Tmax maturity gradient only reaches early oil. By contrast, on the basis of productivity index 14% of the section is peak oil or higher.

Tmax values for the Walcott Member are reliable, but correlate more strongly with their TOC content than with their stratigraphic position. This correlation of Tmax to TOC content is a "delay" effect due to the delayed release of S2 material in high TOC samples. This "delay" effect was also seen in the Walcott Member samples from Nankoweap Canyon and seems to be pronounced in this suite of samples, perhaps due to their great age. A consideration of Tmax analytical reliability leads to the conclusion that the Walcott Member samples range from immature to early mature to the onset of peak oil generation. This is also consistent, in general, with the productivity index values in the Walcott Member samples for which Tmax is reliable, which vary from 0.05 to 0.15. The unusually high productivity index value of sample S10-60-25 may be due to contamination. Samples in the lower part of the Walcott Member (S10-60-18 to S10-60-10) have higher productivity index values due to the very small S1 and S2 values and therefore larger analytical error.

7) Awatubi Kerogen/Hydrocarbon Type: The Awatubi Member is most likely a gas prone source, based on the crossplot of reactive carbon index vs. productivity index (Figure 4), hydrogen index, and S2/S3 ratio; however, between 22% (based on total organic carbon) and 98% (based on generative potential) of the section has poor source rock potential. The modified van Krevelen diagram is not definitive as to kerogen type of the Awatubi Member.

8) Walcott Kerogen/Hydrocarbon Type: The different geochemical indices also show discrepancies in the kerogen/hydrocarbon type predicted for Walcott source rocks. For the Walcott Member oil potential is indicated by the Modified van Krevelen diagram, gas potential alone is indicated by the reactive carbon index vs. productivity index crossplot and by hydrogen index, and mixed oil and gas potential is indicated by the S2/S3 ratio.

The Walcott Member contains Type I and II kerogen based on the Modified van Krevelen diagram (Figure 5) which are oil prone. In contrast, however, the plot of reactive carbon index vs. productivity index (Figure 4) indicates that all but three samples plot in the gas prone region. Hydrogen index indicates that 68% of the section is gas prone and 4% is mixed oil and gas prone (the balance having no hydrocarbon potential). The S2/S3 ratio indicates a greater mix of both oil and gas potential, i.e. 39% gas prone, 35% mixed oil and gas prone, and 11% oil prone (the balance having no hydrocarbon potential).The Walcott Member is definitely a potential gas source, with some indicators suggesting oil potential as well.

9) Migration: For the Awatubi Member hydrocarbons in 40% of the section had a migrated origin, hydrocarbons in 5% of the section had a mixed origin, and hydrocarbons in 55% of the section had an indigenous origin based on productivity index.

For the Walcott Member, hydrocarbons in the bulk of the section (95%) had an indigenous origin, with hydrocarbons in only 2% of the section indicating a migrated origin, and in only 3% of the section indicating a mixed origin, based on productivity index.

10) Thickest organically-rich zones of the Awatubi and Walcott Members occur in the Sixtymile Canyon section: Figure 6 illustrates that thicker organically-rich facies in both the Awatubi and Walcott Members are present in the Sixtymile Canyon section than in the neighboring Carbon Canyon (Walcott Member thin and not sampled) and Nankoweap Canyon sections (Wiley, et al., 1998). This suggests that the Sixtymile Canyon section was deposited in deeper water with more of the section deposited below the anaerobic portion of the water column.

11) Vertical Maturity Anomaly: Average Tmax Walcott maturity exceeding that of underlying Awatubi: In the Sixtymile Canyon section, like the Nankoweap Canyon section, the average Tmax maturity of the Walcott Member (435°C. = immature/early oil boundary) exceeds that of the underlying Awatubi Member (429°C. or 379°C., both immature). This puzzling vertical maturity anomaly is probably a data artifact owing to Awatubi Tmax values being unreliable due to low kerogen S2 values.

12) Tmax Maturity Windows Dipping to the Southeast: Tmax maturities in the Sixtymile Canyon section are consistent with the previously reported pattern from the Carbon Canyon and Nankoweap Canyon sections, whereby Tmax maturity windows have an apparent dip to the southeast. This suggests the pattern is real, not a data artifact. Explanations include: 1) longer and/or deeper burial to the northwest, or 2) higher heat flow to the northwest associated with volcanism and plutonism.

13) Chuar Depositional Environment: Key evidence indicative of the Chuar depositional environment includes stable carbon isotope ratios, sedimentological evidence, and the presence of sulphur in several members (this report; Wiley, et al., 1998; Dehler, et al., 2001), cosmopolitan marine planktonic biofacies and benthonic biofacies (Bloeser, et al., 1977; Vidal and Knoll, 1983; Vidal and Ford, 1985; and Vidal, 1986; Porter and Knoll, 2000), stromatolites and algal beds (Ford and Breed, 1973; Wiley, et al., 1998), evidence of hypersaline deposition (Ford and Breed, 1973, p. 1247, 1251; Summons, et al., 1988), evidence of emergence and desiccation (Ford and Breed, 1973), and common dolomite in the carbonate beds (Ford and Breed, 1973; Wiley, et al., 1998). The Chuar depositional environment is interpreted utilizing the euxinic basin biofacies and lithofacies model of Byers (1977), twelve possible euxinic and oxic basin/organic-rich environment models [primarily from Trask (1939), Friedman and Sanders (1978); Friedman (1980); Huc (1980); Demaison and Moore (1980), Bauld (1981b) and Warren (1986)] and data on the present-day photic zone, stromatolites, nearshore and shelf sands and wave base, ocean temperatures and mixing, and typical shallowing upward carbonate sequences.

a) Thin-bedded, organic-rich, sulphur-bearing, black shales of thin beds of the Tanner and Carbon Canyon Members, the upper part of the Awatubi Member, and most of the Walcott Member indicate deposition in the dysaerobic (50-150 m) or anaerobic (>150 m) water zones, which were toxic to benthos. Their fossil content is limited to a cosmopolitan planktonic biofacies which flourished in the surface aerobic water layer, and settled to the anaerobic bottom waters upon death, where they were preserved. Lack of a benthonic fauna in these units is strongly suggestive of basin depths sufficient to allow tripartite stratified waters (>50 m) with wave-induced oxygenation restricted to the surface aerobic layer. Chuar Group shales, largely lacking sands and storm rip-ups (with the notable exception of the contorted, basal Walcott Member Flaky Dolomite bed, by this interpretation), suggest deposition at least below fairweather wave base (5-20 m; 16-66 ft), and possibly at mid to outer shelf depths [approximately 50 to 150 m (164 to 492 ft) following Ingle (1980, p. 167, 177)] below the inner shelf depths dominated by storm wave processes. (See discussion of alternatives in the "Nearshore and Shelf Sands and Wave Base, Implications for the Chuar Group Shales" section). An alternative model is deposition in the deeper parts of a shallow saline or hypersaline (>37 per mille) oxic lagoon or oxic epeiric sea (< 30 m deep) with a soft fluid clay or semi-liquid bottom and anoxic near-bottom sediments, perhaps during periods of increased water depth and/or sediment influx.

b) Stromatolitic and algal-bearing units contain a benthonic biofacies and indicate deposition under oxygenated conditions in the photic zone (80-200 m maximum depth, or 50 m in nearshore waters). A more likely depth is intertidal or shallow marine (<10 m) based on modern-day domal and columnar stromatolites. The intertidal or shallow marine interpretation is also supported by an intimate association of these units with other facies indicating emergence (Dehler, et al., 2001). These beds record shallow deposition within the aerobic zone (<50 m) Dolomites suggest restricted evaporitic conditions or supratidal sabkha conditions creating dolomitizing magnesium enriched brines, or alternatively post-burial dolomitization. An alternative model is deposition in a shallow saline or hypersaline (>37 per mille) oxic lagoon setting (model 10) or epeiric sea (model 12), perhaps along its margins or during periods of decreased water depth and/or sediment influx. The Flaky Dolomite Bed at the base of the Walcott Member has characteristics of flocculose cyanobacterial mat deposition. Bouyancy produced by entrapped mat photosynthetic oxygen may explain the contorted bedding restricted to this horizon. Other possible explanations for the contorted bedding of the Flaky Dolomite Bed include slumping, storm generated traction currents (rip-up), or deposition in desiccation-flooding-desiccation cycles.

c) The Carbon Butte sandstone was deposited under shallow marine tidal influences (Dehler, 1998; Dehler and Elrick, 1998; Wiley, et al., 1998; Dehler, et al., 1999; Dehler, et al., 2001).

d) The green, gray, and red shales of the Jupiter, Carbon Canyon, and Duppa Members are low in organic content and could represent deposition under oxygenated conditions during reventilation of the deep basin or shallowing of the basin to aerobic zone water depths. The variegated colors could also be due to diagenesis. The shallowing alternative is more likely for the Tanner (?), Jupiter, Carbon Canyon, Carbon Butte, and (basal ?) Awatubi Members which contain ripple marks, and mud cracks, and/or (questionable) rain prints indicative of emergence and desiccation (Ford and Breed, 1973, p. 1250).

e) The range of possible basin models proposed for the Chuar Group include three euxinic models (1, 3, or 4) and two oxic models (10 or 12), all of which are to some degree restricted. The euxinic models include the restricted hypersaline (>37 per mille) euxinic marine basin models with two-way (model 3) or one-way (model 4) flow through the portal, or the isolated tropical humid climate euxinic lake model (model 1). Stable carbon isotope ratios (del C13 Aromatic vs. del C13 Saturate) indicate the lacustrine model is less likely, at least for the Tanner, Carbon Canyon, Awatubi, and Walcott Members (Wiley, et al., 1998). Two oxic, restricted marine models, the shallow saline/hypersaline lagoon (model 10), or an epeiric sea model (model 12) are also possibilities. Some cyclical alternation of these five models is also possible. The lack of bedded gypsum or higher grade evaporites in the Chuar Group implies that for any of the restricted basin depositional models under consideration, the degree of restriction was less than that necessary to concentrate seawater to a salinity of 124‰ at which gypsum precipitation begins. Lucia (1972) has shown that gypsum is not deposited when the ratio (Ao/At) of the surface area of the restricted basin (Ao) to the cross-sectional area of the inlet (At) is less than 10^6.

f) Lower Chuar Group deposition, excepting thin organic-rich shale beds of the Tanner and Carbon Canyon Members, was generally within the aerobic zone at less than 50 m water depth. The organically-rich upper Awatubi and Walcott Members record a deepening episode to dysaerobic and/or anaerobic depths (>50 m) and the initiation of euxinic basin conditions which alternated with up to eight periods of carbonate deposition (Stratigraphic column, Plate 1). Altenatively the upper Awatubi and Walcott Members may record an increase of water depth or sediment influx in a shallow saline or hypersaline (>37 per mille) oxic lagoon or epeiric sea.

References

Aller, R.C., and Yingst, J.Y., 1980, Relationships between microbial distributions and the anaerobic decomposition of organic matter in surface sediments of Long Island Sound, USA: Marine Biology, v. 56, p. 29-42.

Attenborough, D., 1979, Life on Earth-a natural history: Boston, Massachusetts, Little, Brown and Co., 319 p.

Bacescu, M., 1963, Contribution a la bioceanologie de la Mer Noire. L'etage Periozoique et le facies paleodreissenifere, leurs characteristiques: Rapport et proces-verbaux des reunions: Comm. Internat. pour l'exploration scientifique de la Mer Mediterranee, Paris, France, v. 17, p. 107-122.

Bauld, J.,1981a, Occurrence of benthic microbial mats in saline lakes: Hydrobiologia, v. 81, p. 87-111

Bauld, J., 1981b, Geobiological role of cyanobacterial mats in sedimentary environments: production and preservation of organic matter: Bur. Min. Res., Jour. Australian Geology & Geophysics, v. 6, p. 307-317.

Bickford, M.E., et al., 1973, Geology Today: Del Mar, California, CMR Books, Communications Research Machines, Inc., 530 p.

Billingsley, G.H. and Elston, D.P, 1989, Geologic log of the Colorado River from Lees Ferry to Temple Bar, Lake Mead, Arizona, p. 1-36; in Elston, D.P., et al., 1989, Geology of Grand Canyon, northern Arizona (with Colorado River guides): American Geophysical Union, Washington, D.C., 28th International Geological Congress, Field Trip Guidebook T115/315, 239 p.

Bloeser, B., Schopf, J.W., Horodyski, R.J., and Breed, W.J., 1977, Chitinozoans from the Late Precambrian Chuar Group of the Grand Canyon, Arizona: Science, v. 195, p. 676-679.

Bouma, A.H., Berryhill, H.L., Brenner, R.L., Knebel, H.J, 1982, Continental shelf and epicontinental seaways, p. 281-328; in Scholle, P.A. and Spearing, D., 1982, Sandstone depositional environments: Tulsa, Oklahoma, Am. Assoc. Petrol. Geol., Memoir 31, 410 p.

Brenner, R.L., 1980, Construction of process-response models for ancient epicontinental seaway depositional systems using partial analogs: Am. Assoc. Petrol. Geol., Bull., v. 64, no. 8, p. 1223-1244, 17 figs.

Brongersma-Sanders, M., 1957 (reprinted 1963), Mass mortality in the sea, p. 941-1010; in Hedgpeth, J.W., ed., 1957 (reprinted 1963), Treatise on marine ecology and paleoecology: Geological Society of America, Memoir 67, v. 1, Ecology, 1296 p.

Brongersma-Sanders, M., 1966, Metals of Kupferschiefer supplied by normal sea water: Geol. Rundschau (for 1965), v. 55, no. 2, p. 365-375.

Brongersma-Sanders, M., 1968, On the geographical association of strata-bound ore deposits with evaporites: Mineral. Deposita (Berl.), v. 3, p. 286-291.

Brongersma-Sanders, M., and Groen, P., 1970, Wind and water depth and their bearing on the circulation in evaporite basins; in Third symposium on salt: Northern Ohio Geol. Soc., v. 1, p. 3-7.

Busch, D.A., 1974, Stratigraphic traps in sandstones - exploration techniques: Tulsa, Oklahoma, Am. Assoc. Petrol. Geol., Memoir 21, 174 p.

Byers, C.W., 1977, Biofacies patterns in euxinic basins: a general model; in H.E. Cook and P. Enos, eds., 1977, Deep water carbonate environments, Soc. Econ. Paleont. and Min., Spec. Publ. No. 25, p. 5-17.

Calvert, S.E., 1990, Geochemistry and origin of the Holocene sapropel in the Black Sea; in Ittekkot, V., ed., 1990, Facets of modern biogeochemistry: Berlin, Springer-Verlag, p. 327- 353.

Caspers, H., 1957, Chapter 25, Black Sea and Sea of Azov, p. 801-890; in Hedgpeth, J.W., 1957 (reprinted 1963), Treatise on marine ecology and paleoecology: Geol. Soc. Amer., Mem. 67, v. 1, Ecology, 1296 p.

Cook, D.A., 1991, Sedimentology and shale petrology of the upper Proterozoic Walcott Member, Kwagunt Formation, Chuar Group, Grand Canyon, Arizona: M.S. thesis, Northern Arizona Univ., 158 p.

Copeland, B.J., 1967, Environmental characteristics of hypersaline lagoons: Univ.of Texas, Marine Sci. Inst. at Port Aransas, Texas, Contr. Marine Sci., v. 12, p. 207-218.

Core Laboratories, Inc., 1983, Geochemical well profile.

Degens, E.T. and Ross, D.A., eds., 1974, The Black Sea- geology, chemistry, and biology: Am. Assoc. Petrol. Geol., Mem. 20, 633 p.

Degens, E.T., Von Herzen, R.P., and Wong, H.-K., 1971, Lake Tanganyika: water chemistry, sediments, geological structure: Naturwissenschaften, v. 58, p. 229-241.

Dehler, C.M., in preparation, Basin analysis and C-isotope stratigraphy of the marine Chuar Group, Grand Canyon: Ph.D. dissertation, University of New Mexico, Albuquerque.

Dehler, C.M., 1998, Facies analysis and environmental interpretation of the middle Chuar Group (Proterozoic): implications for the timing of Rodinian breakup (Abstract): Am. Assoc. Petrol. Geol., National Convention, Salt Lake City, Utah.

Dehler, C.M., Des Marais, D.J., Bowring, S., Sharp, Z., Karlstrom, K.E., and Elrick, M., 1999, Chuar Group (1.1-0.74 Ga), Grand Canyon: carbon isotope systematics at the onset of Sturtian glaciation (Abstract): Geol. Soc. Amer., Abstracts with Programs, v. 31, no. 7, p. A-487.

Dehler, C.M. and Elrick, M.E., 1998, Implications for paleoenvironments and areal extent of the Chuar Basin from facies analyses of the middle Chuar Group (Neoproterozoic), Grand Canyon (Abstract): Geol. Soc. Amer., Regional Convention, Flagstaff, Arizona.

Dehler, C.M., Elrick, M.E., Karlstrom, K.E., Smith, G.A., Crossey, L.J., and Timmons, J.M., 2001, Neoproterozoic Chuar Group (~800-742 Ma), Grand Canyon: a record of cyclic marine deposition during global cooling and supercontinent rifting: Sedimentary Geology, v. 141, p. 465-499.

Demaison, G.J., and Moore, G.T., 1980, Anoxic environments and oil source bed genesis: Amer. Assoc. Petrol. Geol., Bull., v. 64, no. 8, p. 1179-1209, 18 figs.

Dill, R.F., Shinn, E.A., Jones, A.T., Kelly, K., and Steinen, R.P., 1986, Giant subtidal stromatolites forming in normal salinity waters: Nature, v. 324, p. 55-58.

Dow, W.G., and O'Connor, D.I., 1982, Kerogen maturity and type by reflected light microscopy applied to petrolem exploration: Soc. Econ. Paleont. and Min., How to assess maturation and paleotemperatures, Short Course No. 7, p. 133-157.

Dresser Atlas, 1979, Log Interpretation Charts: Houston, Texas, Dresser Industries, Inc., 108 p.

Dunbar, C.O. and Rodgers, J., 1957, Prinicples of stratigraphy, New York, New York, John Wiley and Sons, Inc., 356 p.

Eggleston, J.R., and Dean, W.E., 1976, Freshwater stromatolitic bioherms in Green Lake, New York, Chapter 8.7, p. 479-488; in Walter, M.R., ed., 1976, Stromatolites-developments in sedimentology 20: Amsterdam, Elsevier Scientific Publishing Co., 790 p.

Elston, D.P., 1989, Chapter 9: Middle and late Proterozoic Grand Canyon Supergroup, Arizona, p. 94-105; in Elston et al., 1989, Geology of Grand Canyon, northern Arizona (with Colorado River guides): American Geophysical Union, 28th International Geological Congress, Field Trip Guidebook T115/315, 239 p.

Elston, D.P., Billingsley, G.H., and Young, R.A., eds., 1989, Geology of Grand Canyon, northern Arizona (with Colorado River guides): American Geophysical Union, 28th International Geological Congress, Field Trip Guidebook T115/315, 239 p.

Elston, D.P., and McKee, E.H., 1982, Age and correlation of the late Proterozoic Grand Canyon disturbance, northern Arizona: Geological Society of America, Bull., v. 93, p. 681-699.

Eugster, H.P., and Hardie, L.A., 1975, Sedimentation in an ancient playa-lake complex: the Wilkins Peak Member of the Green River Formation of Wyoming: Geol. Soc. America, Bull., v. 86, p. 319-334.

Flint, R.F., 1971, Glacial and Quaternary Geology: New York, New York, John Wiley and Sons, Inc., 892 p.

Ford, T.D., 1990, Chapter 4 - Grand Canyon Supergroup: Nankoweap Formation, Chuar Group, and Sixtymile Formation, p. 49-70; in Beus, S.S., and Morales, M., 1990, Grand Canyon Geology: New York-Oxford, Oxford University Press-Museum of Northern Arizona Press, 518 p.

Ford, T.D., and Breed, W.J., 1973, Late Precambrian Chuar Group, Grand Canyon, Arizona: Geological Society of America, Bull., v. 84, p. 1243-1260, 12 figs.

Force, E.G., and McCarty, 1970, Anaerobic decomposition of algae: Environ. Sci. and Technology, v. 4, p. 842-849.

Fortey, R.A., 1998, Life- a natural history of the first four billion years of life on Earth: New York, New York, Alfred A. Knopf, 346 p.

Friedman, G.M.,1980, Review of depositional environments in evaporite deposits and the role of evaporites in hydrocarbon accumulation: Bulletin des Centres de Recheches Exploration-Production Elf-Aquitaine, v. 4, p. 589-608.

Friedman, G.M., and Sanders, J.E., 1978, Principles of sedimentology: New York, New York, John Wiley and Sons, 792 p.

Galloway, W.E. and Hobday, D.K., 1983, Terrigenous clastic depositional systems - applications to petroleum, coal, and uranium exploration, 1st edn.: New York, New York, Springer-Verlag, 423 p.

Galloway, W.E. and Hobday, D.K., 1996, Terrigenous clastic depositional systems - applications to fossil fuels and groundwater resources, 2nd edn.: Heidelberg, Germany, Springer-Verlag, 484 p.

Gebelein, C.D., 1976, Open marine subtidal and intertidal stromatolites (Florida, the Bahamas and Bermuda), Chapter 8.1, p. 381-388; in Walter, M.R., ed., 1976, Stromatolites-developments in sedimentology 20: Amsterdam, Elsevier Scientific Publishing Co., 790 p.

Goldman, M.I., 1924, "Black Shale" formation in and about Chesapeake Bay: Am. Assoc. Petrol. Geol., Bull., v. 8, p. 195-201.

Golubic, S., 1976a, Organisms that build stromatolites, Chapter 4.1, p. 113-126; in Walter, M.R., ed., 1976, Stromatolites-developments in sedimentology 20: Amsterdam, Elsevier Scientific Publishing Co., 790 p.

Golubic, S., 1976b, Taxonomy of extant stromatolite-building cyanophytes, Chapter 4.2, p. 127-140; in Walter, M.R., ed., 1976, Stromatolites-developments in sedimentology 20: Amsterdam, Elsevier Scientific Publishing Co., 790 p.

Gripenberg, S., 1939, Sediments of the Baltic Sea, p. 298-321; in Trask, P.D., ed., 1939, Recent marine sediments- a symposium: Tulsa, Oklahoma, Amer. Assoc. Petrol. Geol., 736 p.

Hallam, A., 1965, Environmental causes of stunting in living and fossil marine benthonic invertebrates: Paleontology, v. 8, pt. 1, p. 132-155.

Halley, R.B., 1976, Textural variation within Great Salt Lake algal mounds, Chapter 8.5, p. 435-446; in Walter, M.R., ed., 1976, Stromatolites- developments in sedimentology 20: Amsterdam, Elsevier Scientific Publishing Co., 790 p.

Harms, J.C., Southard, J.B., Spearing, D.R., Walker, R.G., 1975, Depositional environments as interpreted from primary sedimentary structures and stratification sequences: Tulsa, Oklahoma, Soc. Econ. Paleont. and Mineralogists, Short Course No. 2, Dallas, 1975, 161 p.

Hayes, M.O., 1967, Relationship between coastal climate and bottom sediment type on the inner continental shelf: Marine Geology, v. 5, p. 111-132.

Heckel, P.H., 1972, Recognition of ancient shallow marine environments, p. 226-286; in Rigby, J.K. and Hamblin, W.K., eds., 1972, Recognition of ancient sedimentary environments: Tulsa, Oklahoma, Soc. Econ. Paleont. and Mineralogists, Special Publ. No. 16, 340 p.

Hedgpeth, J.W., 1957 (reprinted 1963), Classification of marine environments, p. 17-27; in Hedgpeth, J.W., ed., 1957 (reprinted 1963), Treatise on marine ecology and paleoecology: Geological Society of America, Memoir 67, v. 1, Ecology, 1296 p.

Hintze, L.H., 1988, Geologic history of Utah: Brigham Young University Geology Studies, Special Publication 7, 202 p.

Hite, R.J., 1972, Shelf carbonate sedimentation controlled by salinity in the Paradox Basin, southeast Utah: Rocky Mountain Assoc. of Geol., The Mountain Geologist, v. 9, no. 2-3, p. 329-344.

Hoffman, P.F., Kaufman, A.J., Halverson, G.P., and Schrag, D.P., 1998, A Neoproterozoic Snowball Earth: Science, v. 281, (28 August 1998), p. 1342-1346.

Hoffman, P.F., and Schrag, D.P., 2000, Snowball Earth: Scientific American, January 2000, p. 68-75.

Holmes, A., 1965, Principles of Physical Geology, Second Edition: New York, The Ronald Press Company, 1288 p.

Hood, A, Gutjahr, C.C.M., and Heacock, R.L., 1975, Organic metamorphism and the generation of petroleum: Am. Assoc. Petrol. Geol., Bull., v. 59, no. 6, p. 986-996, 7 figs.

Hsu, K.J., 1972, Origin of saline giants: a critical review after the discovery of the Mediterranean Evaporite: Earth-Sci. Rev., v. 8, p. 371-396.

Hsu, K.J., Ryan, W.B.F., and Cita, M.B., 1973, Late Miocene desiccation of the Mediterranean: Nature, v. 242, p. 240-244.

Huc, A.Y., 1980, Chapter 14, Origin and formation of organic matter in recent sediments and its relation to kerogen, p. 445-474; in Durand, D., ed., 1980, Kerogen: insoluble organic matter from sedimentary rocks: Paris, Technips, 519 p.

Huntoon, P.W., 1989, Chapter 7 - Phanerozoic tectonism, Grand Canyon, Arizona, p. 76-89; in Elston, et al., 1989, Geology of Grand Canyon, northern Arizona (with Colorado River guides): American Geophysical Union, Washington, D.C., 28th International Geological Congress, Field Trip Guidebook T115/315, 239 p.

Huntoon, P.W. 1990, Chapter 14 - Phanerozoic structural geology of the Grand Canyon, p. 261-309; in Beus, S.S. and Morales, M., 1990, Grand Canyon Geology: New York-Oxford, Oxford University Press-Museum of Northern Arizona Press, 518 p.

Huntoon, P.W., Billingsley, G.H., Sears, J.W., Ilg, B.R., Karlstrom, K.E., Williams, M.L., Hawkins, D., Breed, W.J., Ford, T.D., Clark, M.D., Babcock, R.S., and Brown, E.H., 1996, Geologic map of the eastern part of the Grand Canyon National Park, Arizona: Museum of Northern Arizona and Grand Canyon Association.

Imbrie, J., and Imbrie, K.P., 1986, Ice Ages - Solving the Mystery: Cambridge, Massachussets, Harvard University Press, 224 p.

Ingle, J.C, 1980, Cenozoic paleobathymetry and depositional history of selected sequences wthin the southern California continental borderland, p. 163-195; in Sliter, W.V., 1980, Studies in marine micropaleontology and paleoecology- a memorial volume to Orville L. Bandy, Cushman Foundation for Foraminiferal Res., Spec. Publ. No. 19, 300 p.

James, N.P., 1984, Shallowing upward sequences in carbonates (Chapter 14), p. 213-228; in Walker, R.G., 1984, Facies models, 2nd edn.: St. John's, Newfoundland, Canada, Geological Association of Canada, Geoscience Canada Reprint Series 1, 317 p.

Jewell, W.J., and McCarty, P.L., 1971, Aerobic decomposition of algae: Envir. Sci. and Technology, v. 5, p. 1023-1031.

Jones, D.J., 1969, Introduction to Microfossils: New York, New York, Hafner Publishing Co., Inc., 406 p.

Karlstrom, K.E., Dehler, C.M., Sharp, Z.D., Geissman, J.W., Elrick, M.E., Timmons, J.M., Crossey, L.J., Bowring, S.A., Keefe, K., Knoll, A.H., Porter, S.M., Des Marais, D.J., and Weil, A.B., 2000, The Chuar Group of the Grand Canyon: record of breakup of Rodinia, associated change in the global carbon cycle, and ecosystem expansion by 740 Ma: Geology, v. 28, no. 7, p. 619-622.

Keen, M.J., 1969, An Introduction to Marine Geology: Oxford, Great Britain, Pergamon Press, 218 p.

Kendall, A.C., 1984, Evaporites, p. 259-296; in Walker, R.G., 1984, Facies Models, 2nd edn.: St. John's, Newfoundland, Canada, Geological Association of Canada, Geoscience Canada Reprint Series 1, 317 p.

Keulegan, H.G. and Krumbein, W.C., 1949, Stable configuration of bottom slope in a shallow sea and its bearing on geological processes: Am. Geophys. Union Trans., v. 30, p. 855-861.

Kinsman, D.J.J., Boardman, M., and Borcsik, M., 1973, An experimental determination of the solubility of oxygen in marine brines; in Fourth international symposium on salt: Northern Ohio Geol. Soc., v. 1, p. 325-327.

Kirkland, D.W., and Evans, R., 1981, Source-rock potential of evaporitic environment: Am. Assoc. Petrol. Geol., Bull., v. 65, no. 2, p. 181-190.

Klemme, H.D., and Ulmishek, G.F., 1991, Effective petroleum source rocks of the world: stratigraphic distribution and controlling depositional factors: Amer. Assoc. Petrol Geol., Bull., v. 75, no. 12, p. 1809-1851, 29 figs., 1 table.

Klubov, B.A., 1983, Prirodnye bitumy severa (Natural bitumens of the Arctic): Moscow, Nauka, 205 p.

Lagutenkova, N.S., and Chepikova, I.K., 1982, Verkhnedokem-briyskiye otlozheniya Volgo-Uralskoy oblasti i perspektivy ikh neftegazonosnosti (Upper Precambrian rocks of the Volga-Ural region and their petroleum potential): Moscow, Nauka, 111 p.

Lankford, R., 1967, Foraminiferal Zoogeography of the inner continental shelf, p. RL-1-RL-8A; in Bandy, O.L., Ingle, J.C., Lankford, R.R., and Lowenstam, H.A., 1967, Washington, D.C, American Geological Institute, Paleoecology, AGI Short Course Lecture Notes, New Orleans, Louisiana, November 17-19, 1967.

Laporte, L.F.,1968, Ancient environments: Englewood Cliffs, New Jersey, Prentice-Hall, Inc., 116 p.

Lucia, F.J., 1972, Recognition of evaporite-carbonate shoreline sedimentation, p. 160-191; in Rigby, J.K. and Hamblin, W.K., eds., 1972, Recognition of ancient sedimentary environments: Tulsa, Oklahoma, Soc. Econ. Paleont. and Mineralogists, Special Publ. No. 16, 340 p.

McAlester, A.L., 1968, The history of life: Engelewood Cliffs, New Jersey, Prentice-Hall, Inc., 152 p.

McHenry, R. (General Editor), 1992a, Burundi: The New Encyclopedia Britannica, Micropaedia, v. 2, p. 669-670.

McHenry, R. (General Editor), 1992b, Dead Sea: The New Encyclopedia Britannica, Micropaedia, v. 3, p. 937.

McHenry, R. (General Editor), 1992c, Mediterranean Sea: The New Encyclopedia Britannica, Micropaedia, v. 7, p. 1008.

McHenry, R. (General Editor), 1992d, Tanganyika, Lake: The New Encyclopedia Britannica, Micropaedia, v. 11, p. 541.

McHenry, R. (General Editor), 1992e, Tide: The New Encyclopedia Britannica, Micropaedia, v. 11, p. 760.

Middleton, L.T., and Elliot, D.K., 1990, Chapter 6 - Tonto Group, p. 83-106; in Beus, S.S., and Morales, M., 1990, Grand Canyon Geology: New York-Oxford, Oxford University Press-Museum of Northern Arizona Press, 518 p.

Mintz, L.W., 1972, Historical geology- the science of a dynamic earth: Columbus, Ohio, Charles E. Merrill Publishing Co., 785 p.

Murray, J.W., 1973, Distribution and ecology of living benthic foraminiferids: London, Great Britain, Heinemann Educational Books Limited, 274 p.

Neev, D., and Emery, K.O., 1967, The Dead Sea: depositional processes and environments of evaporites: Jerusalem, Israel Min. Develop. Geol. Surv., Bull. no. 42, 147 p., 59 figs., 50 tables.

Nuccio, V.F., and Fouch, T.D., 1992, Thermal maturity of the Mesaverde Group, Uinta Basin, Utah, p. 70-78; in Magoon, L.B., ed., 1992, The petroleum system- status of research and methods, 1992: U.S. Geol. Surv., Bull. 2007.

Ochsenius, C., 1877, Die bildung der steinsalzlager und ihrer mutterlaugensalze: Halle, C.E.M. Pfeffer, , 172 p.

Ochsenius, C., 1888, On the formation of rock-salt beds and mother liquor salts: Proc. Acad. Nat. Sci. Philadelphia, v. 40, p. 181-187.

Otsuki, A., and Hanya, T., 1972a, Production of dissolved organic matter from dead algal cells, I; aerobic microbial decomposition: Limnology and oceanography, v. 7, p. 248-257.

Otsuki, A., and Hanya, T., 1972b, Production of dissolved organic matter from dead algal cells, II; anaerobic microbial decomposition: Limnology and oceanography, v. 7, p. 258-264.

Parker, R.H., 1964, Zoogeography and ecology of some macroinvertebrates, particularly molluscs, in the Gulf of California and the continental slope off Mexico: Dansk Naturhistorisk Foren. Videnskabelige Medd., Bd. 126, 178 p.

Parrish, J.T., 1982, Upwelling and petroleum source beds, with reference to Paleozoic: Am. Assoc. Petrol. Geol., Bull., v. 66, no. 6, p. 750-774, 12 figs., 2 tables.

Parrish, J.T. and Curtis, R.L., 1982, Atmospheric circulation, upwelling, and organic-rich rocks in the Mesozoic and Cenozoic eras: Paleogeography, Paleoclimatology, Paleoecology, v. 40, p. 31-66.

Pedersen, T.F., and Calvert, S.E., 1990, Anoxia vs. productivity: what controls the formation of organic-carbon-rich sediments and sedimentary rocks?: Am. Assoc. Petrol. Geol., Bull., v. 74, no. 4, p. 454-466, 8 figs.

Pelet, R., and Debyser, Y., 1977, Organic geochemistry of Black Sea cores: Geochim. et Cosmochim. Acta, v. 41, p. 1575-1586.

Peters, K.E., 1986, Guidelines for evaluating petroleum source rock using programmed pyrolysis: Amer. Assoc. Petrol. Geol., Bull., v. 70, no. 3, p. 318-329, 15 figs., 4 tables.

Peters, K.E., and Cassa, M.R., 1994, Chapter 5 - Applied source rock geochemistry, p. 93-120; in Magoon, L.B., and Dow, W.G., eds., 1994, The petroleum system-from source to trap: Am. Assoc. Petrol. Geol., Memoir 60.

Phleger, F.B., 1960, Ecology and distribution of Recent Foraminifera: Baltimore, Maryland, The Johns Hopkins Press, 297 p.

Pickard, G.L., 1956, Physical features of British Columbia inlets: Roy. Soc. Canada, Trans., v. L, ser. III, p. 47-58, 4 figs., 2 tables.

Playford, P.E., and Cockbain, A.E., 1969, Algal stromatolites: deepwater forms in the Devonian of Western Australia: Science, v. 165, p. 1008-1010.

Playford, P.E., and Cockbain, A.E., 1976, Modern algal stromatolites at Hamelin Pool, a hypersaline barred basin in Shark Bay, Western Australia, Chapter 8.2, p. 389-412; in Walter, M.R., ed., 1976, Stromatolites- developments in sedimentology 20: Amsterdam, Elsevier Scientific Publishing Co., 790 p.

Porter, S.M., and Knoll, A.H., 2000, Testate amoebae in the Neoproterozoic Era: evidence from vase-shaped microfossils in the Chuar Group, Grand Canyon: Paleobiology, v. 26, no. 3, p. 345-370.

Rand McNally and Company, 1973, Rand McNally Illustrated World Atlas: Chicago, Illinois, Rand McNally and Company, 222 p.

Rauzi, S.L., 1990. Distribution of Proterozoic hydrocarbon source rock in northern Arizona and southern Utah: Arizona Geological Survey, Arizona Oil and Gas Conservation Commission, Special Publication 6, 19 p., 1 sheet, scale 1:500,000 [now available as Arizona Geological Survey Oil and Gas Publication OG - 31].

Rhoads, D.C., and Morse, J.W., 1971, Evolutionary and ecologic significance of oxygen-deficient marine basins: Lethaia, v. 4, p. 413-428.

Richards, F.A., 1957, Oxygen in the ocean, p.185-238; in Hedgpeth, J.W., ed., 1957, Treatise on marine ecology and paleoecology: Geol. Soc. America, Mem. 67, v. 1, Ecology, 1296 p.

Rusnak, G.A., 1960, Sediments of Laguna Madre, Texas, p. 153-196, 30 figs., 8 tables; in Shepard, F.P., Phleger, F.B., and van Andel, T.H., 1960, Recent sediments, northwest Gulf of Mexico: Tulsa, Oklahoma, Am. Assoc. Petrol. Geol., 394 p.

Ryan, W.B.F., Hsu, K.J., Nesteroff, D., Pautot, G., Wezel, F.C., Lort, J.M., Cita, M., Mayne, W., Stradner, H., and Dumitrica, P., 1972, Initial Reports of the Deep-Sea Drilling Project, Lisbon to Lisbon, 13: U.S. Government Printing Office, Washington, D.C.

Schlumberger Limited, 1972, Log Interpretation, Volume 1- Principles: New York, New York, 113 p.

Schlumberger Well Surveying Corporation, 1979, Log interpretation charts: Houston, Texas, 97 p.

Scruton, P.C., 1953, Deposition of evaporites: Amer. Assoc. Petrol. Geol., Bull., v. 37, no. 11, p. 2498-2512, 4 figs., 2 tables.

Sears, J.W., 1990, Chapter 5 - Geologic structure of the Grand Canyon Supergroup, p. 71-82; in Beus, S.S., and Morales, M., 1990, Grand Canyon Geology: New York-Oxford, Oxford University Press-Museum of Northern Arizona Press, 518 p.

Shaw, A.B., 1977, A review of some aspects of evaporite deposition: Rocky Mountain Assoc. Geol., The Mountain Geologist, v. 14, no. 1, p. 1-16.

Shepard, F.P., 1963, Submarine geology (2nd edn.): New York, New York, Harper and Row, Publishers, 557 p.

Shepard, F.P., 1969, The earth beneath the sea: New York, New York, Atheneum, 242 p.

Sofer, Z., 1984, Stable carbon isotope composition of crude oils: application to source depositional environments and petroleum alteration: Amer. Assoc. Petrol. Geol., Bull., v. 68, no. 1, p. 31-49, 8 figs., 1 table.

Steno, N., 1669, De solido intra solidum naturaliter contento dissertationis prodromus: Florence.

Stoakes, F.A., and Creaney, S., 1985, Sedimentology of a carbonate source rock: the Duvernay Formation of Alberta Canada, p. 343-375; in Longman, M.W., Shanley, K.W., Lindsay, R.F., and Eby, D.E., 1985, Rocky Mountain carbonate reservoirs: a core workshop: Soc. Econ. Paleont. and Min., Core Workshop No. 7, Golden, Colorado, August 10-11, 1985, 482 p.

Strom, K.M., 1936, Land-locked waters- hydrography and bottom deposits in badly-ventilated Norwegian fjords with remarks upon sedimentation under anaerobic conditions: Oslo, Skrifter utgitt av det Norske Videnskaps-Akademi i Oslo, I. Mat.-naturv. klasse, 1936, no. 7, p. 1-85, 43 figs., 9 pls.

Strom, K.M., 1937, Two land-locked fjords in northern Norway: Oslo, Skrifter utgitt av det Norske Videnskaps-Akademi i Oslo, I. Mat.-naturv. klasse, 1937, no. 7, p. 1-12, 5 figs.

Strom, K.M., 1939, Land-locked waters and the deposition of black muds, p. 356-372; in Trask, P.D., ed., 1939, Recent marine sediments- a symposium: Tulsa, Oklahoma, Amer. Assoc. Petrol. Geol., 736 p.

Summons, R.E., Brassell, S.C., Eglinton, G., Evans, E., Horodyski, R.J., Robinson, N., and Ward, D.M., 1988, Distinctive hydrocarbon biomarkers from fossiliferous sediment of the late Proterozoic Walcott Member, Chuar Group, Grand Canyon, Arizona: Geochemica et Cosmochemica Acta, v. 52, p. 2625-2637.

Tang Zeyao and Zhan Shenyu, 1984, Forming conditions of the Sinian gas pool in Sichuan basin: Beijing Petroleum Geology Symposium Preprint, 21 p.

Timmons, M.J., Karlstrom, K.E., Dehler, C.M., Geissman, J.W., Heizler, M.T., 2001, Proterozoic multistage (ca. 1.1 and 0.8 Ga) extension in the Grand Canyon Supergroup and establishment of northwest- and north-trending tectonic grains in the southwestern United States: Geol. Soc. Amer., Bull., v. 113, no. 2, p. 163-181.

Tissot, B.P., and Welte, D.H., 1978, Petroleum formation and occurrence- a new approach to oil and gas exploration: Berlin, Springer-Verlag, 699 p.

Toombs, R.B., 1956, Some characteristics of Bute Inlet sediments: Royal Soc. Canada, Trans., v. L, ser. III, p. 59-65, 3 figs., 1 table.

Trask, P.D., 1932, Origin and environment of source sediments of petroleum: Houston, Gulf Pub. Co., 323 p.

Trask, P.D., 1939, Organic content of recent marine sediments, p. 428-453; in Trask, P.D., ed., 1939, Recent marine sediments- a symposium: Tulsa, Oklahoma, Amer. Assoc. Petrol. Geol., 736 p.

Trewartha, G.T., 1961, The Earths Problem Climate: Madison, Wisconsin, The University of Wisconsin Press, 334 p.

Turekian, K.K., 1968, Oceans: Englewood Cliffs, New Jersey, Prentice-Hall, Inc., 120 p.

van Gijzel, P., 1982, Characterization and identification of kerogen and bitumen and determination of thermal maturation by means of qualitative and quantitative microscopical techniques, p. 159-205; in 1982, How to assess maturation and paleotemperatures: Soc. Econ. Paleontologists and Mineralogists, Short Course No. 7.

Vassoyevich, N.B., Korchagina, Y.I., Lopatin, N.V., and Chernyshev, V.V., 1970, Principal phase of oil formation: Moskov. Univ. Vestnik, no. 6, p. 3-27 (in Russian); English transl.: Internat. Geology Rev., v. 12, p. 1276-1296.

Vidal, G., 1986, Acritarch-based biostratigraphic correlations and the upper Proterozoic in Scandinavia, Greenland, and North America (Abstract): Geological Society of America, Abstracts with Programs, v. 18, no. 5, p. 420.

Vidal, G., and Ford, T.D., 1985, Microbiotas from the late Proterozoic Chuar Group (northern Arizona) and Uinta Mountain Group (Utah) and their chronostratigraphic implications: Precambrian Research, v. 28, p. 349-389.

Vidal, G., and Knoll, A.H., 1983, Proterozoic plankton; in Medaris, L.G., Jr., Byers, C.W., Mickelson, D.M., and Shanks, W.C., eds., International Proterozoic symposium (1981: University of Wisconsin-Madison) Proterozoic geology: Selected papers from an international Proterozoic symposium: Geological Society of America, Memoir 161, p. 265-277.

Wagner, F.J.E., 1970, Faunas of the Pleistocene Champlain Sea: Ottawa, Canada, Geol. Surv. of Canada, Bull. 181, 104 p., 2 figs., 7 pls., 3 tables.

Walker, R.G., 1984, Facies models, 2nd edn.: St. John's, Newfoundland, Canada, Geological Association of Canada, Geoscience Canada Reprint Series 1, 317 p.

Warren, J.K., 1986, Perspectives: shallow-water evaporitic environments and their source rock potential: Soc. Econ. Paleont. and Mineral., Jour. Sed. Petrol., v. 56, no. 3, p. 442-454, 9 figs., 2 tables.

Warren, J.K., and Kendall, C.G.S.C., 1985, Comparison of sequences formed in marine sabkha (subaerial) and salina (subaqueous) settings- modern and ancient: Am. Assoc. Petrol. Geol., Bull., v. 69, no. 6, p. 1013-1023, 6 figs., 1 table.

Waples, D.W., 1980, Time and temperature in petroleum formation: application of Lopatin's method to petroleum exploration: Am. Assoc. Petrol. Geol., Bull., v. 64, no. 6, p. 916-926, 13 figs.

Watson, S.W., and Waterbury, J.B., 1969, The sterile hot brines of the Red Sea, p. 272-281, 1 fig., 6 tables; in Degens, E.T., and Ross, D.A., eds., 1969, Hot brines and recent heavy metal deposits in the Red Sea: New York, Springer-Verlag.

Weil, A.B., Van der Voo, R., Geissman, J.W., and Karlstrom, K.E., 1999, Preliminary paleomagnetic results from the Neoproterozoic Chuar Group, Grand Canyon Supergroup, Arizona: Geol. Soc. America, Abstracts with Programs, v. 31, no. 7, p. A-317.

Wiley, B.H., Rauzi, S.L., Cook, D.A., Clifton, E.H., Kuo, Lung-Chuan, and Moser, J.A., 1998, Geologic description, sampling, petroleum potential, and depositional environment of the Chuar Group, Grand Canyon, Arizona: Arizona Geological Survey, Open-File Report 98-17, 83 p., 6 tables, 12 figs., 2 pls.

Woolnough, W.G., 1937, Sedimentation in barred basins, and source rocks of oil: Am. Assoc. Petrol. Geol., Bull., v. 21, no. 9, p. 1101-1157.

Zenkevitch, L., 1963, Biology of the seas of the U.S.S.R.: London, George Allen and Unwin Ltd. and New York, Interscience Pub., 955 p.

Table 1. Measured thicknesses of Awatubi and Walcott Members, Kwagunt Formation, Chuar Group in this* and previous studies and number of samples per study.

Rock Unit	Ford, 1990; Ford and Breed, 1973, p. 1244	Hintze, 1988, p. 199	Elston, 1989, p. 96	Wiley and others, 1998 Nankoweap Canyon Area	Wiley and others, 1998 Carbon Canyon Area	Cook, 1991 Nankoweap Butte	Cook, 1991 Sixtymile Canyon	This Study Sixtymile Canyon
Walcott Member	838 ft	840 ft	922 ft	887 ft (36 samples)	50 ft est. (0 samples)	793 ft (57 samples)	763 ft (9 samples)	827 ft (21 samples)
Awatubi Member	1128 ft	1230 ft	988 ft	855 ft (31 samples)	771 ft+ (27 samples)	Not sampled	Not sampled	653 ft (9 samples)

*Total of 1480 ft of section measured and 30 samples collected in the present study

Table 2. Summary of source rock data. Walcott and Awatubi Members, Kwagunt Formation, Chuar Group, Sixtymile Canyon Section.

ROCK UNIT	SOURCE ROCK POTENTIAL (This Study)						SOURCE ROCK POTENTIAL (Cook, 1991)					
	Organic richness (% TOC)			Organic maturity (Tmax °C)			Organic richness (% TOC)			Organic maturity (Tmax °C)		
	#sp	Range	Ave	#sp	Range	Ave	#sp	Range	Ave	#sp	Range	Ave
Walcott Member	21	0.96-9.39 (fair - excellent)	2.83 (very good)	21	427-447 (immature - peak oil)	435 (immature/early oil boundary)	9	0.03-5.61 (poor - excellent)	2.22 (very good)	8	436-451 (early oil - late oil)	443 (early oil)
Awatubi Member	9	0.39-1.87 (poor - good)	1.11 (good)	9	301-436 (immature - early oil)	389 (immature)		NOT SAMPLED				
				6*	416-436 (immature - early oil)	428 (immature)						

*Excluding samples with Tmax < 380°C

Table 3. Hydrocarbon Source Rock Potential of Awatubi and Walcott Members, Kwagunt Formation, Chuar Group. Sixtymile Canyon Section.

ROCK UNIT	HYDROCARBON TYPE INDICATOR		SOURCE RICHNESS		SOURCE MATURITY		INDIGENOUS/ MIXED/MIGRATED
	HI: Hydrogen Index	S2/S3	TOC (%)	Genetic Potential	Tmax	PI = TR	PI = TR
Walcott Member	35 ft mixed oil & gas prone	92 ft oil prone	117 ft excellent	52 ft excellent	432°C (immature) @ top	358 ft immature	20 ft migrated
	555 ft gas prone	282 ft mixed oil & gas prone	303 ft v. good (420 ft v. good +)	40 ft good (92 ft good +)	437°C (early oil) @ base	139 ft early oil (456 ft early oil +)	22 ft mixed (42 ft mixed or migrated)
	224 ft no hydrocarbon potential	321 ft gas prone	388 ft good (808 ft good +)	397 ft moderate (489 ft moderate +)	upper 420 ft immature	205 ft early oil-peak oil gap (317 ft early oil-peak oil gap +)	772 ft indigenous
		119 ft no hydrocarbon potential	6 ft fair (814 ft fair +)	325 ft non oil source, some gas potential	basal 407 ft early oil	92 ft peak oil (112 ft peak oil +)	
						20 ft late oil and post-mature	
	814 ft sampled	814 ft sampled	814 ft sampled	814 ft sampled	827 ft total section	814 ft sampled	814 ft sampled
Awatubi Member	37 ft gas prone	100 ft gas prone	100 ft v. good	10 ft moderate	All 653 ft early oil	22 ft immature	182 ft migrated
	419 ft no hydrocarbon potential	356 ft no hydrocarbon potential	238 ft good (338 ft good +)	446 ft non oil source, some gas potential	437°C @ top	97 ft early oil (434 ft early oil +)	22 ft mixed (204 ft mixed or migrated)
			17 ft fair (355 ft fair +)		440°C @ base	119 ft early oil-peak oil gap (337 ft early oil-peak oil gap +)	252 ft indigenous
			101 ft poor			36 ft peak oil (218 ft peak oil +)	
						182 ft late oil and post-mature (gas window)	
	456 ft sampled	456 ft sampled	456 ft sampled	456 ft sampled	653 ft total section	456 ft sampled	456 ft sampled

Table 4: Modern Euxinic and Oxic Basin/Organic–Rich Environment Classification and Comparison of % Organic Matter, Depths, and Sediments of Anoxic vs. Oxic Facies. Compiled from (1) Strom, 1936; (2) Strom, 1937; (3) Gripenberg, 1939; (4) Strom, 1939; (5) Trask, 1939; (6) Toombs, 1956; (7) Pickard, 1956; (8) Caspers, 1957; (9) Rusnak, 1960; (10) Neev and Emery, 1967; (11) Turekian, 1968; (12) Watson and Waterbury, 1969; (13) Shaw, 1977; (14) Friedman and Sanders, 1978; (15) Demaison and Moore, 1980; (16) Huc, 1980; (17) Ingle, 1980; (18) Bauld, 1981a; (19) Bauld, 1981b; (20) Kirkland and Evans, 1981; (21) Warren, 1986; and (22) Pedersen and Calvert, 1990. Assumes: Org. carbon = 0.56 x Org. matter (Trask, 1939, p. 449).

Category and Examples and (Sources)	% Organic Carbon		Depth		Sediments	
	Anoxic Facies	Oxic Facies	Anoxic Facies	Oxic Facies	Anoxic Facies	Oxic Facies
I. Large Deep Lakes						
A. Large Anoxic, Permanently Stratified Tropical Lakes						
1. Lake Tanganyika (15, 21)	7-11%	1-2%	150-1500 m	< 150 m	Varving. Common diatoms.	Varving. Common diatoms.
2. Lake Kivu (15, 21)	Up to 15%		60-500 m	< 60 m		
3. Pre-1979 Dead Sea (10, 14, 15, 21)	4-2.0% → ?		> 50 m	< 50 m	Dark layers of equal amts. of calcite & aragonite + white layers w/ 4X as much aragonite as calcite (pre-overturn).	Gypsum ubiquitous. Aragonite pptd. when surf. water temp. > 35° C. (every 5th yr. +/-) (pre-overturn).
B. Large Oxic Lakes –Temperate to cold climates with seasonal overturn						
1. Lake Albert, E. Africa (15)						
2. Lake Victoria, E. Africa (15)						
3. Lake Baikal, Siberia (15)						
4. Great Lakes, North America (15)						
5. Great Slave Lake, W. Canada (15)						
II. Silled, Restricted (Semi-Isolated) Basins						
A. Positive Water Balance – Rainfall, runoff, and stream inflow exceed evaporation						
1. Anoxic – Portals with one-way flow. Outflowing freshwater blocks freshwater threshold.						
a. Black Sea (8, 14, 15, 16, 22) (Holocene sapropel excluded)	1-6% or 1.7-5.6% (5)	< 2.5%	>250 m @ edges; > 150 m @ center	<250 m @ edges; < 150 m @ center.	Alternating white coccolith & black organic-rich laminates (50-100 cm). Gray clay and gray calcareous clay or marl.	
b. Baltic Sea (3, 5, 14, 15)	1.7-5.8%	2.9-4.1% (?)	Gothland Deep		Black or gray muds.	Gray muds.

67

Table 4 (continued).

II. Silled, Restricted (Semi-Isolated) Basins (Cont.)						
A. Positive Water Balance -- Rainfall, runoff, and stream inflow exceed evaporation (Cont.)						
1. Anoxic -- Portals with one-way flow. Outflowing freshwater blocks threshold (Cont.).						
c. Lake Maracaibo (15, 16)		< 6% dry wt				
d. Saanich Inlet, British Columbia (15, 22)		0.5-16.8%; 12% common			Black (pyritic), organic mud.	
e. Few Norwegian Fjords (1, 2, 4, 5, 14)						
f. Kaoe Bay on coast of Halmahera, Indonesia (1, 4, 14, 16)		3-4% → ?	470-500 m			
2. Oxic -- Portals with two-way flow. Outflowing freshwater doesn't block threshold.						
a. Most Fjords on coast of British Columbia, Canada (6, 7, 14)	Absent	0.3-2.5%; av. 0.8%	Absent	6-732 m		Green-brown, green-grey, to grey, fine-grained silt and mud. Abundant diatoms.
b. Many Norwegian Fjords (1, 2, 4, 14)	Absent	0.6-1.4%	Absent			Gray or green mud.
c. Jervis Inlet, British Columbia (22)	Absent	< 6% dry wt				
3. Occassional Marine Inflow						
a. Anoxic -- Inflow less dense than basin water and forms interflow (14).						
b. Oxic -- Inflow denser than basin water. Sinks to and oxygenates bottom (14).						
B. Negative Water Balance -- Basins losing large amounts of water by evaporation.						
1. Portals with Two-way Flow (14).						
a. Anoxic -- Basins with stratified brines and sub-threshold salinities ≥ 124-199 ‰ NaCl, i.e. precipitating gypsum or halite or higher grade evaporites. Most saline evaporites at margin opposite portal (teardrop pattern) (20).						
b. Oxic -- Basins without stratified brines or with stratified sub-threshold salinities < 124-199 ‰ NaCl, i.e. not precipitating gypsum or higher grade evaporites.						
1) Mediterranean Sea (5, 14, 15)	Absent	0.6-1.7%	Absent	0-4000 m	Absent	Absent
2) Red Sea (12, 13, 14, 15, 21)	Anoxic Deeps: 0.22%. [4% if ignore the metals pptd. fr. brine (95% of seds.)].	0.26-0.66%	2040-2175 m	0-2040 m	95% of sediments = metals pptd. fr. brine.	
3) Persian Gulf (15)	Absent	To 2.5%	Absent			Absent

Table 4 (continued).

II. Silled, Restricted (Semi-Isolated) Basins (Cont.)					
B. Negative Water Balance – Basins losing large amounts of water by evaporation (Cont.)					
2. Portals with One-way Flow (14).					
a. Anoxic – Basins with stratified brines and sub-threshold salinities ≥ 124-199 ‰ NaCl, i.e. precipitating gypsum and/or halite or higher grade evaporites. Most saline evaporites at center (bullseye pattern) (20).					
b. Oxic – Basins without stratified brines or stratified with sub-threshold salinities < 124-199 ‰ NaCl, i.e. not precipitating gypsum or higher grade evaporites.					
III. Anoxic Depression in Oxic Open Ocean (Closed Basins on the Sea Floor)					
A. Cariaco Trench, North of Venezuela (14, 15, 16, 21)	3-6%	Av. 0.8%	300-1400 m	< 300 m	Abundant fish bones.
B. Orca Basin, N.W. Gulf of Mexico (15)	0.8-2.9% (May be diluted by slumping.)		2200-2400 m	< 2200 m	
C. Continental Borderland, off S. California (Santa Barbara Basin) (5, 14, 16)	To 4.5%				
D. Moluccas, Indonesian Archipelago (14)					
IV. Upwelling Areas					
A. Anoxic Layers Caused by Upwelling: California, Peru, Chile, S.W. Africa, Morocco, W. Australia (15).					
1. S.W. African Shelf, Namibia: Walvis Bay & Cape Cross (Benguela Current) (15, 16). (Also a closed basin on the sea floor III)	3-26% (or 30% (15)	< 3%	Mostly < 500 m		OM = mostly planktonic. Abnormal conc. of Cu, Ni, U, P, & Mo. U incorporated in apatite & conc. in phosphate nodules & laminae.
2. Peru (Humbolt) Current (15, 21)	3-11%. Av. 3.33%	0.5-3%	100-500 m	> 500 m	Silty clays & laminated diatomaceous oozes. U-enriched phosphorite nodules @ upper & lower boundaries O_2 min. zone.
B. Upwelling without Anoxic Layers: Antarctica, the N. Pacific (Offshore Japan & Kuriles), off S.E. Brazil (15).					
1. Antarctica (15)	Absent	0.10-0.94 %			Absent
2. Argentine Basin (11)	Absent	To 2.8%			

69

Table 4 (continued).

V. Open Ocean Water Masses						
A. Anoxic Open Ocean (Oxygen Minimum Zones)						
1. Indian Ocean (15)	2-11%	< 0.5-1%	250-1200 m	<250m.; >1200 m	Laminated mud & olive-gray mud	Dark- & light-brown mud.
2. N.E. Pacific Ocean, Offshore Oregon & Washington (15)	1-3%	Approx. 1%				Lamination lacking. Active bioturbation.
3. Gulf of California (Mexico) (5, 15, 22)	>5-5.6%	<2%	300-1200 m	<300m.; >1200 m	Finely laminated, richly diatomaceous seds. Burrowers scarce or absent.	
4. Angola Basin (15)	No data.	No data.				
5. E. Tropical Pacific (22)			O_2 Min. with free H_2S: 200-1200 m			
6. E. Arabian Sea (22)	To 6.9% wt.		200-1500 m			
7. Southern California (17) (Also an Upwelling Area, IVA) (5)			200-500 m to 1000-1500 m		Thin bedded or laminated sed. enriched in OM.	
8. Gulf of Mexico (5, 14)	0.8-2.8%(O_2 minimum but nearly fully oxic)	≤0.8 or 1.1	100 – 250 m	<100 m & >250 m		
B. Oxic Open Ocean						
1. Offshore N.W. Africa (Mauritania & Cape Verde) (15, 22).	Absent	0.5-4%	O_2 min. centered @ 400 m & doesn't extend to OC max. depths.	OC max = 1000-2000 m below center of intense upwelling off Cap Blanc & off Senegal R.		
2. Offshore Ivory Coast & Ghana (15)	Absent	3-5% (high terrestrial OM)			Absent	High terrestrial plant OM.
3. Niger Delta (15)	Absent	0.5-1% (Dilution by high sedn. rates.)			Absent	Prodelta clays.

Table 4 (continued).

V. Open Ocean Water Masses (Cont.)						
B. Oxic Open Ocean (Cont.)						
4. Grand Banks, Newfoundland (15)	Absent	Av. 0.5%			Absent	
VI. Non-Euxinic (Oxic) Categories						
A. Shallow, Saline/Hypersaline, Coastal and Continental Oxic Lakes - Shallow enough for wind mixing.						
1. Solar Lk., Gulf of Aquaba, Israel (18, 19, 21)	Absent?	8-15%		4-6 m		Cyanobact. mat. sed
2. Laguna Guerrero Negro, Baja, Calif. (19, 21)	Absent?	9.1-29.6%				Cyanobact. mat. seds.
3. Laguna Lejia, Antofagasta, Chile (19, 21)	Absent?	1.2-3.1%				Cyanobact. mat. sed
4. Coast Lk., Ross Island, McMurdo Snd. (19, 21)	Absent?	To 24%				Cyanobact. mat. seds.
5. Coorong Ephemeral Lks., S. Australia, (14, 16, 21)	To 12% (Anoxic Holocene Lk.)	To 2% (Present Ephemeral Lks., Seasonally vadose.)		2-10 m	Cyanobact. mat. Seds (Anoxic Holocene lk.)	
B. Deltas						
1. Mississippi Delta (5)	Absent	1.1-1.7%			Absent	Fine-grained deps.
C. Lagoons						
1. Bays of Texas (5)	Absent	0.6-1.7%			Absent	
a. Kleberg Point Lagoon, Baffin Bay, TX (9, 19, 21)	Absent?	2.2-5.0%		2.44-3.05 m	Absent?	Cyanobact. mat. seds.
b. Harbor Island, Texas (19, 21)	Absent?	To 32%	Absent?		Absent	Cyanobact. mat. seds
c. Laguna Madre, Southern Texas (9, 20)	Absent?	0.1-3.9%; av. 0.2%	Absent?	To 2.44 m; av. 1.2 m	Absent?	Highest OM = 6-7% = Cyanobact. mat deposits in anoxic near-surface seds.
2. Lagoona Mormona, Baja California, Mexico (16, 18, 19)	Absent?	To 5.4%		0.01-<1.0 m		Cyanobact. mat seds
3. Pamlico Sound, E. Coast U.S. (5)	Absent?	0.6-3.9%				Possible OM influx from bordering swamps.
4. Abidjan Lagoon, Ivory Coast (16, 21)	Absent?	4-12%			Absent?	
D. Areas of Limestone Deposition, Bahamas & Florida (5)						
1. Shallow marl banks in 0.3-1 m of water (5)	Absent	1.7-3.4%	Absent	0.3-1 m	Absent	Marl.
2. Adjacent deeper oceanic water (5)	Absent	0.6-3.4%				
a. Bahamian Oolite (21)	Absent	3-5%				

Table 4 (continued).

VI. Non-Euxinic (Oxic) Categories (Cont.)			
D. Areas of Limestone Deposition, Bahamas & Florida (5) (Cont.)			
2. Adjacent deeper oceanic water (5) (Cont.)	Absent	0.6-3.4%	
b. Gulf of Batabano, Cuban Shelf (21)	Absent	To 16%	Lack of iron reductant for S^{-2} results in high, sterilizing levels of H_2S in near-surface sediments, killing even sulfate-reducing bacteria.

72

Table 5.   Summary of Range of Organic Carbon Percentage in Euxinic and Oxic Organic-rich Model Environments from Data in Table 4.

Basin or Environment Type	% Organic Carbon of Anoxic Facies	% Organic Carbon of Oxic Facies
Euxinic Basins		
1) Large Tropical Lakes and Desiccating Inland Seas	0.4 - 15	1 - 2
2) Semi-isolated, Positive Water Balance Basins	1 - 16.8	0.3 - 4.1? (or <6)
3) Semi-isolated, Negative Water Balance Basins - Portals with Two-way Flow	0.22 - 4?	0.26 - 2.5
4) Semi-isolated, Negative Water Balance Basins - Portals with One-way Flow	?	?
5) Closed Anoxic Depressions in the Oxic Open-ocean	0.8 - 6	Av. 0.8
6) Anoxic Layers Caused by Upwelling	3 - 26 or 30	0.1 - 3.0
7) Anoxic Open-ocean Water Masses	1 - 11	<0.5 - 5
Total Range for Euxinic Basins	**0.22 - 26 or 30**	**0.1 - 5 (or < 6)**
Non-euxinic (Oxic) Environments		
8) Saline/Hypersaline Lakes	To 12 (Holocene)	1.2 - 29.6
9) Deltas	Absent	1.1 - 1.7
10) Lagoons	Absent	0.1 - 32
11) Areas of Limestone Deposition	Absent	0.6 - 16
12) Epeiric Sea	Absent	?
Total Range for Non-euxinic (Oxic) Environments	**To 12 (Holocene)**	**0.1 -32**
Total Range for all Organic-rich Environments	**0.22 - 26 or 30**	**0.1 - 32**

Figure 1. Index Map, Chuar Terrane, Eastern Grand Canyon, Arizona (from Ford and Breed, 1973, Fig. 1.)

74
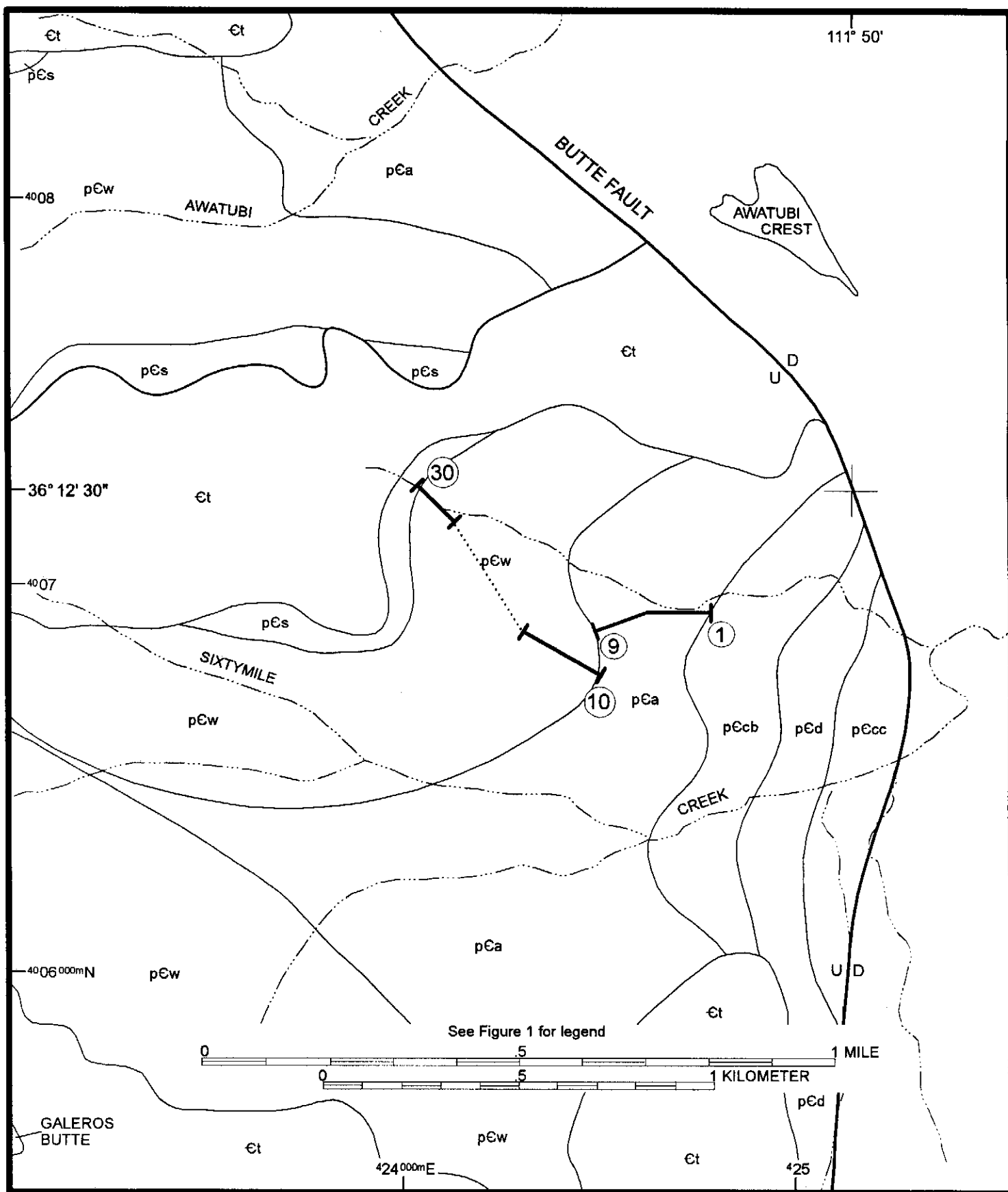
Figure 2. Sample Localities and Geology from Ford and Breed (1973, Fig. 1). Sixtymile Canyon Area, Cape Solitude 7.5' Quadrangle, Arizona.
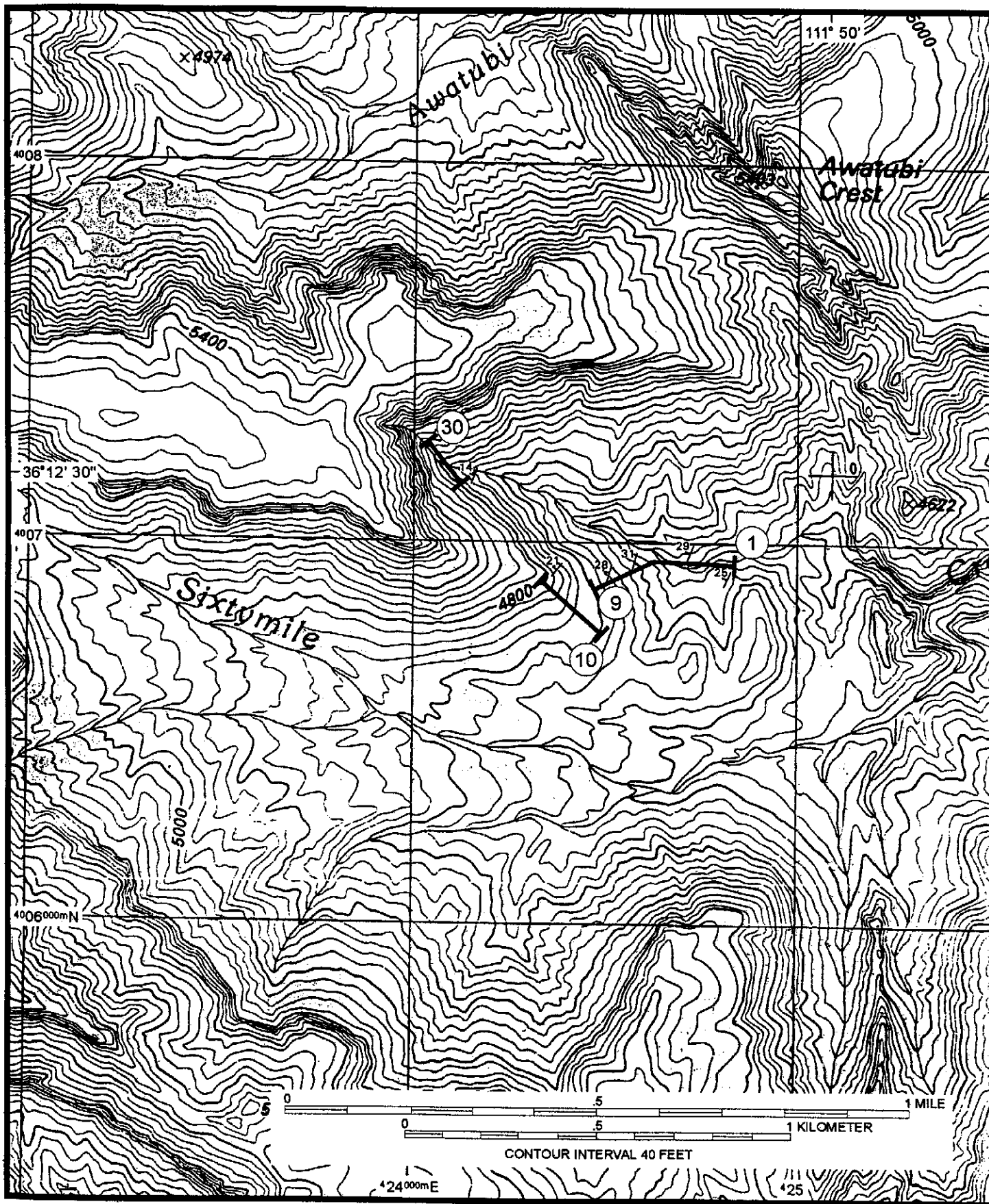
Figure 3. Sample Localities and Topography Sixtymile Canyon Area, Cape Solitude 7.5' Quadrangle, Arizona.
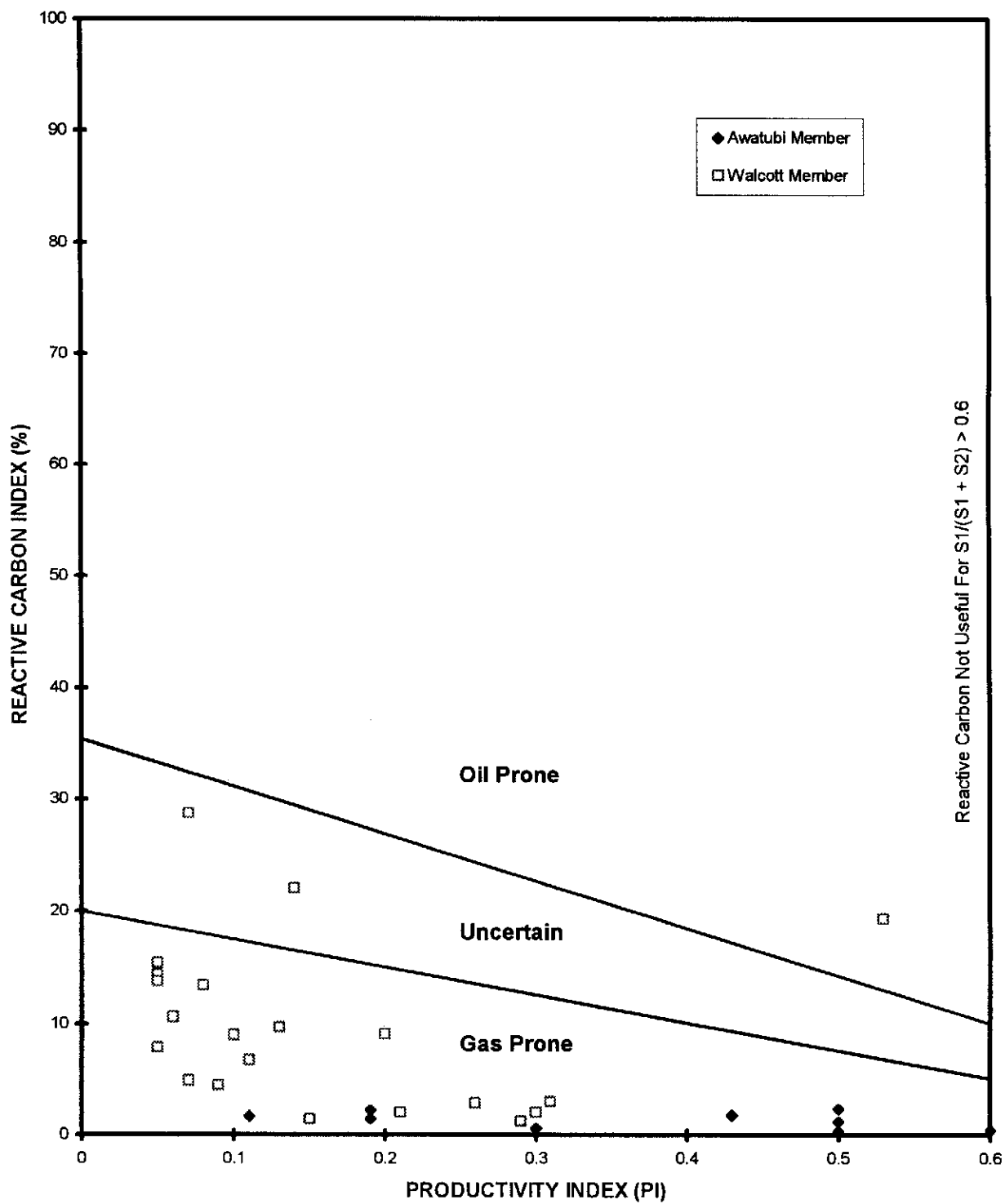
Figure 4. Cross-plot of Reactive Carbon Index vs. Productivity Index with Hydrocarbon Type. Awatubi and Walcott Members, Sixtymile Canyon Area, Grand Canyon, Arizona.
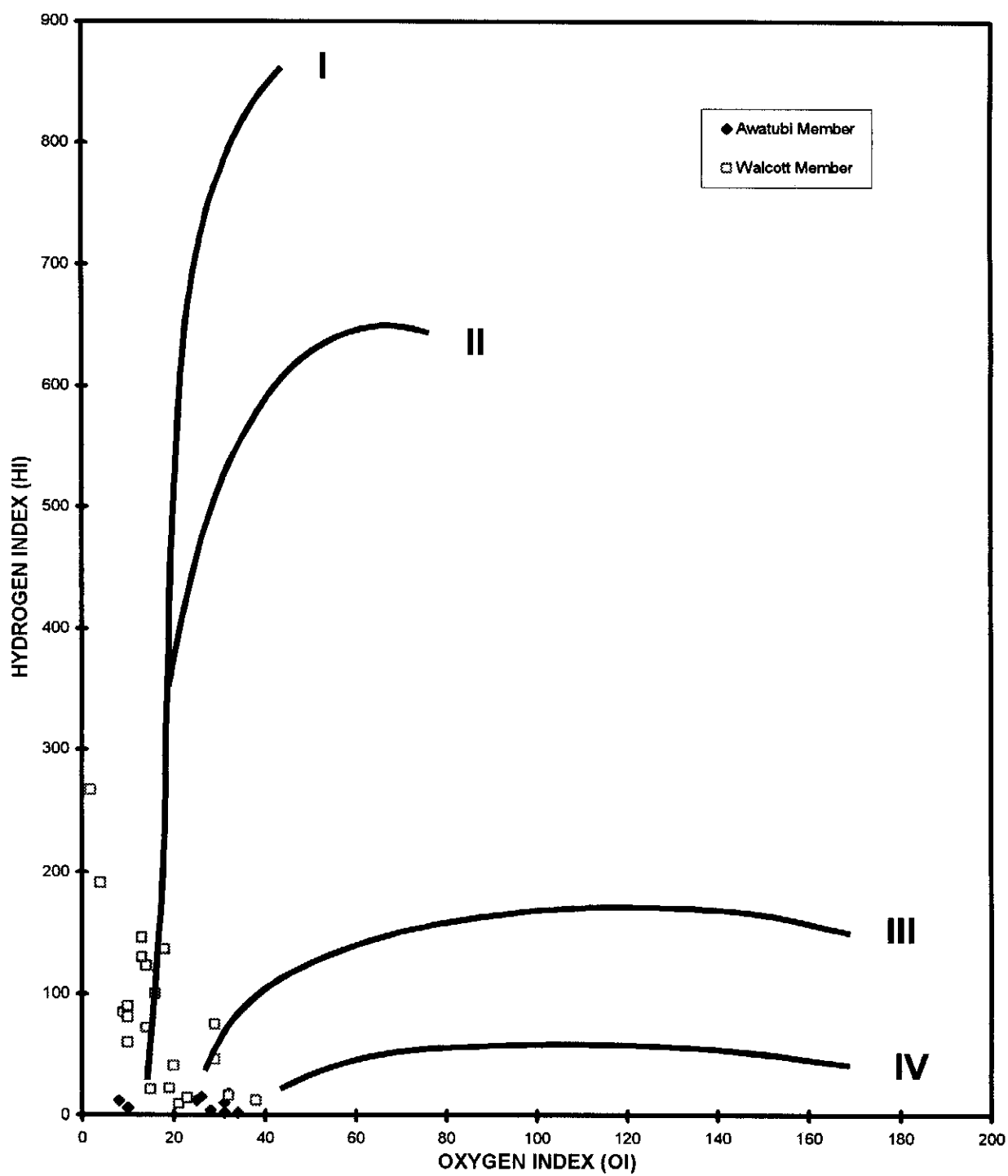
Figure 5. Modified van Krevelen diagram. Awatubi and Walcott Members, Sixtymile Canyon Area, Grand Canyon, Arizona.
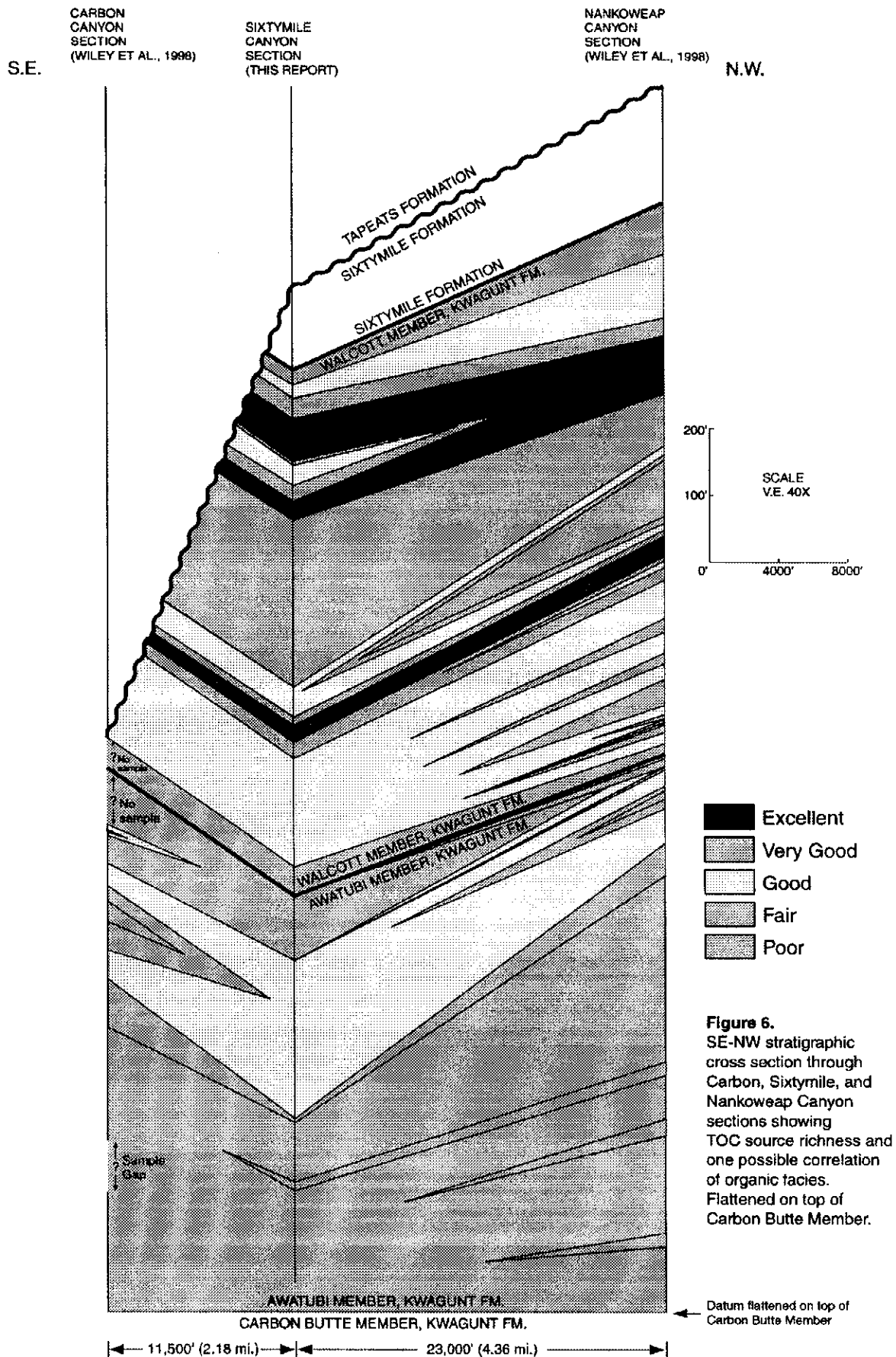
Figure 6.
SE-NW stratigraphic cross section through Carbon, Sixtymile, and Nankoweap Canyon sections showing TOC source richness and one possible correlation of organic facies. Flattened on top of Carbon Butte Member.

Figure 7.
SE-NW stratigraphic cross section through Carbon, Sixtymile, and Nankoweap Canyon sections showing TMAX source maturity windows (Red) superimposed. Flattened on top of Carbon Butte Member.

B. Wiley 12/05/99

80
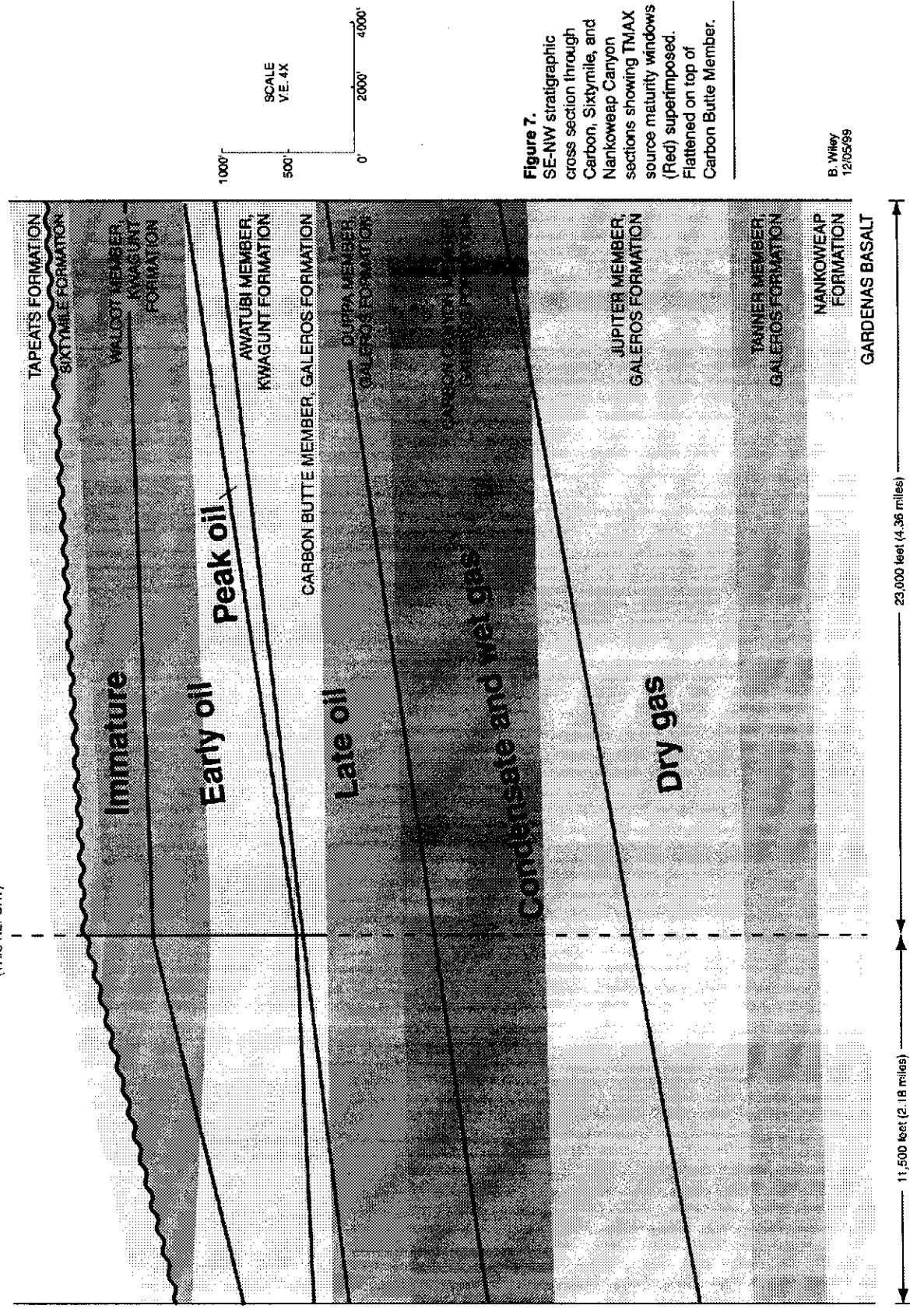
Appendix 1: Analytical Data and Source Rock Analyses. Sixtymile Canyon Area, Grand Canyon, Arizona

Member	Sample No.	Cum. Height (feet)	TOC (wt%)	S1 (mg/g)	S2 (mg/g)	S3 (mg/g)	Tmax (°C)	HI	OI	S2/S3	GP (mg/g)	PI	RCI (%)	S1/ TOC
Walcott	S10-60-30	1467	2.96	0.22	3.86	0.38	435	130	13	10.16	4.08	0.05	13.78	7
	S10-60-29	1452	1.46	0.11	0.88	0.15	432	60	10	5.87	0.99	0.11	6.78	8
	S10-60-28	1417	2.48	0.22	2.01	0.26	431	81	10	7.73	2.23	0.10	8.99	9
	S10-60-27	1388	5.32	1.60	10.16	0.22	442	191	4	46.18	11.76	0.14	22.11	30
	S10-60-26	1358	9.39	2.02	24.00	0.22	447	266	2	113.59	27.01	0.07	28.76	22
	S10-60-25	1334	1.50	1.55	1.35	0.15	427	90	10	9.00	2.90	0.53	19.33	103
	S10-60-24	1294	2.03	0.25	1.72	0.18	434	85	9	9.56	1.97	0.13	9.70	12
	S10-60-23	1270	5.14	0.42	7.53	6.69	439	146	13	10.91	7.95	0.05	15.47	8
	S10-60-22	1209	2.38	0.08	1.10	0.68	432	46	29	1.62	1.18	0.07	4.96	3
	S10-60-21	1096	3.63	0.26	4.96	0.65	441	137	18	7.63	5.22	0.05	14.38	7
	S10-60-20	1066	2.52	0.16	2.51	0.41	437	100	16	6.12	2.67	0.06	10.60	6
	S10-60-19	983	2.02	0.22	2.49	0.28	435	123	14	8.89	2.71	0.08	13.42	11
	S10-60-18	938	1.13	0.07	0.16	0.26	434*	14	23	0.62	0.23	0.30	2.04	6
	S10-60-17	909	5.14	0.20	2.12	1.03	437	41	20	2.06	2.32	0.09	4.51	4
	S10-60-16	874	2.07	0.09	0.33	0.67	431*	16	32	0.49	0.42	0.21	2.03	4
	S10-60-15	845	1.06	0.08	0.23	0.20	433*	22	19	1.15	0.31	0.26	2.92	8
	S10-60-14	820	0.96	0.09	0.20	0.14	434*	21	15	1.43	0.29	0.31	3.02	9
	S10-60-13	796	1.73	0.32	1.25	0.25	430	72	14	5.00	1.57	0.20	9.08	18
	S10-60-12	715	1.80	0.04	0.22	0.68	435*	12	38	0.32	0.26	0.15	1.44	2
	S10-60-11	702	1.37	0.05	0.12	0.29	436*	9	21	0.41	0.17	0.29	1.24	4
	S10-60-10	682	3.30	0.13	2.48	0.96	437	75	29	2.58	2.61	0.05	7.91	4
Awatubi	S10-60-09	543	1.87	0.08	0.34	0.59	434*	18	32	0.58	0.42	0.19	2.25	4
	S10-60-08	512	1.27	0.02	0.02	0.39	302*	2	31	0.05	0.04	0.50	0.31	2
	S10-60-07	477	1.15	0.03	0.02	0.39	301*	2	34	0.05	0.05	0.60	0.43	3
	S10-60-06	443	1.69	0.03	0.07	0.48	416*	4	28	0.15	0.10	0.30	0.59	2
	S10-60-05	413	1.06	0.02	0.16	0.28	431*	15	26	0.57	0.18	0.11	1.70	2
	S10-60-04	315	1.09	0.03	0.13	0.09	436*	12	8	1.44	0.16	0.19	1.47	3
	S10-60-03	308	0.50	0.03	0.03	0.05	330*	6	10	0.60	0.06	0.50	1.20	6
	S10-60-02	205	0.39	0.03	0.04	0.12	429*	10	31	0.33	0.07	0.43	1.79	8
	S10-60-01	197	0.93	0.11	0.11	0.23	420*	12	25	0.48	0.22	0.50	2.37	12

* = Tmax data not reliable due to low kerogen S2 value

HI = 100(S2)/TOC

OI = 100(S3)/TOC

GP = S1 + S2

PI = S1/(S1 + S2)

RCI = 10(S1 +S2)/TOC

S1/TOC = 100(S1)/TOC

TOC = Weight Percent Organic Carbon

S1, S2, GP = mg hydrocarbons/g rock

S3 = mg carbon dioxide/g rock

Awatubi and Walcott Members of the Kwagunt Formation, Chuar Group. Sixtymile Canyon Stratigraphic Section, Grand Canyon National Park, Cape Solitude 7.5' Topographic Quadrangle, Coconino County, Arizona by Samir A. Ghazi

Sample designations are S10-60-#, which indicate S for the collector, Samir Ghazi, 10 for the **tenth** trip of the University of New Mexico to the Chuar Group of the Grand Canyon, 60 for Sixtymile Canyon Section, followed by the **sample number** of 1 through 30. Samples S10-60-1 through S10-60-9 were from the Awatubi Member of the Kwagunt Formation. Samples S10-60-10 through S10-60-30 were from the Walcott Member of the Kwagunt Formation. The section was measured November 7 through November 9, 1997, by S. Ghazi, A. Knoll, and C. Dehler. The section begins at the contact between the Carbon Butte and Awatubi Members of the Kwagunt Formation, located 8550 feet S71°W from the junction of Sixtymile Creek and the Colorado River. It is measured up section. It ends at the contact between the Walcott Member of the Kwagunt Formation and the Sixtymile Formation, located 16,200 feet S81°W from the junction of Sixtymile Creek and the Colorado River. The section is along the northern tributary of the Sixtymile Creek and along the ridge on the south flank of this tributary.

SIXTYMILE FORMATION: The contact with the Sixtymile Formation is put at the base of the carbonate in this area. The carbonate is believed to be a slide block by Elston and is reddish to terra cotta in color.

WALCOTT MEMBER, KWAGUNT FORMATION (251 m = 823.5 ft)

	251 m	(823.5 ft)	= Top Walcott Member, Kwagunt Formation = Base of boudin-like carbonate of the Sixtymile Formation.
	248-251 m	(814-823.5 ft)	Shale.
S-10-60-30	248 m	(814 ft)	Shale.
	245-248 m	(804-814 ft)	Shale.
	245 m	(804 ft)	20 cm (8 in) of crystalline dolomite (?).
	243.5-245 m	(799-804 ft)	Shale.
S-10-60-29	243.5 m	(799 ft)	Shale.
	233-243.5 m	(764-799 ft)	Shale.
S-10-60-28	233 m	(764 ft)	Shale.
	224-233 m	(735-764 ft)	Shale.
S-10-60-27	224 m	(735 ft)	Shale.
	215-224 m	(705-735 ft)	Shale.
S-10-60-26	215 m	(705 ft)	Shale.
	207.5-215 m	(681-705 ft)	Shale.
S-10-60-25	207.5 m	(681 ft)	Shale.
	195.5-207.5 m	(641-681 ft)	Shale with a 25 cm (10 in) thick bed of pisolitic grainstone dolomite which is very hard and may be inversely graded (sample 4). Note: Should this be sample 24?
S-10-60-24	195.5 m	(641 ft)	Shale (or see note immediately above).
	188-195.5 m	(617-641 ft)	Very thick section of black claystones, hard, fractured, and weathered, some sulphurous smell. Consistent petroliferous odor upon striking. When clay breaks, abundant yellowish white powder on cleavage planes (sulfur?).
S-10-60-23	188 m	(617 ft)	Shale.
	182-188 m	(597-617 ft)	Shale.
	178.5-182 m	(586-597 ft)	Upper unit of the Double Dolomite. The upper unit contains two beds and is undulose.
	175.5-178.5 m	(576-586 ft)	Lower unit of the Double Dolomite. It has a sharp base and chert lenses throughout.
	169.5-175.5 m	(556-576 ft)	Mostly covered.
S-10-60-22	169.5 m	(556 ft)	Hard black claystone, weathered.
	160.5-169.5 m	(527-556 ft)	Lower half of interval has apparent cross-beddding with topsets truncated, present in one area. Low angle cross-laminations and trough cross-bedding. Upper half of interval is mostly covered.
	157-160.5 m	(515-527 ft)	3 m (10 ft) thick dolomite, tan to terra cotta, petroliferous, with lamellar, stromatolitic texture and intervals of rip-up clasts

Appendix 2: Field Notes for Plate 1

			(character similar to flaky dolomite). Layers with contorted lamellations/bedding present and layers with silica lenses present.
	157 m	(515 ft)	Base of Dolomite doublet. Sharp undulose contact. Wavelegth remains nearly constant
	154-155 m	(505-508.5 ft)	Thinly laminated, almost rhythmic (varved) crystalline dolomite with petroliferous odor.
	153-154 m	(502-505 ft)	About 1 m (3.2808 ft) of thinly laminated dolomitic (?) claystones.
	151.5-153 m	(497-502 ft)	1.5 m (5 ft) thick stromatolitic (silicified), intraclastic, tan dolostone with hydrocarbon odor. Intraclasts appear to be ripped up stomatolitic fragments. Sucrosic texture in dolomite. Intraclasts parallel to sub-parallel to laminae.
	147-151.5 m	(482-497 ft)	Covered.
	147 m	(482 ft)	Silicified (?) Dolostone, finely crystalline, cleaving along laminations about 50 cm (20 in) thick, with hydrocarbon odor.
	135-147 m	(443-482 ft)	Covered.
S-10-60-21	135 m	(443 ft)	As below. Dark clays, with paper structure.
	126-135 m	(413-443 ft)	Covered.
S-10-60-20	126 m	(413 ft)	Dark gray, black fissile clays, with sulfurous odor.
	124.5-126 m	(408.5-413 ft)	Dark gray, black fissile clays, with sulfurous odor.
	124.5 m	(408.5 ft)	Pisolitic packstone (?) with wavy laminations, badly weathered and hard, encased in paper clays. About 30 cm (12 in) thick.
	115.5-124.5 m	(379-408.5 ft)	Covered slope.
	115.5 m	(379 ft)	Black pisolitic grainstone in black matrix, chert matrix and cement (?), very hard with vertical fractures, about 30-50 cm (12-20 in) thick. No apparent sorting or grading.

Note: From 22.5 to 115.5 m (74 to 379 ft) is mostly covered, dark gray slope with skree.

S-10-60-19	100.5 m	(330 ft)	Weathered claystones with Chuaria (???).
S-10-60-18	87 m	(285 ft)	Weathered claystones with Chuaria (???).
S-10-60-17	78 m	(256 ft)	Black to dark gray, weathered claystones with yellowish weathering surface.
S-10-60-16	67.5 m	(221 ft)	Claystones as below.
S-10-60-15	58.5 m	(192 ft)	
S-10-60-14	51 m	(167 ft)	Dark gray to black claystone.
S-10-60-13	43.5 m	(143 ft)	As above.
	22.5-41.5 m	(74-136 ft)	Covered slope with skree and alluvium. Most likely black shales.
	22.5 m	(74 ft)	Pisolitic and stromatolitic (?) grainstone, silica cemented. Very hard. Brown (weathered), about 1.5 m (5 ft) thick. In places it appears to be thinly laminated = stromatolitic ?? No apparent sorting of pisolites.
S-10-60-12	19 m	(62 ft)	Dominantly black claystones.
	15-18.75 m	(49-62 ft)	Dominantly black claystones.
S-10-60-11	15 m	(49 ft)	Dominantly black claystones.
	12 m	(39 ft)	50 cm (20 in) thick dolostone, hard with hydrocarbon odor.
S-10-60-10	9 m	(29.5 ft)	
	7.5 m	(25 ft)	Hard cherty (?) claystone.
	4.5-6 m	(15-20 ft)	Generally pisolitic grainstone, chertified/silicified interbedded with stromatolitic (flaky) dolomite, very hard with hydrocarbon odor.
	0-4.5 m	(0-15 ft)	Flaky dolomite about 4.5 m (14.76 ft) thick, with chert lenses comprising pisolites. Lower beds consist of contorted bedding/laminations in stromatolitic dolomite, with local fractures present with small microfractures cemented. Middle beds consist of pisolite silica lenses floating in flaky (stromatolitic) dolomite. Stromatolite laminae very contorted in places. Upper beds consist of pisolitic grainstones. Majority of pisolites greater than 2 mm,

Appendix 2: Field Notes for Plate 1

	0 m	(0 ft)	white to dark gray in white silica matrix cement. Extremely tight. Base of Walcott Member = Base of Flaky Dolomite = Top of Awatubi Member. Note: Walcott Member section measured from base of Walcott Member.

AWATUBI MEMBER, KWAGUNT FORMATION (199 m = 653 ft)

	199 m	(653 ft)	Top Awatubi Member, Kwagunt Formation = Base Walcott Member, Kwagunt Formation = Base Flaky (filamentous) Dolomite.
	196-199 m	(643-653 ft)	Section covered with skree (fallen boulders from flaky dolomite). At base of contact with dolomite is a 50 cm (20 in) thick bed of red and green claystone which passes downward to a slightly dolomitic dark gray claystone. (No Chuaria observerd). Red color may be diagenetic. Probably low TOC (also calcareous).
	196 m	(643 ft)	60 to 80 cm (24-31 in) thick bedded dolomite, non-pisolitic.
	165.5-196 m	(543-643 ft)	Covered ?
S-10-60-9	165.5 m	(543 ft)	Black fissile shale with Chuaria throughout. Weathers to pale-dark yellow.
	156-165.5 m	(512-543 ft)	Shale.
S-10-60-8	156 m	(512 ft)	As below. Chuaria in paper thin silty shales of Awatubi.
	150-156 m	(492-512 ft)	Silty shales and claystones.
	150 m	(492 ft)	Claystones, same as below.
S-10-60-7	145.5 m	(477 ft)	Same as below.
S-10-60-6	135 m	(443 ft)	Same as below.
S-10-60-5	126 m	(413 ft)	Grey (dark) claystone, very rich in Chuaria, slightly silty.
	100.5-126 m	(330-413 ft)	All covered with rock debris. From slope character, section is probably same as below.
	100.5 m	(330 ft)	Same shale as below.
S-10-60-4	96 m	(315 ft)	Grey shale with Chuaria (weathered).
S-10-60-3	94 m	(308 ft)	Weathered silty claystone (yellowish orange due to oxidation). Fresher surface is grey to light grey. Slightly fissile, fractured with Chuaria circularis.
	69-93 m	(226-305 ft)	Covered with bushes and fallen claystones and Tapeats boulders.
	69 m	(226 ft)	Maroon silty claystones, weathered. Migrating ripples with surface of axial trough oriented N65°W.
	63-64 m	(207-210 ft)	80 to 100 cm (31-39 in) unit which is silty at the top, underlain by sandstone beds which are 15 to 20 cm (6-8 in) thick and are tabular to channel form with rip-up clasts in clayey (green) matrix, well cemented. Recessive units of silt present in interbeds.
	63 m	(207 ft)	Sandstone, greyish-green, hard, ripple marked, thinly laminated, slightly argillaceous.
S-10-60-2	62.5 m	(205 ft)	Silty shale as below, grey.
S-10-60-1	60 m	(197 ft)	Blocky silty shale. Weathers to maroon, but grey (fresh) breaks. Breaks to flakes (silty).
	44-60 m	(144-197 ft)	Mudstones and silty mudstones. Maroon and variegated.
	44 m	(144)	Sandstone, rippled and mud-cracked with drapes of medium sandstone, silica cemented.
	26-44 m	(85-144 ft)	18 m (59 ft) of covered section with floatstone and clays.
	3-3.5 m	(10-11.5 ft)	0.5 m (1.6 ft) of interbedded clays and limestone.
	0-3 m	(0-10 ft)	3 m (10 ft) of stromatolitic limestone, tan (weathered) with vertical columnal algal heads. Very tight, however fractured.
	0 m	(0 ft)	Base of stromatolitic limestone = Base of Awatubi Member. Below stromatolites are claystones of Carbon Butte Member.